RP TU Rheinland-Pfälzische Technische Universität Kaiserslautern Landau

Analysis of associative olfactory learning and memory in *Drosophila*

vom Fachbereich Biologie
der Rheinland-Pfälzischen Technischen Universität Kaiserslautern-Landau zur Verleihung des akademischen Grades Dr. rer. nat. genehmigte

Dissertation

von

Vanessa Burre, M.Sc.

Mündliche Prüfung:	11.09.2026
Dekan:	Prof. Dr. Stefan Kins
Prüfungsvorsitz:	Prof. Dr. Tanja Maritzen
Betreuer:	Prof. Dr. Jan Pielage
Korreferent:	Prof. Dr. Stefan Kins

D 386

Declaration in lieu of oath

I hereby declare under oath that I have prepared the submitted thesis myself and that I have not used any other media or materials than the ones referred to in this thesis I have not previously submitted this dissertation or any part of it for a state or scientific examination. Likewise, I have not submitted this or any other dissertation to another department or university.

Ich erkläre wahrheitsgemäß, dass ich die eingereichte Dissertation selbst angefertigt und alle für die Arbeit benutzten Hilfsmittel und Hilfestellungen in der Arbeit angegeben habe. Die Dissertation oder Teile hiervon habe ich bisher nicht als Prüfungsarbeit für eine staatliche oder andere wissenschaftliche Prüfung eingereicht. Ebenso habe ich die gleiche oder eine andere Abhandlung nicht bei einem anderen Fachbereich oder einer anderen Universität als Dissertation eingereicht.

Place, Date Vanessa Burre

Parts of this thesis have been published in the following research articles:

Zhou F, Tichy A-M, Imambocus BN, Sakharwade S, Rodriguez Jimenez FJ, González Martínez M, Jahan I, Habib M, Wilhelmy N, Burre V, Lömker T, Sauter K, Helfrich-Förster C, Pielage J, Grunwald Kadow IC, Janovjak H, Soba P (2023)
'Optimized design and *in vivo* application of optogenetically functionalized Drosophila dopamine receptors'
Published in: Nature Communications, https://doi.org/10.1038/s41467-023-43970-0

Darlegung des Eigenanteils

Vanessa Burre

Analysis of associative olfactory learning and memory in *Drosophila*

Die in den Abbildungen 18–19 sowie 21–22 dargestellten Daten wurden in gleichwertiger Zusammenarbeit mit Nina Wilhelmy erhoben. Auch die Daten, die der Abbildung 17 zugrunde liegen, stammen aus einer ebenso gleichwertigen Kooperation mit Nina Wilhelmy. Die anschließende Datenanalyse erfolgte vollständig durch mich. Die Konzeption der Experimente wurde in beiden Fällen gleichermaßen von Nina Wilhelmy und mir gemeinsam entwickelt.

Die für die Quantifizierung der Daten in Abbildung 25 verwendete Software wurde vollständig von Hannes Euler programmiert.

Die zugrunde liegenden Daten der Abbildung 25 wurden in gleichwertiger Zusammenarbeit mit Benjamin Escribano erhoben. Die anschließende Datenanalyse erfolgte vollständig durch mich. Die Konzeption der Experimente wurde hierbei gleichermaßen von Benjamin Escribano und mir gemeinsam entwickelt.

Teile dieser Arbeit wurden zudem in Zusammenarbeit mit Prof. Dr. Peter Soba von der Friedrich-Alexander-Universität Erlangen-Nürnberg im Rahmen einer gemeinsamen Publikation erhoben. Die Konzeption der Experimente erfolgte in gleichwertiger Zusammenarbeit mit Nina Wilhelmy und in Absprache mit Prof. Dr. Peter Soba sowie Prof. Dr. Jan Pielage. Die in den Abbildungen 28–31 gezeigten Daten wurden zusammen mit Nina Wilhelmy erhoben und ausgewertet.

Natalie Foth unterstützte mich bei der Etablierung des Färbeprotokolls für Puppen, war jedoch nicht an der Erhebung der in dieser Arbeit verwendeten Daten beteiligt.

Die vorliegende Einschätzung der von Dritten erbrachten Leistungen wurde mit den genannten Personen einvernehmlich abgestimmt.

Datum, Unterschrift Doktorandin	Datum, Unterschrift Betreuer

Table of contents

List of figures ..... **IV**

List of tables ..... **V**

List of abbreviations ..... **VI**

1. Summary **1**

2. Zusammenfassung **3**

3. Introduction **5**

3.1 Olfactory pathway 5
3.2 Classical olfactory conditioning 8
3.3 Memory formation 9
3.4 The engram 12
3.5 Binary expression system 13
3.6 CREB-signaling pathway 15
3.7 FUNCAT 16
3.8 Aim of the thesis 19

4. Materials and methods **20**

4.1 Buffers, solutions and media 20
4.1.1 Standard fly food 20
4.1.2 Odor-free food 20
4.1.3 Retinal food 20
4.1.4 Phosphate buffered saline (PBS) 21
4.1.5 PBS with Triton X-100 (PBST) 21
4.1.6 PBS with Tween-20 21
4.1.7 Paraformaldehyde (PFA) in PBS 21
4.1.8 Hemolymph-like physiological solution (HL3) 22
4.1.9 PFA in HL3 22
4.1.10 Normal goat serum (NGS) 22
4.1.11 Poly-L-lysine hydrobromide (PLL) 22
4.1.12 B-Block 22
4.1.13 PFA lysine phosphate buffer (PLP-fix) 23
4.1.14 PBS with dimethyl sulfoxide, Triton and Tween (PBS-DTT) 23
4.1.15 FUNCAT Solution 23
4.1.16 FUNCAT washing buffer 23
4.2 Experimental animals 24
4.2.1 Fly breeding 24

4.2.2 ANL feeding 26
4.3 Immunohistochemistry 26
4.3.1 Old immunohistochemical labeling protocol 27
4.3.2 Improved immunohistochemical labeling protocol 27
4.3.3 FUNCAT labeling protocol 28
4.3.4 Quantification and microscopy 29
4.4 Behavior 29
4.4.1 Regulation of environmental influences 29
4.4.2 Appetitive olfactory conditioning 32
4.4.3 Aversive olfactory conditioning 33
4.4.4 Artificial aversive conditioning 35
4.4.5 Odor preference test 37
4.4.6 Light preference test 38
4.5 Statistical analysis 39
5. Results 40
5.1 Natural experiences modulate CAMEL-tool activity 40
5.1.1 Experience-dependent labeling of CAMEL-cells 41
5.1.2 Optogenetic reactivation of CAMEL-cells encoding natural memories 46
5.2 Establishment of an improved immunohistochemical labeling protocol 49
5.3 LTM-dependent CAMEL-tool activity 51
5.3.1 Conditioning-dependent labeling of CAMEL-cells 51
5.3.2 Visualization of newly synthesized LTM proteins 53
5.3.3 Recall of conditioning-dependent appetitive memories 56
5.4 Artificial aversive conditioning 63
5.5 Characterization of light activatable DopRs 65
5.5.1 Light activatable DopRs are incorporated into neuronal membranes 65
5.5.2 DopR activity in KCs is required but not sufficient for learning 68
6. Discussion 72
6.1 Experience-dependent CAMEL-tool activity 72
6.1.1 CAMEL-tool activity in sensory-deprived pupae 73
6.1.2 Neural impact of social isolation 74
6.1.3 Increased environmental stimulation enhances CAMEL-activity 75
6.1.3.1 CAMEL-labeling through mechanical stimulus 75
6.1.3.2 Combined Environmental Stimulation Enhances CAMEL-Activity 76
6.1.4 Experience-dependent memory modulates behavior 77
6.2 Appetitive memory formation and engram cell recruitment 79
6.3 Visualization of newly synthesized proteins in engram cells 81
6.4 Optogenetic approach to generate an artificial olfactory memory 83

6.5 Functional characterization of light-activated DopRs 85
6.6 Conclusion 87
7. References **89**
1. Appendix ..... **I**
1.1 Results of statistical analysis I
1.2 Curriculum Vitae IV
1.3 Acknowledgements V

List of figures

Figure 1: Olfactory pathway of the adult fly. 7
Figure 2: Balance model of associative memory formation. 11
Figure 3: Schematic of the Gal4-UAS binary expression system....14
Figure 4: Memory formation in KCs based on the CREB signaling pathway 15
Figure 5: Schematic of FUNCAT technique. 18
Figure 6: Experimental setup for controlled environmental influences. 31
Figure 7: Experimental setup for appetitive olfactory conditioning. 33
Figure 8: Experimental setup for aversive olfactory conditioning. 34
Figure 9: Experimental setup for artificial aversive conditioning. 36
Figure 10: Experimental setup for odor preference test. 37
Figure 11: Experimental setup for light preference test. 38
Figure 12: Schematic of the CAMEL-tool. 40
Figure 13: Sensory deprivation minimizes number of labeled CAMEL-cells. 42
Figure 14: Successive increase of environmental inputs leads to an increasing number of labeled CAMEL-cells. 44
Figure 15: Summary of the number of positive CAMEL-cells in relation to different environmental inputs. 45
Figure 16: Artificial recall of natural memory requires a combination of environmental inputs. 48
Figure 17: The number of CAMEL-cells depends on the reporter gene expressed. 49
Figure 18: The new protocol improves the quality of antibody labeling. 50
Figure 19: The time point of fixation has a minor influence on the quality of the labeling. ..51
Figure 20: Appetitive memory formation increases the number of CAMEL positive cells. ..52
Figure 21: Visualization of EGFP-tagged MetRS^{L262G} and newly synthesized proteins. 54
Figure 22: Visualization of protein synthesis in CAMEL-somata. 55
Figure 23: Optogenetic reactivation of conditioning-dependent CAMEL-cells. 56
Figure 24: Retinal feeding test. 57
Figure 25: Automated data analysis of arena videos. 60
Figure 26: Comparison of memory recall in the circular arena and the T-maze. 62
Figure 27: Artificial aversive conditioning of CAMEL-cells using red LEDs. 64
Figure 28: Subcellular localization of light activatable DopRs. 66
Figure 29: Localization of light activatable DopR in single neurons. 67
Figure 30: Analysis of DopR knock down and overexpression for learning. 69
Figure 31: Activation of exogenous D1R1 is not sufficient to induce learning. 71

List of tables

Table 1: Fly stocks. 24
Table 2: Experimental genotypes. 25
Table 3: List of antibodies. 26
Table 4: List of detailed statistical results for boxplots and scatter plots. I

List of abbreviations

4-EG	4-ethylguaiacol
AD	activation domain
AHA	azidohomoalanine
ANL	azidonorleucine
ARM	anesthesia-resistant memory
BDSC	bloomington drosophila stock center
BONCAT	bioorthogonal non-canonical amino acid tagging
CAMEL	CRE-activity-dependent memory engram label
cAMP	cyclic Adenosine Monophosphate
CRE	cAMP responsive element
CREB	cAMP responsive element binding protein
CS	conditioned stimulus
DAN	dopaminergic neuron
DBD	DNA binding domain
DMSO	dimethyl sulfoxide
DNA	deoxyribonucleic acid
DopR	dopamine receptor
DPX	dibutylphthalate polystyrene xylene
EDTA	ethylenediaminetetraacetic acid
EGFP	enhanced GFP
FUNCAT	fluorescent non-canonical amino-acid tagging
GABA	gamma-aminobutyric acid
GFP	green fluorescent protein
HL3	hemolymph-like physiological solution
HPG	homopropargylglycine
KC	kenyon cell
LH	lateral horn
LTM	long-term memory
MB	mushroom body
MBON	mushroom body output neuron
MCH	4-methyl-cyclohexanol
MetRS	methionyl-tRNA synthetase
mRNA	messenger RNA
MTM	middle-term memory
ncAA	non-canonical amino acids
NGS	normal goat serum

OCT	3-octanol
OR	odorant receptor
ORN	olfactory receptor neuron
PAM	protocerebral anterior medial
PBS	phosphate buffered saline
PBS-DTT	PBS with dimethyl sulfoxide, Triton and Tween
PBST	phosphate buffered saline with triton
PFA	paraformaldehyde
PKA	protein kinase A
PLL	poly-L-lysine hydrobromide
PLP-Fix	PFA lysine phosphate buffer
PN	projection neuron
PPL	protocerebral posterior lateral
RNA	ribonucleic acid
RNA_i	RNA-interference
RT	room temperature
SEM	standard error of the mean
STM	short-term memory
TAMRA	tetramethylrhodamine
TBTA	tris [(1-benzyl-1H-1,2,3-triazol-4-yl) methyl] amines
TCEP	tris (2-carboxyethyl) phosphine hydrochloride
tRNA	transfer RNA
UAS	upstream activating sequence
US	unconditioned stimulus

1. Summary

Throughout their lives organisms encounter a wide range of complex sensory stimuli and must be able to flexibly adjust their behavior. Innate behavior, which is genetically programmed, differs from learned behavior, which relies on experience. The output of both behavioral pathways is integrated to generate appropriate responses to environmental cues. The detection and evaluation of these stimuli are essential for survival and show remarkable similarities between vertebrates and insects, especially in the olfactory system. Memory enables organisms to use past experiences by storing relevant information that can be accessed later to guide behavior and adapt to future changes. In *Drosophila melanogaster* the mushroom body (MB) acts as the key brain region for learning and memory formation. Through associative learning, where sensory cues are linked with either positive or negative reinforcement, behavioral changes can become lasting. The establishment of long-term memory in the MB involves local molecular adaptation and synaptic remodeling.

In this thesis I investigate the formation and function of memory traces in the olfactory system of the fruit fly. Central to this study is the CRE-activity-dependent memory engram label (CAMEL)-tool, a genetic reporter that labels and manipulates memory-relevant Kenyon cells (KCs). I demonstrated that the number of fluorescently labeled CAMEL cells was modulated dynamically by sensory input. Environmental enrichment led to a significant increase in CAMEL-labeled KCs within the MB, indicating that CAMEL activity reflects experience-dependent memory encoding. Optogenetic reactivation of these CAMEL-cells after exposure to specific stimuli resulted in behavioral changes, confirming their functional relevance.

To investigate molecular changes within individual engram cells, I combined the fluorescent non-canonical amino-acid tagging (FUNCAT) technique with the CAMEL-tool to visualize newly synthesized proteins. FUNCAT relies on the incorporation of a methionine analog into nascent proteins, which can subsequently be fluorescently labeled using bioorthogonal click chemistry. This approach enables sensitive and specific detection of protein synthesis at the single-cell level, allowing precise analysis of translational activity within defined neuronal populations without relying on conventional antibody staining.

I established an optimized immunohistochemical labeling protocol to improve the detection of sparsely labeled neuronal populations by increasing signal-to-noise ratio and overall staining consistency. This enabled more reliable detection of sparsely labeled neuronal populations and helped to overcome limitations observed with previous protocols.

In an artificial aversive conditioning paradigm the odor cue was replaced by optogenetic activation of CAMEL cells during training. In the subsequent light preference test using the circular arena, we were not able to recall artificial aversive memory using this approach.

Finally, I optogenetically manipulated dopaminergic signaling pathways by expressing a light-activatable variant of the dopamine receptor D1R1 in MB neurons. I confirmed proper subcellular localization of the receptor, and behavioral experiments demonstrated that D1R1 function in KCs is required for learning. However, when the electric shock was replaced by light-induced activation of D1R1 during odor presentation, this artificial activation alone was insufficient to induce associative memory formation

2. Zusammenfassung

Im Verlauf ihres Lebens sind Organismen einer Vielzahl komplexer Sinneseindrücke ausgesetzt und müssen ihr Verhalten flexibel anpassen können. Angeborenes Verhalten, das genetisch festgelegt ist, unterscheidet sich von erlerntem Verhalten, das auf Erfahrung basiert. Angeborenes und erlerntes Verhalten wirken zusammen, um passende Reaktionen auf Umweltreize zu erzeugen. Die Wahrnehmung und Bewertung dieser Reize ist für das Überleben essenziell und zeigt bemerkenswerte Parallelen zwischen Wirbeltieren und Insekten – insbesondere im olfaktorischen System. Gedächtnis ermöglicht es Organismen, frühere Erfahrungen zu speichern und diese bei Bedarf abzurufen, um ihr Verhalten zu steuern und sich an neue Situationen anzupassen. Bei *Drosophila melanogaster* übernimmt der Pilzkörper (mushroom body, MB) eine zentrale Rolle bei Lernprozessen und der Gedächtnisbildung. Durch assoziatives Lernen, bei dem Sinneseindrücke mit positiver oder negativer Verstärkung verknüpft werden, können Verhaltensänderungen dauerhaft etabliert werden. Die Ausbildung von Langzeitgedächtnis im MB geht mit synaptischer Plastizität und molekularen Anpassungen einher.

In dieser Arbeit untersuche ich die Bildung und Funktion von Gedächtnisspuren im olfaktorischen System der Fruchtfliege. Im Mittelpunkt steht das CAMEL-Werkzeug (CRE-activity–dependent memory engram label, CAMEL) – ein genetischer Reporter, der Kenyon-Zellen (KCs) auf Basis von CRE-Aktivität markiert und manipuliert, wenn sie an der Gedächtnisbildung beteiligt sind. Ich konnte zeigen, dass die Anzahl Fluoreszenz markierter CAMEL-Zellen dynamisch durch sensorische Reize beeinflusst wird. Umgebung mit erhöhter sensorischer Stimulation führte zu einer signifikanten Zunahme CAMEL-positiver KCs, was darauf hindeutet, dass CAMEL-Aktivität erfahrungsabhängige Gedächtnisprozesse widerspiegelt. Die optogenetische Reaktivierung dieser CAMEL-Zellen nach definierter Reizexposition führte zu Verhaltensänderungen, was ihre funktionelle Relevanz bestätigt.

Um molekulare Veränderungen in einzelnen Engrammzellen zu untersuchen, kombinierte ich das CAMEL-Werkzeug mit der FUNCAT-Technik (fluorescent non-canonical amino-acid tagging, FUNCAT) zur Visualisierung neu synthetisierter Proteine. FUNCAT basiert auf dem Einbau eines Methionin-Analogons in naszierende Proteine, die anschließend über bioorthogonale Click-Chemie fluoreszent markiert werden können. Diese Methode erlaubt eine sensitive und spezifische Detektion von Proteinsynthese auf Einzelzellebene und ermöglicht eine präzise Analyse translationaler Aktivität in definierten neuronalen Populationen ohne den Einsatz konventioneller Antikörperfärbungen.

Ich etablierte ein optimiertes immunhistochemisches Färbeprotokoll, dass das Kontrastverhältnis zwischen Signal und Hintergrund erhöht. Dadurch wurde die Detektion

schwach markierter neuronaler Populationen zuverlässiger und Einschränkungen früherer Protokolle konnten überwunden werden.

In einem künstlichen aversiven Konditionierungsparadigma wurden die Elektroschocks während des Trainings beibehalten, der Geruchsreiz jedoch durch optogenetische Aktivierung von CAMEL-Zellen ersetzt. Im anschließenden Lichtpräferenztest innerhalb der zirkularen Arena konnte auf diese Weise jedoch kein aversives Gedächtnisverhalten ausgelöst werden.

Zur Manipulation dopaminerger Signalwege exprimierte ich eine lichtaktivierbare Variante des Dopaminrezeptors D1R1 in Neuronen des MB. Die korrekte subzelluläre Lokalisation wurde bestätigt, und Verhaltensexperimente zeigten, dass D1R1 in KCs für Lernprozesse erforderlich ist. Wenn jedoch der Elektroschock durch lichtinduzierte Aktivierung von D1R1 während der Geruchsdarbietung ersetzt wurde, war diese künstliche Aktivierung allein nicht ausreichend, um eine assoziative Gedächtnisbildung zu induzieren.

3. Introduction

During its lifetime an organism experiences a dynamic and complex sensory environment and its survival depends on the ability to adapt behavior to these stimuli. However, a distinction is made between innate behavior, which is genetically encoded through hardwired networks, and learned behavior, which is experience dependent. Innate behavior, encoded through hardwired neural circuits, ensures the survival of the organism. However, to cope with the wide variety of environmental influences, the organism must also adapt its behavior. This adaptability is enabled through learned behavior. Neural circuits integrate information from both innate and learned behavioral pathways to compute appropriate responses to complex environmental inputs.

For many decades, research has focused on the localization of memory traces, as this provides great potential to understand how the brain functions at synaptic level. More importantly, it may allow us to intervene in traumatic memories causing stress disorders. However, there are limited possibilities to conduct research on the brain of living humans. For this reason, model organisms provide a good opportunity to perform basic research and extend findings to more complex organisms due to the conserved basic principles across evolution. The fruit fly *Drosophila melanogaster*, for example, exhibits complex behaviors based on simple and largely known neuroanatomy. In addition, a rich genetic toolbox is available to manipulate individual neurons in a targeted and reproducible manner. Thus, the fruit fly is used as a model organism to gain a better understanding of neuronal circuits underlying behavior (Kazama, 2015; Owald et al., 2015b; Shin et al., 2018).

3.1 Olfactory pathway

The detection and subsequent evaluation of sensory cues in the natural environment is essential for animals to ensure their survival. It is plausible that a variety of different receptors and signaling pathways are used in the animal kingdom to accomplish this task. However, looking at the olfactory system, a striking overlap between vertebrates and insects can be observed (Kaupp, 2010; Yu et al., 2004).

Vertebrates have a large repertoire of G protein-coupled odorant receptors (ORs). The number of OR genes varies widely among species and mostly ranges between 600 and 1,300. ORs are localized in the olfactory epithelium of the nose, where they detect odorant molecules. Olfactory receptor neurons (ORNs) transmit sensory information to the olfactory bulb where they innervate so-called glomeruli. Neurons expressing the same OR gene converge on a particular position within the olfactory bulb, forming a glomerulus. Projection neurons (PNs), specifically mitral cells and tufted cells, then transmit the information from the olfactory bulb to

central brain regions to elicit appropriate behavioral output (Kaupp, 2010; Smith and Bhatnagar, 2019; Wachowiak and Shipley, 2006).

Two types of behavior can be distinguished in this context: innate behavior, which follows a stereotypical pattern, and memory-based learned behavior. To recall innate behavior, mitral cells transmit olfactory information to the amygdala. For memory-based behavior, the information is conveyed by tufted cells and mitral cells to the olfactory cortex. However, it should be noted that many behaviors are the result of the interaction between learned and innate behavior and cannot be separated strictly (Dolan et al., 2018; Eschbach et al., 2021; Kobayakawa et al., 2007; Mori and Sakano, 2021).

Fruit flies perceive odors via their antennae and maxillary palps, which house ~1,300 ORNs expressing 62 different ORs (Figure 1, Busto et al., 2010; Davis, 2004; Vosshall and Stocker, 2007). Although the fly's nervous system is relatively simple in terms of the number and diversity of neurons compared to vertebrates, whose brains contain hundreds of ORs, it is still capable of reliable odor discrimination. In the apical dendrites of the ORNs, usually only one type of the 62 ORs is expressed together with the co-receptor Or83b, called Orco (Kaupp, 2010; Larsson et al., 2004; Robertson et al., 2003; Vosshall et al., 1999; Vosshall and Stocker, 2007). In some ORNs a second OR or an additional gustatory receptor is expressed in a single neuron. ORNs project through the antennal nerve into the ~50 glomeruli of the antennal lobe. ORNs expressing the same OR converge onto the same glomerulus, forming a dense and stereotyped representation of receptor identity (Couto et al., 2005; Fishilevich and Vosshall, 2005). As a result, odor identity is encoded combinatorially. Natural odors typically consist of multiple odorants that activate distinct receptor subsets, giving rise to characteristic and reproducible patterns of glomerular activity across individuals (Ng et al., 2002; Yu et al., 2004).

In the antennal lobe glomeruli ORNs synapse onto PNs. The ~150 PNs relay information to two higher brain regions, the lateral horn (LH) and the mushroom body (MB) (Jefferis et al., 2007; Keene and Waddell, 2007). In the LH innate behavior is collected and processed, particularly for odors such as carbon dioxide and geosmin, which are detected via dedicated circuits eliciting hard-wired avoidance responses (Das Chakraborty and Sachse, 2021; Huoviala et al., 2018; Stensmyr et al., 2012; Suh et al., 2004; Varela et al., 2019). The MB is the center for learning and memory in the fly (Davis, 1993; Heisenberg, 2003; Heisenberg et al., 1985; Keene and Waddell, 2007; Takemura et al., 2017).

The MB consists of ~2,000 Kenyon cells (KCs) per hemisphere. The dendritic branches of the KCs form a bulbous structure, the MB calyx. Here, the sensory information from the PNs is transmitted to the KCs (Baltruschat et al., 2021; Gruntman and Turner, 2013; Tanaka et al., 2008). An odor is represented by the activity of a sparse set of KCs (Campbell et al., 2013; Honegger et al., 2011; Siegenthaler et al., 2019; Wang et al., 2004). The axons of the KCs bundle together to form the peduncle and the lobes of the MB. Based on their branching, the

following three main subtypes have been distinguished: α/β, α'/β', and γ KCs (Ito et al., 1997; Lee et al., 1999; Tanaka et al., 2008).

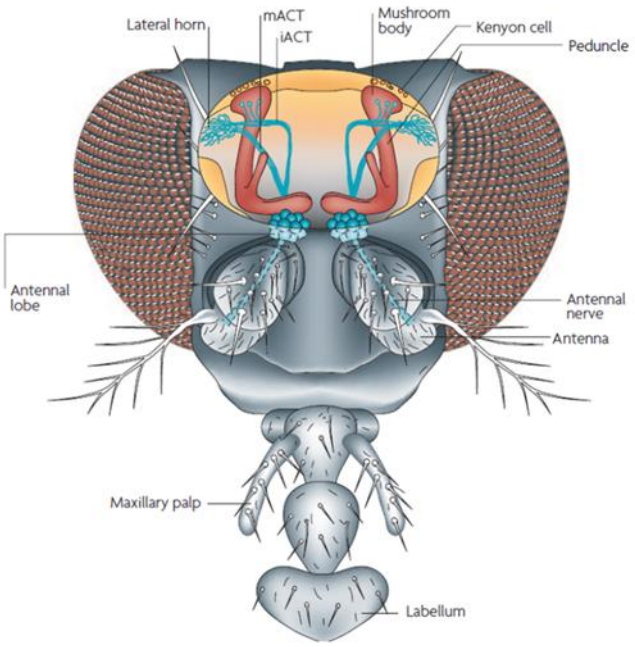


Figure 1: Olfactory pathway of the adult fly.
A schematic fly head is shown depicting the anatomical key components of the olfactory pathway. Odors are perceived by ORNs in the antennae and the maxillary palps. Along the antennal nerve, the ORNs project into the antennal lobe glomeruli, where they synapse onto PNs. The PNs transmit the information to the LH (blue) or the MB (red). Adapted from (Keene and Waddell, 2007).

During the larval stage, all MB neurons branch into a vertical and a horizontal lobe. During the pupal stage, however, γ axons are pruned and subsequently only re-extend/regrow medially. The α/β and α'/β' neurons bifurcate into a vertical (α and α') and a horizontal (β and β') lobe. (Aso et al., 2009; Crittenden et al., 1998; Lee et al., 1999). The KCs form en passant synapses along their axonal projections and converge onto a total of 34 mushroom body output neurons (MBONs) per hemisphere, which integrate this input to shape behavioral output (Aso et al., 2014a; Tanaka et al., 2008). Different MBONs promote either approach or avoidance behavior and thereby determine the behavioral valence of an odor (Aso et al., 2014b; Owald et al., 2015a). The MB is additionally innervated by dopaminergic neurons (DANs). If flies perceive an odor in conjunction with a negative or positive stimulus, the activity of the DANs modulates the KC>MBON synapses, thereby altering the output of the MBONs and assigning a valence to that odor. This ultimately leads to a behavioral change (Aso et al., 2014a; Mao and Davis, 2009). Hence, the fruit fly provides a common model organism for better understanding of the neuronal circuits underlying associative learning (Kazama, 2015; Owald et al., 2015b; Shin et al., 2018).

3.2 Classical olfactory conditioning

The Russian physiologist Ivan Petrovich Pavlov is considered the founder of associative memory formation. He postulated that a previously neutral stimulus without a specific response produces a conditioned response after learning. He tested his hypothesis with a behavioral experiment on dogs. In 1927 Pavlov observed that dogs always respond to food by salivating, which is an unconditioned response (unconditioned stimulus, US). As a neutral stimulus he used a metronome in his experiment. During conditioning, the click of the metronome was presented to the dog immediately followed by food presentation. After several repetitions of this training the dogs associated the sound with the food and began to salivate as soon as they heard the metronome. The neutral stimulus had become the conditioned stimulus (CS) and a conditioned response is produced. The presentation of the CS alone is now sufficient to cause salivation (Pavlov, 1927).

Adaptations of this simple experiment have been used in neuroscience to study the principles of adaptive decision-making. In *Drosophila melanogaster*, olfactory classical conditioning has become a common method to study the molecular and cellular mechanisms underlying learning and memory. One major advantage is the large homology of the olfactory system in insects and mammals. This allows a direct transfer of findings from the relatively simple nervous system of flies to the complex nervous system of mammals. In addition, olfactory conditioning reliably induces associative memory and provides a robust behavioral readout to quantify learned associations in *Drosophila* (Davis, 2004; Kaupp, 2010).

In olfactory conditioning, flies learn to associate a specific odor (CS^+) with a reward or punishment, while a second odor (CS^-) is presented without reinforcement. Appetitive conditioning uses sugar as a positive reinforcer, whereas aversive conditioning uses electric shocks. Training can be performed as a single trial or can be repeated in spaced cycles. The time interval between training and testing induces different forms of memory. Accordingly, four different forms of memory can be distinguished, depending on the conditioning protocol: short-term memory (STM), middle-term memory (MTM), anesthesia-resistant memory (ARM) and long-term memory (LTM) (Dubnau and Tully, 1998; Keene and Waddell, 2007). STM is tested a few minutes after a single conditioning trial and lasts only 7 min. STM transitions sequentially to MTM, which lasts for 1-3 h. These early memory phases are independent of new protein expression, the behavioral changes are caused by changes in synaptic transmission (Bilz et al., 2020; Dubnau and Tully, 1998; Heisenberg, 2003; Yu et al., 2004). In contrast, repeated aversive training trials separated by rest intervals (spaced training) and a single cycle of appetitive training induce protein synthesis-dependent LTM. Whereas repeated trials without rest intervals (massed training) resulted in protein synthesis-independent ARM. ARM persists for approximately two days, while LTM can last up to nine days (Heisenberg, 2003; Hirano et al., 2016; Tully et al., 1994).

In the early 1970s scientists began to establish olfactory conditioning of flies. Although the technical equipment has improved considerably since its inception, the basic procedure of the assay has remained the same. Modern setups allow conditioning of several cohorts of flies simultaneously under identical conditions, thereby reducing experimental variability between trials.

3.3 Memory formation

Olfactory conditioning in *Drosophila melanogaster* induces experience-dependent behavioral changes via associative learning. A specific odor (CS^+) is associated with a reinforcing stimulus (US), such as sugar reward or electric shock (see section 3.2). However, not every pairing of CS and US leads to stable memory formation. The strength and persistence of the resulting memory critically depend on the training paradigm. In standard aversive conditioning, flies are repeatedly exposed to an odor (CS^+) paired with electric shocks (US), while a second odor (CS^-) is presented without reinforcement. If these training cycles are separated by rest intervals (spaced training), protein synthesis-dependent LTM is formed. In contrast, repeated training without rest intervals (massed training) results in ARM, which is independent of protein synthesis and less persistent (Hirano et al., 2016; Tully et al., 1994; Tully and Quinn, 1985). In addition, memory expression can be modified after initial learning. For example, repeated presentation of the CS^+ without reinforcement (i.e. odor without shock) reduces the conditioned response. This process, known as extinction, does not result in the erasure of the original memory but instead in the formation of a new inhibitory memory trace that suppresses its expression (Felsenberg et al., 2018).

A widely accepted model of associative learning in *Drosophila* is based on the anatomical and functional organization of the MB (Adel and Griffith, 2021; Heisenberg, 2003). The MB is formed by KCs, which receive sensory information from the olfactory pathway via PNs (see section 3.1). Each odor activates only a distinct and sparse subset of KCs, providing a highly specific representation of sensory input (Campbell et al., 2013; Honegger et al., 2011; Siegenthaler et al., 2019; Wang et al., 2004). The axons of KCs form the characteristic MB lobes, which are subdivided into 15 anatomical compartments defined by the dendritic fields of MBONs (Aso et al., 2014a; Hige et al., 2015). MBONs belong to two broad functional categories: approach-mediating and avoidance-mediating neurons, using different neurotransmitters such as acetylcholine, gamma-aminobutyric acid (GABA), or glutamate (Figure 2A, Aso et al., 2014b, 2014a; Modi et al., 2020; Zhang et al., 2019). Approach-promoting MBONs mainly innervate the vertical MB lobes, whereas avoidance-promoting MBONs are located in the horizontal lobes. Each MB compartment is additionally innervated by DANs, which convey information about reinforcement stimuli such as sugar or electric shocks and can be grouped into three major clusters: protocerebral anterior medial (PAM),

protocerebral posterior lateral 1 (PPL1), and PPL2ab (Figure 2B, Mao and Davis, 2009). Rewarding stimuli activate PAM neurons, which mainly innervate compartments associated with avoidance-mediating MBONs (Busto et al., 2010; C. Liu et al., 2012; Mao and Davis, 2009; Yamagata et al., 2015), whereas aversive stimuli activate PPL1 neurons that project to compartments innervated by approach-mediating MBONs (Busto et al., 2010; Claridge-Chang et al., 2009; Mao and Davis, 2009). PPL2ab neurons target the calyx and may modulate plasticity in earlier MB processing stages. A minority of DANs, such as PAM-γ3, deviate from this organization and have been shown to encode punishment (Yamagata et al., 2016).

During conditioning, presentation of the CS^+ activates a specific subset of KCs, while the US activates DANs. The coincidence of KC activity and dopamine release induces compartment-specific synaptic depression of KC>MBON synapses. For aversive conditioning, dopamine release from PPL1. PPL1 neurons selectively weakens the synapse between KCs and approach-mediating MBONs in a compartment-specific manner, thereby reducing their output and shifting behavior toward avoidance. Conversely, during appetitive conditioning, PAM neuron activity weakens KC synapses onto avoidance-mediating MBONs, biasing the overall behavior towards approach.

This principle is described by the balance model, which proposes that MBON activity is balanced in naïve animals and shifted by learning through selective weakening of the KC>MBON synapse (Hige and Turner, 2015). Pairing of CS and US induces synaptic depression, whereas unpaired presentations, in which the US precedes the CS, can result in synaptic potentiation, indicating bidirectional plasticity depending on stimulus timing (Cohn et al., 2015).

Dopamine is the primary neurotransmitter conveying reinforcement signals in *Drosophila*. During aversive conditioning the US information is mediated exclusively by dopamine. During appetitive conditioning signal transmission involves not only dopamine but also octopamine, which is released by octopaminergic neurons (Burke et al., 2012; Guven-Ozkan and Davis, 2014; Schwaerzel et al., 2003). The *Drosophila* genome encodes four dopamine receptors (DopRs): D1R1, D1R2, D2R and DopEcR (Berry et al., 2012; Sun et al., 2020). It is assumed that D1R1 is required for memory acquisition, whereas D1R2 is necessary for forgetting (Berry et al., 2012; Y.-C. Kim et al., 2007).

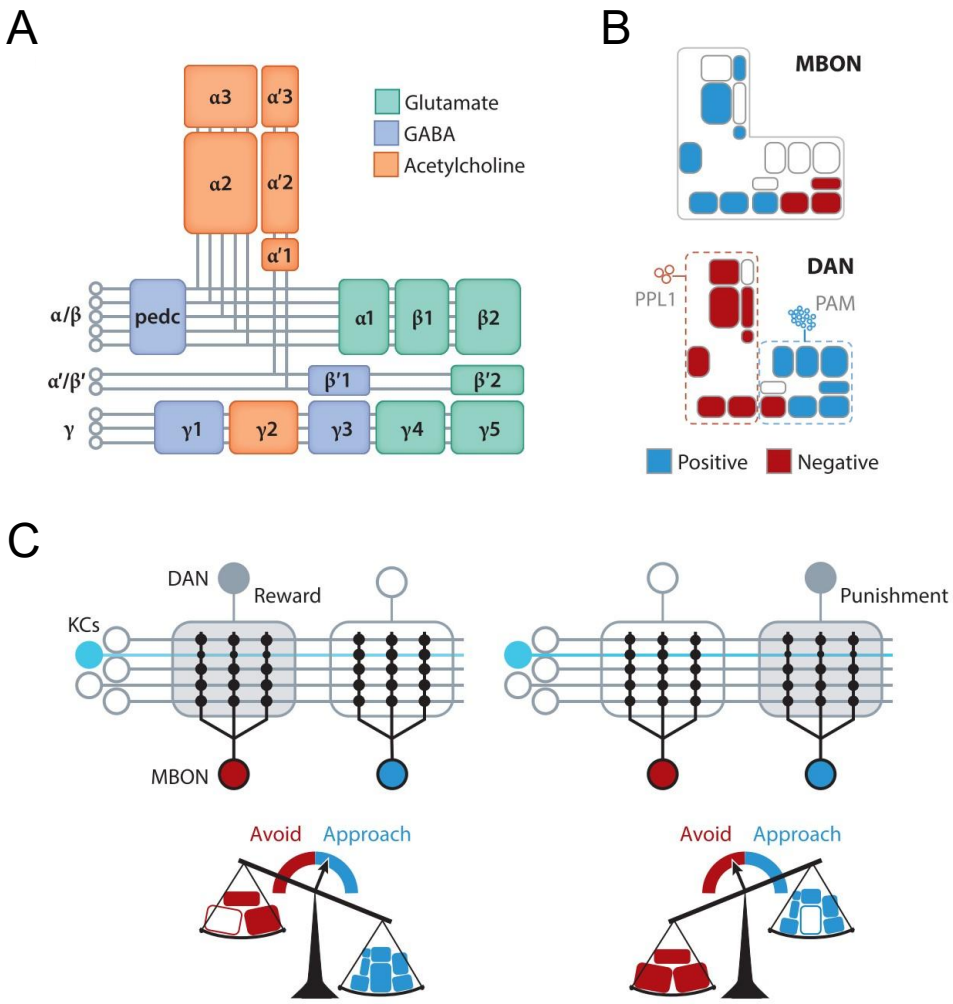


Figure 2: Balance model of associative memory formation.
(A) Schematic representation of the MB lobes with the three main KC types: α/β, α'/β' and γ, as well as the dendritic fields of MBONs. Shown as boxes are the 15 compartments of the MB with their respective designation. The colors indicate the neurotransmitters of the corresponding MBONs. (B) The dendritic arbors of the approach promoting MBONs (blue) mainly innervate the vertical lobe, the avoidance promoting MBONs (red) innervate the horizontal part (upper panel). The PPL1 neurons (red) innervate the vertical lobe of the MB and the PAM neurons (blue) project to the horizontal part of the MB (lower part). White compartments indicate regions for which no clear valence-associated behavioral phenotype has been identified so far. (C) The paired presentation of odor and sugar (reward, left) or shock (punishment, right) during conditioning modulates the KC>MBON synapse. Odor presentation leads to sparse activity of KCs (light blue). During appetitive conditioning, reward-activated PAM neurons release dopamine into a MB compartment innervated by negative valence MBONs. The KC>MBON synapse is depressed, shifting the behavioral balance towards approach. During aversive conditioning, PPL1 neurons release dopamine elicited by punishment into MB compartments innervated by positive valence MBONs. The KC>MBON synapse is depressed, which shifts the balance of behavior towards avoidance. Adapted from Modi et al., 2020.

Plasticity is not limited to the KC>MBON synapse (Figure 2C; Felsenberg et al., 2018; Heisenberg, 2003; Hige et al., 2015; Owald and Waddell, 2015) but may also occur at upstream sites, such as the PN>KC synapse (Kremer et al., 2010; Leiss et al., 2009; Tavosanis, 2012). Furthermore, MBON–MBON interactions and feedback from MBONs to DANs contribute to memory consolidation and retrieval by shaping circuit dynamics (Aso et al., 2014a; Bennett et al., 2021; Cervantes-Sandoval et al., 2017; Takemura et al., 2017).

3.4 The engram

The concept of the engram, originally defined by Richard Semon, describes the physical trace of a memory in the brain (Semon, 1921). In modern neuroscience, engrams are defined as the neuronal substrate of memory, consisting of sparse populations of neurons that are recruited during learning and reactivated during recall (Josselyn et al., 2017; Tonegawa et al., 2015). Their identification relies on four specific criteria: they must be active during memory formation and undergo molecular and functional changes; their artificial activation must be sufficient to trigger recall; their inhibition must block memory expression; and they must represent a minority of neurons specifically responsive to the learned cue (Guan et al., 2016).

To investigate these mechanisms *in vivo*, engram-labeling and manipulating techniques have been established in vertebrate models. These allow both the visualization and targeted manipulation of memory-relevant neuronal populations. One approach relies on activity-dependent expression of transgenes under the control of immediate early genes such as c-fos, enabling reactivation of neurons tagged during learning (Ohkawa et al., 2015; Redondo et al., 2014; Tayler et al., 2013). In fear-conditioning paradigms, artificial activation of such labeled cells can induce behavioral responses that mimic natural memory recall, whereas silencing them disrupts retrieval (X. Liu et al., 2012). Another strategy increases the probability of neuronal recruitment into an engram through elevated CRE binding protein (CREB) levels, thereby enhancing their excitability during learning. Selective ablation of these neurons has been shown to abolish memory expression, highlighting their causal role in storage (Sano et al., 2016; Sekeres et al., 2012; Yiu et al., 2014; Zhou et al., 2009).

In *Drosophila*, the MB is the central brain structure of olfactory learning and memory and thus a primary site for investigating cellular engrams. KCs, the intrinsic neurons of the MB, respond to sensory stimuli such as odors and undergo learning-induced changes in intracellular signaling (Cognigni et al., 2018; Honegger et al., 2011; Yu et al., 2006). Furthermore, their inactivation consistently blocks memory retrieval (Krashes et al., 2007; Miyashita et al., 2018; Siegenthaler et al., 2019; Trannoy et al., 2011), and only a small proportion appears to be reactivated during recall, fulfilling multiple engram criteria (Campbell et al., 2013; Honegger et al., 2011; Miyashita et al., 2018; Siegenthaler et al., 2019; Wang et al., 2004). However, most genetic tools in *Drosophila* target large KC populations rather than sparse subsets, making it difficult to directly test engram sufficiency. To overcome this limitation, Dr. Dominique Siegenthaler, a former member of our lab, developed the CRE-activity-dependent memory engram label (CAMEL)-tool, which enables activity-dependent tagging of putative engram cells (Siegenthaler et al., 2019). CAMEL is based on the activation of the cAMP/CREB signaling pathway during memory formation and uses cAMP responsive element (CRE) -dependent transcription to label neurons that were active during conditioning. By restricting expression to KCs and coupling it to CREB2 activity, CAMEL selectively targets a sparse population of

neurons involved in LTM formation. This allows subsequent visualization and functional manipulation of these cells, providing a powerful approach to study the neuronal basis of memory in *Drosophila*. Altogether, these findings support the notion that memory is not localized in a single structure or molecular event but emerges from the dynamic interaction of sparsely active neurons embedded within larger networks.

3.5 Binary expression system

Binary gene expression systems are widely used to achieve cell type-specific expression of target genes in *Drosophila* melanogaster (Owald et al., 2015b). The Gal4 system is based on the insertion of the yeast transcription factor Gal4 into the fly genome. A tissue-specific promoter or enhancer drives Gal4 expression, and the transcription factor binds to upstream activating sequences (UAS) to induce expression of a downstream target gene (Figure 3A; Brand and Perrimon, 1993). The system consists of two separate components: a driver line providing Gal4 expression and a responder line carrying the UAS-controlled transgene. Upon crossing these lines, Gal4-dependent expression of the effector occurs in the progeny (Duffy, 2002). The modular nature of the Gal4-UAS system enables a wide range of genetic manipulations by combining different driver and effector lines. To further expand targeting possibilities, additional binary systems such as LexA-LexAop and the Q-system have been developed, which function independently of Gal4-UAS and allow parallel manipulation of distinct neuronal populations within the same organism (Kazama, 2015; Lai and Lee, 2006; Potter et al., 2010; Viktorinová and Wimmer, 2007).

To further increase the specificity the Gal4 system was improved by splitting the transcription factor into the deoxyribonucleic acid (DNA) binding domain (DBD) and activation domain (AD). The two parts are independently expressed under control of two different enhancers. Only in cells in which both parts of the transcription factor are present a functional Gal4 can be reconstituted (Figure 3B; Luan et al., 2006; Owald et al., 2015). Based on this principle, the CAMEL-tool was developed to enable activity-dependent targeting of putative engram cells (Bräuler, 2019; Siegenthaler, 2019; Siegenthaler et al., 2019). CAMEL combines the split-Gal4 system with a CREB-dependent reporter to restrict target gene expression to neurons that are both anatomically defined and functionally engaged during memory formation. Specifically, the Gal4-DBD is expressed under control of the MB-specific enhancer R21B06, restricting expression to αβ surface and γ KCs, which are known to be required for LTM(Cervantes-Sandoval et al., 2013; Huang et al., 2013; Isabel et al., 2004). The Gal4-AD is driven by a synthetic promoter containing multiple cAMP response elements (CRE) and is therefore only expressed in cells with active cAMP/CREB signaling (Siegenthaler, 2019; Siegenthaler et al., 2019).

An augmentation of the Gal4-UAS system is the yeast repressor Gal80. The simultaneous expression of Gal80 and Gal4 enables the inhibition of Gal4 and can therefore be used to limit the activity of Gal4 spatially (Figure 3C; Lee and Luo, 1999). The temperature-sensitive variant of Gal80 (Gal80ts) provides temporal control over Gal4-driven gene expression. Below 25°C Gal80 suppresses Gal4 activity. If the temperature is increased to 30°C, Gal80ts inhibition of Gal4 is abolished (McGuire et al., 2003). Temporal control makes it possible to identify the timepoint at which the expression of a transgene causes a certain phenotype. In addition, genes required for development can be inhibited in the adult fly without affecting the animal's viability.

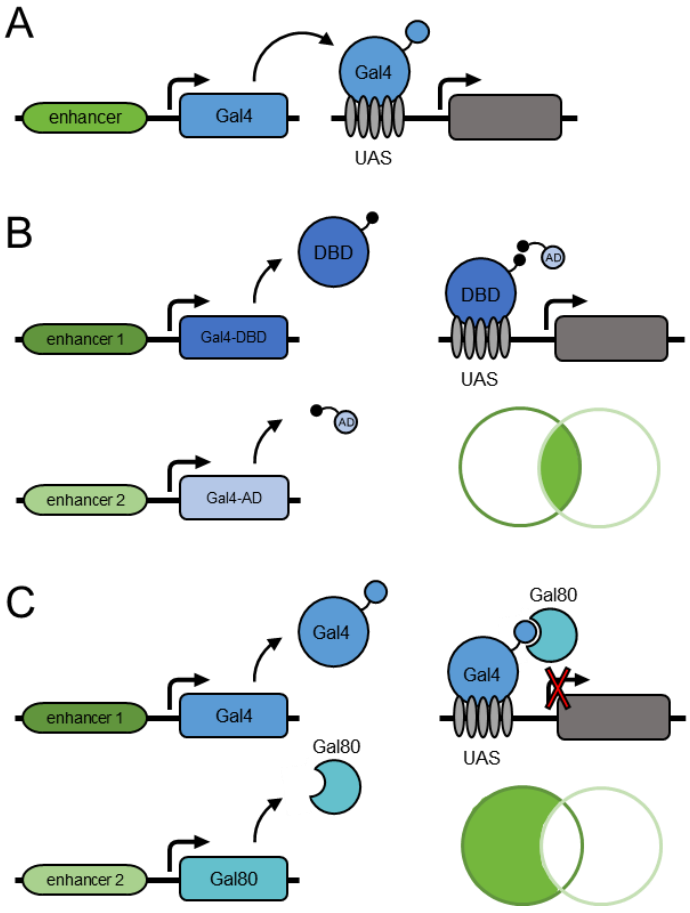


Figure 3: Schematic of the Gal4-UAS binary expression system.
Binary expression systems allow cell-specific, partially temporally inducible expression of effector proteins. (A) The transcription factor Gal4 is controlled by a cell-specific enhancer. The Gal4 protein binds to UAS, which causes expression of the target gene. (B) The specificity of the Gal4-UAS system was increased by splitting the Gal4 transcription factor into two parts, which are controlled by different enhancers. If the AD and DBD fragments are present, a functional Gal4 is reconstituted and the effector is expressed. The two different enhancers enrich specificity, which enables targeted manipulation. (C) The Gal80 repressor can spatially limit Gal4 activity. Gal4 and Gal80 are controlled by two independent enhancers. In cells in which both Gal4 and Gal80 are present, Gal80 suppresses the expression of the target gene by binding to Gal4.

3.6 CREB-signaling pathway

The molecular model of learning and memory during aversive olfactory conditioning is based on the cAMP-signaling pathway in *Drosophila* (Androschuk et al., 2015; Kida and Serita, 2014; Livingstone et al., 1984). The perception of an odor causes neuronal activity of the ORNs and leads to a Ca^{2+} influx in a subset of KCs (Figure 4). The electrical shock leads to PPL1 neuron dependent dopamine release, which activates G-protein coupled DopRs in the vertical lobe of the MB. The simultaneous occurrence of both stimuli induces the activation of Ca^{2+}/calmodulin-sensitive adenylyl cyclase (Levin et al., 1992; Livingstone et al., 1984). Adenylyl cyclase then catalyzes the conversion of adenosine triphosphate to cAMP, increasing intracellular cAMP levels, which in turn activate Protein kinase A (PKA). PKA can modulate synaptic transmission either short-term by altering the conductance of the cell, or long-term via synaptic plasticity (Akalal et al., 2010; Castellucci et al., 1980; Corbin and Krebs, 1969; Kandel, 2012; Riabowol et al., 1988). LTM-dependent structural changes are mediated by the transcription factor CREB2. PKA activates CREB2 through phosphorylation, which allows CREB2 to bind the CRE site of the DNA, inducing protein expression (DeZazzo and Tully, 1995; Kandel, 2012; Widmer et al., 2018; Yin et al., 1994).

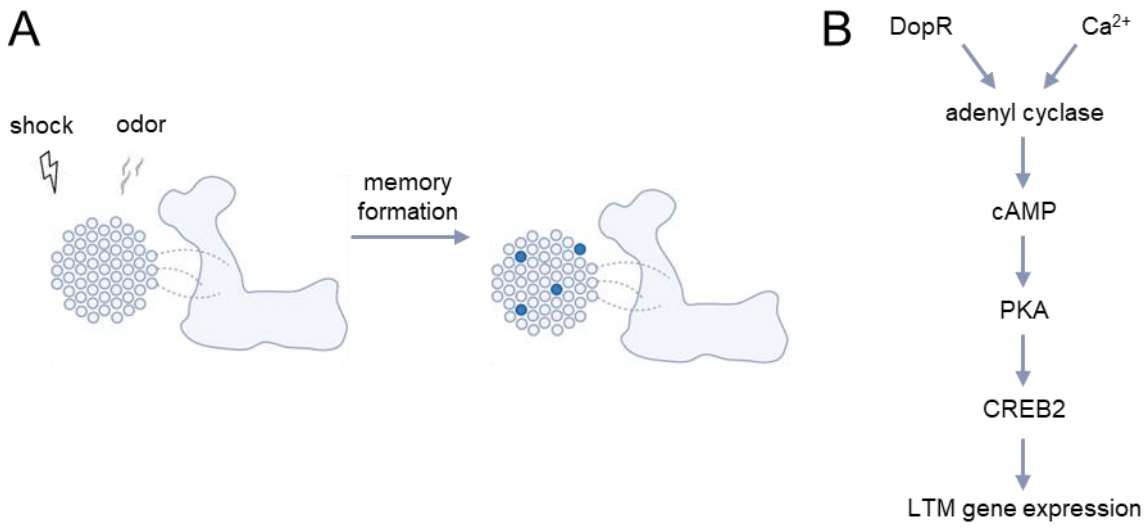


Figure 4: Memory formation in KCs based on the CREB signaling pathway
(A) Schematic of the MB during aversive olfactory conditioning. The simultaneous presentation of electric shock and odor leads to memory formation in a sparse set of KCs resembling engram cells. The CAMEL-tool can e.g. be used to visualize engram cells by expressing enhanced GFP (EGFP). It also enables to manipulate the targeted engram cells. (B) Memory formation is based on the molecular mechanism of the CREB signaling pathway. The adenylyl cyclase is activated by the paired aversive conditioning, which in turn stimulates cAMP synthesis. The increased cAMP levels lead to the activation of PKA, which phosphorylates CREB2. The phosphorylated CREB2 binds to its upstream CRE element, resulting in the expression of LTM genes.

The transcription factor CREB is not only essential for memory consolidation in flies (Miyashita et al., 2018; Siegenthaler et al., 2019; Widmer et al., 2018; Yin et al., 1994), but also in a variety of other animal models, such as *Caenorhabditis elegans* (Amano and Maruyama, 2011), *Aplysia* (Dash et al., 1990; Kandel, 2012) and vertebrates (Brightwell et al., 2005; Gass et al., 1998; Kida et al., 2002), highlighting its evolutionarily conserved role in memory formation. This central role makes CREB activity a suitable entry point for identifying neurons involved in memory encoding.

Based on this principle, CAMEL-tool was developed to enable activity-dependent tagging of putative engram cells (Bräuler, 2019; Siegenthaler, 2019; Siegenthaler et al., 2019). During associative olfactory conditioning, simultaneous odor-induced Ca^{2+} influx and dopaminergic input triggered by reinforcing stimuli, such as sugar or electric shocks, activate adenylyl cyclase in KCs. Subsequently, cAMP levels increase resulting in activation of PKA, and phosphorylation of CREB2. This induces transcription of memory-related genes and drives expression of the Gal4-AD under the control of CRE elements. Functional Gal4 is therefore reconstituted only in αβ surface and γ KCs in which CREB signaling is active, resembling putative LTM engram cells, thereby enabling their specific labeling or manipulation via UAS-controlled effector genes.

3.7 FUNCAT

Although scientists have made progress in identifying the engram by allocating small cell populations to specific memories, the question of which molecules cause the cellular and molecular changes remains unclear. Therefore, it is of great interest to investigate proteomic changes during memory consolidation. However, it is difficult to identify newly synthesized proteins because old and new proteins are chemically indistinguishable (Dieterich et al., 2010). To enable differentiation proteins must be labeled conditionally or in an inducible fashion. The revolutionary invention of click chemistry provides the basis to label newly synthesized proteins. The term click chemistry refers to stereospecific reactions that are modular, and wide in scope. They take place under simple reaction conditions, deliver a high yield of a stable product and only harmless byproducts (Kolb et al., 2001). Click chemistry has rapidly expanded and evolved as an important tool across disciplines (Agard et al., 2004; Saleh et al., 2019). Scientists have succeeded in incorporating click chemistry into the cellular translational apparatus via non-canonical amino acids (ncAAs; Link et al., 2003; Ngo et al., 2009). Protein biosynthesis is divided into two sub-processes. During transcription, messenger ribonucleic acid (mRNA) is synthesized based on the DNA sequence of a gene in the nucleus. The enzyme RNA polymerase binds to the DNA, unwinds the double helix, and synthesizes mRNA by moving along the DNA and adding complementary RNA nucleotides to the DNA template. At the end of transcription, the mRNA is released and moves into the cytoplasm, and the double helix closes again. The subsequent process, translation, takes place at the ribosomes and

translates the mRNA into an amino acid sequence. In the cytoplasm, aminoacyl-transfer RNA (tRNA) synthetases load the amino acids onto the appropriate tRNA. The ribosome assembles around the mRNA. Each tRNA has an anticodon that is complementary to a mRNA codon (base triplet). The ribosome catalyzes the formation of peptide bonds between the amino acids, causing the polypeptide chain to grow. At the end of translation the ribosome releases the polypeptide. The ribosomal complex remains intact and moves on to the next mRNA to be translated (Girbig et al., 2022; Scheper et al., 2007; Webster and Weixlbaumer, 2021).

In this process, a ncAA carrying a click chemistry group is introduced into a host system. In the host cells, ncAAs compete with the native amino acids to be bound to an aminoacyl-tRNA synthetase. This enzyme then loads the ncAA onto the corresponding tRNA. In the ribosome, the ncAA is bioorthogonally incorporated into the growing polypeptide chain. Small molecular probes such as affinity markers can then bind to the ncAA-containing proteins by means of click chemistry reaction (Saleh et al., 2019).

In 2010 fluorescent non-canonical amino-acid tagging (FUNCAT) was introduced, which allows *in situ* visualization of newly synthesized proteins (Figure 5). Methionine analogs azidohomoalanine (AHA) and homopropargylglycine (HPG) were used as ncAAs. The binding kinetics of AHA and HPG to methionyl-tRNA synthetase (MetRS) are slower than that of methionine. But sufficiently fast that both ncAAs are loaded onto methionine tRNA by endogenous MetRS and are incorporated into the growing polypeptide chain. They synthesized fluorescent tags that bind to AHA and HPG using copper-catalyzed [3+2] azide-alkyne cycloaddition (click chemistry; Dieterich et al., 2010; Kiick et al., 2002). Tracking nascent proteins with AHA and HPG has already been applied in various systems such as *Escherichia coli* (Kiick et al., 2002; Ngo et al., 2009), mammalian cell culture and slices (Beatty et al., 2006; Beatty and Tirrell, 2008; Dieck et al., 2012; Mockett et al., 2019; Ngo et al., 2009; Tcherkezian et al., 2010), *Xenopus* cell culture (Yoon et al., 2012), *Drosophila* (Deal et al., 2010; Niehues et al., 2015), larval zebrafish (Hinz et al., 2012) and mice (Du et al., 2021).

The FUNCAT technique is a powerful tool to study proteomic changes. However, ncAA incorporation does not allow cell type-specific resolution, since MetRS incorporates AHA and HPG, respectively, into proteins in any cell. Tirrell and colleagues found MetRS mutants that were able to integrate ncAA into nascent proteins, allowing cell specificity for FUNCAT experiments (Link et al., 2006). The point mutation L262G replaces leucine with glycine within MetRS ($MetRS^{L262G}$). This mutation leads to an altered binding site that allows azidonorleucine (ANL) to be loaded onto the methionine tRNA and enables incorporation of ANL into nascent proteins instead of methionine in *Drosophila melanogaster*. The red-fluorescent dye Tetramethylrhodamine (TAMRA) was used to visualize the newly synthesized proteins. The alkyne tag of TAMRA binds the azide group of ANL by cycloaddition (Erdmann et al., 2015; Niehues et al., 2015).

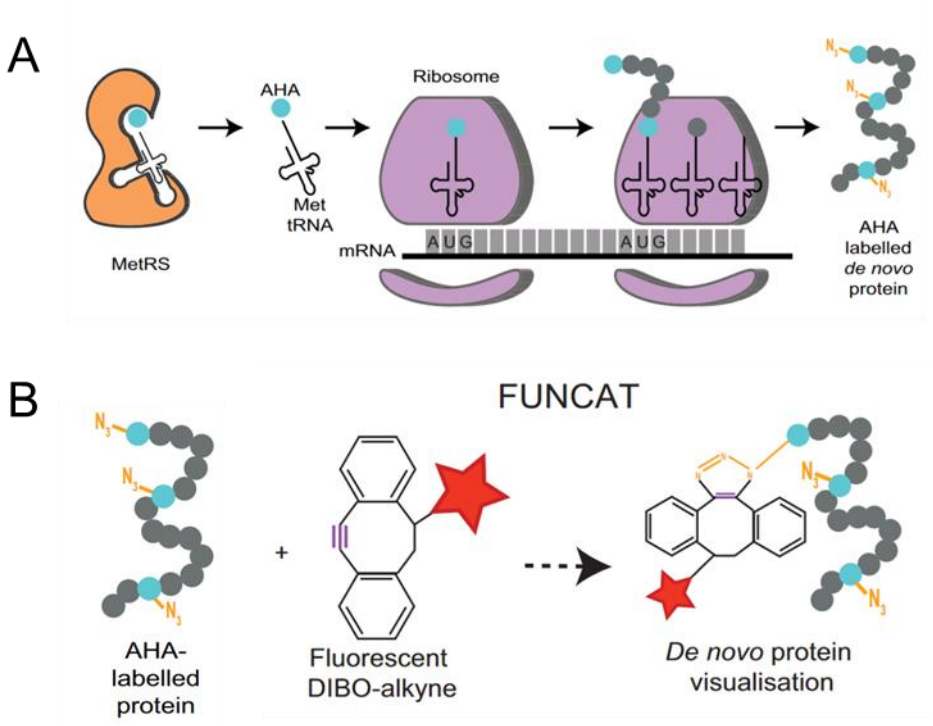


Figure 5: Schematic of FUNCAT technique.
(A) The enzyme MetRS (orange) catalyzes the binding of methionine or the methionine analog AHA (blue) to the methionine tRNA. During translation, the ribosome (purple) migrates along the mRNA until it recognizes the start codon AUG. With its matching anti codon, the methionine tRNA binds to the mRNA. Methionine respectively AHA is incorporated into the growing polypeptide strand repeatedly. (B) The azide group (orange) of AHA binds covalently to the alkyne group (purple) of the fluorescent tag. Thus, the *de novo* proteins are visualized. Modified from (Evans et al., 2020).

In a next step, targeted expression of mutant MetRS in engram cells can be used to visualize proteomic changes during memory formation. The CAMEL-tool, for example, offers the possibility of tagging memory engram cells (Siegenthaler et al., 2019). When FUNCAT is combined with the CAMEL-tool, newly synthesized proteins are exclusively tagged in engram cells; these proteins are potentially involved in LTM formation. However, since FUNCAT labels all newly synthesized proteins unspecifically, it does not allow to identify the labeled proteins. For protein identification, bioorthogonal non-canonical amino acid tagging (BONCAT) must be used. This approach differs little from FUNCAT, only an alkyne affinity tag is used instead of an alkyne fluorescent tag. The affinity-tagged proteins can then be quantified through immunoblot analysis or separated by affinity purification and identified using mass spectrometry (Dieterich et al., 2006; Hinz et al., 2013).

3.8 Aim of the thesis

A major goal of modern neuroscience is to elucidate the cellular and molecular mechanisms of memory formation, consolidation, and maintenance which largely relies on the ability to manipulate memory engram cells. To specifically label and manipulate memory engram cells, a former member of the group, Dr. Dominique Siegenthaler, developed the CAMEL-tool during his PhD thesis (Siegenthaler et al., 2019). We previously showed that removal of the food odor during fly raising resulted in a reduced number of labeled CAMEL cells (Siegenthaler et al., 2019). We concluded that CAMEL-activity depends on olfactory experience and probably reflects natural memory formation. Whether CAMEL positive cells could represent the memory engrams beyond olfaction remains to be known. Hence, first aim of this thesis was to understand the behavioral and cellular changes that might occur in response to environmental influences such as social interaction, and upon deprivation and enhancement of sensory stimuli.

Further, the long-lasting phase of memory formation has been shown to depend upon regulated protein expression (Davis and Squire, 1984; Rosenberg et al., 2014). Hence, the second aim of this thesis was to unravel whether CAMEL positive cells result in LTM related protein synthesis. This was done by deploying FUNCAT technique to identify *de novo* proteins (Dieterich et al., 2010).

The third aim of this thesis was to establish artificial conditioning in *Drosophila* melanogaster by replacing CS with optogenetic activation of CAMEL neurons.

Lastly, this thesis focused on characterizing light-activatable DopRs and elucidating their role in memory formation. To this end, genetically engineered DopRs were expressed in KCs and optogenetically activated to assess whether targeted DopR signaling is sufficient to induce memory-relevant plasticity.

4. Materials and methods

4.1 Buffers, solutions and media

The source of the chemicals used is indicated in the main text when they were first mentioned. If no manufacturer is indicated, chemicals were either obtained from the chemical dispensary of the TU Kaiserslautern or multiple manufacturers were used, as this did not alter the efficiency of the experiments.

The pH of the solutions was buffered using sodium hydroxide or hydrochloride acid, unless stated otherwise.

4.1.1 Standard fly food

The fly food was prepared by the animal house of the TU Kaiserslautern. For a total volume of 45 l fly food, 180 g filamentous agar (Serva) and 120 g USB agar (Biomol) were dissolved in 15 l boiling water. Afterwards, 721.5 g dry yeast (Fala), 393 g potassium sodium tartrate, 33 g Calcium chloride, 1420.5 g sucrose (Roth), 2838 g glucose and 1490 g cornmeal (NewStart Center) were added and boiled for 20 min. By adding cold water, the food was cooled down to 55 °C. Then, water was added until the final volume of 45 l was reached. Subsequently 160 ml propionic acid, 96 g nipagin (Roth/Sigma-Aldrich) and 300 ml ethanol were added. The food was portioned into standard food vials or bottles, sealed, and stored at 4 °C.

4.1.2 Odor-free food

The odor-free food contained 2 % agarose (VWR) and 1 M D-sorbitol (Sigma-Aldrich). To prepare the food, 1 g of agarose was added to 50 ml of tap water and briefly heated in a microwave until the agarose was completely dissolved. To ensure that the food remained liquid, it was kept on a magnetic stirrer at approximately 80 °C. Then, 9.11 g of D-sorbitol were added and stirred until fully dissolved. Finally, the food was poured into sterile 5 ml reaction vials and stored at 4 °C.

4.1.3 Retinal food

For optogenetic activation, Chrimson channels require the cofactor all-trans-retinal (Sigma-Aldrich) and D1R1 9-cis-retinal (Sigma-Aldrich). The flies ingested the respective retinal via the food, except for appetitively conditioned flies. They received the retinal in water to maintain their starvation state. First, a stock solution of 100 mM all-trans-retinal and 50 mM 9-cis-retinal was prepared in 100 % ethanol. These stock solutions were wrapped in aluminum foil and stored at -20 °C. To prepare the retinal food, standard fly food was heated in a microwave until

it was completely liquefied. It was then cooled to approximately 40 °C with constant stirring on the magnetic stirrer. Then, 0.4 mM all-trans or 9-cis-retinal were added and stirred to ensure an even distribution of the retinal. The retinal food was poured into food vials or bottles, allowed to cool in the dark and sealed with foam plugs. It was stored in the dark at 4 °C.

4.1.4 Phosphate buffered saline (PBS)

To prepare 1 l of 10x PBS, 50 PBS tablets (Sigma-Aldrich) were dissolved in 800 ml distilled water, and the final volume was filled up to 1 l and the solution was autoclaved. Due to use of the tablets, the pH was always between 7.2 and 7.6. For 1x PBS, the stock solution was diluted 1:10 with distilled water and stored at room temperature (RT). The FUNCAT reaction requires an exact pH value of 7.4 or 7.8; the pH of the 1x PBS was adjusted for this purpose.

4.1.5 PBS with Triton X-100 (PBST)

1 ml (for 0.1 %), 2 ml (for 0.2 %) or 5 ml (for 0.5 %) Triton X-100 (Sigma-Aldrich) were added to 1 l 1x PBS. The mixture was heated to about 70 °C on a magnetic stirrer until the Triton X-100 was completely dissolved. The solution was then stored at RT. The pH of the 0.1 % PBST was buffered to 7.8 for the FUNCAT protocol. For the other solutions, no further adjustments were made to the pH value.

4.1.6 PBS with Tween-20

The FUNCAT protocol requires PBS with Tween-20 (VWR) in addition to the PBST already described. For 1 l, 1 ml of Tween-20 was dissolved in 1 l of 1x PBS at pH 7.4.

4.1.7 Paraformaldehyde (PFA) in PBS

The preparation of PFA took place exclusively under the fume hood. For 100 ml 4 % PFA (Sigma-Aldrich), 50 ml distilled water and 4 g PFA were added to a measuring beaker. The mixture was stirred on a magnetic stirrer at a maximum of 60 °C until PFA dissolved completely. Then, 10 ml of 10x PBS were added, the solution was cooled down and the pH was adjusted to 7.4. Next, the solution was filtered, and distilled water was added until the final volume of 100 ml was reached. Lastly, 10 ml aliquots were prepared and stored at -20 °C. The old labeling protocol requires the addition of 0.2 % Triton X-100.

4.1.8 Hemolymph-like physiological solution (HL3)

The HL3 solution was adapted to the recipe of Stewart et al., 1994, except for $MgCl_2$, the ion concentrations of all components were identical. Stock solutions of 1 M NaCl, 0.5 M KCl, 0.5 M HEPES (Fluka), 0.5 M trehalose (Sigma-Aldrich), 1 M $CaCl_2$ and 1 M $MgCl_2$ were prepared first. The stock solutions simplify the preparation of HL3 as they can be stored long-term at 4 °C and only $NaHCO_3$ and sucrose need to be weighed in. For 250 ml HL3, 200 ml distilled water was poured into a graduated cylinder. Successively, 17.5 ml NaCl, 2.5 ml KCl, 2.5 ml HEPES, 0.21 g $NaHCO_3$, 2.5 ml trehalose, 9.84 g sucrose, 0.357 ml $CaCl_2$ and 2.5 ml $MgCl_2$ were added. Then, the final volume was adjusted to 250 ml with distilled water and the solution was buffered to a pH of 7.2. HL3 was stored at 4°C and used for one to two weeks.

4.1.9 PFA in HL3

PFA was prepared under a fume hood. To manufacture 80 ml of 2 % PFA, 10 ml of 16 % PFA (Alfa Aesar) were added to 70 ml HL3. The solution was mixed on the magnetic stirrer and stored in 10 ml aliquots at -20 °C.

4.1.10 Normal goat serum (NGS)

For the old labeling protocol, 1 ml of NGS (BIO-RAD) was diluted in 9 ml of 0.2 % PBST. For improved labeling protocol, 500 µl were diluted in 9.5 ml 0.5 % PBST. Both solutions were stored at -20 °C.

4.1.11 Poly-L-lysine hydrobromide (PLL)

PLL (Sigma Aldrich) was dissolved in distilled water to a concentration of 1 mg/ml, and stored at -20 °C. To prepare the 0.078 % (w/v) solution for coverslip coating, 3 ml of the stock were mixed with 846 µl of milliQ water and 7.7 µl of Photo-Flo (Kodak Photo-Flo 200 Solution) by shaking or vortexing. The solution was transferred to a brown glass bottle, stored in a light-tight box at 4 °C, and used within three months.

4.1.12 B-Block

To prepare 100 ml of B-Block, 50ml 1x PBS were measured in a graduated cylinder. 10 ml normal horse serum (Sigma-Aldrich), 5 g sucrose and 2 ml bovine serum albumin (Roth) were added. The final volume was filled up to 100 ml and the solution was filtered. Aliquots of 10 ml were stored at -20 °C. Before usage, 50 µl Triton X-100 per aliquot were added. The solution was used for up to five days.

4.1.13 PFA lysine phosphate buffer (PLP-fix)

Two stock solutions were prepared for the PLP-fix, which could be stored at 4 °C for a long time. The ready-to-use PLP-fix, on the other hand, could only be stored for up to one week. The first stock solution was lysine phosphate buffer: for 100 ml, 3.66 g of lysine monohydrochloride (Sigma-Aldrich) were added to 100 ml distilled water and the pH was buffered to 7.4 with 0.1 M disodium phosphate (Sigma-Aldrich). The second solution was PFA: 0.54 g of glucose were weighed into 10 ml of 16 % PFA and the solution was mixed. Finally, three parts of the lysine phosphate buffer were mixed with one part of PFA and 0.01 M sodium periodate (Acros Organics, Thermo Fisher) were added.

4.1.14 PBS with dimethyl sulfoxide, Triton and Tween (PBS-DTT)

To prepare 5 ml of PBS-DTT, 5 ml of 1x PBS pH 7.4 were measured and 50 µl of dimethyl sulfoxide (DMSO, Fluka), 125 µl of Triton-X100 and 5 µl of Tween-20 were added. The solution could be stored at RT for up to one week.

4.1.15 FUNCAT Solution

The FUNCAT solution always had to be prepared immediately before usage. 200 mM tris[(1-benzyl-1H-1,2,3-triazol-4-yl) methyl]amines (TBTA, Alfa Aesar, Thermo Fisher) were dissolved in DMSO and stored in 2-5 µl aliquots at -20 °C. 2 mM 5/6 carboxytetramethylrhodamine-PEG4-alkyne, acetylene-fluor 545 (TAMRA, Jena Bioscience) were dissolved in DMSO and also stored in 2-5 µ aliquots at -20 °C. 200 mM Copper(II) sulphate pentahydrate (Sigma-Aldrich) and 500 mM Tris(2-carboxyethyl) phosphine hydrochloride (TCEP, Sigma-Aldrich) were each dissolved in LC-MS grade water (Fisher Scientific, Thermo Fisher) prior to application of the FUNCAT solution.

Single components as well as the FUNCAT solution were protected from light. 1 µl of 20 mM TBTA was added to 1 ml 1x PBS pH 7.8, the solution was vortexed for 10 s at 2,700 rpm. Then, 1 µl of 500 mM TECEP was added and vortexed for another 10 s. Next, 1 µl of 2 mM TAMRA was added and vortexed for 10 s. Last, 1 µl of 200 mM Copper(II) sulphate pentahydrate was added to the solution and vortexed for 30 s.

4.1.16 FUNCAT washing buffer

10 µl 0.25 M ethylenediaminetetraacetic acid (EDTA, Roth) and 50 µl Tween-20 were dissolved in 1x PBS pH 7.8. The solution was stored at RT and was used for a maximum of four days.

4.2 Experimental animals

4.2.1 Fly breeding

All flies were bred on standard fly food in incubators with day-night lighting (12 h/ 12 h) and constant humidity of 70 %. Stocks were kept in an 18 °C incubator or at RT with unregulated humidity. The original fly stocks used in this study are listed in Table 1. The stocks were used to generate experimental genotypes in Table 2.

Table 1: Fly stocks.
Listed are all fly stocks used in this thesis. If available, the corresponding Bloomington *Drosophila* Stock Center (BDSC) number and the original source are mentioned.

genotype	BDSC number	source
10xUAS-myr::tdTomato	32223	Pfeiffer et al., 2010
10xUAS-mCD8::GFP	32186	Pfeiffer et al., 2010
20xUAS-Chrimson$_{VENUS}$	55135	Klapoetke et al., 2014
2xUAS-EGFP	23867	Halfon et al., 2002
6xCRE-splitGal4$^{AD\ attP2}$	-	Siegenthaler et al., 2019
6xCRE-splitGal4^{AD} $_{VK00027}$	-	Siegenthaler, 2019; Zhou et al., 2023
elav-splitGal4^{AD}	23868	Luan et al., 2006
elav-splitGal4^{DBD}	23867	Luan et al., 2006
Gr66a-Gal4	-	Scott et al., 2001
MB077B Gal4	-	Aso et al., 2014a
OK107-Gal4	854	Lee et al., 1999
R21B06-splitGal4^{DBD} (MB364B)	68318	Aso et al., 2014b
tub-Gal80^{ts}	7019	McGuire et al., 2004
UAS-D1R2-V2	-	Zhou et al., 2023
UAS-D1R1-V2	-	Zhou et al., 2023
UAS-D1R1-RNAi	-	Zhou et al., 2023
UAS-MetRS^{L262G}-EGFP	-	Erdmann et al., 2015
wild type (2U)	-	Tully et al., 1994

If large quantities of virgins were needed (300-400 virgins per week) the fly stocks were kept at 18 °C overnight. Crossings of experimental genotypes were stored at 28 °C until the first filial generation reached the third instar larval stage. Crosses containing a temperature-sensitive component were shifted to 20 °C to prevent uncontrolled activation, all other crosses were shifted to 22 °C.

Table 2: Experimental genotypes.
Listed are the designations of the experimental flies, their exact genotype with breakdown of chromosomal expression of all components, and the corresponding figure.

designation	genotype	figure
6xCRE^{AD} ∩ elav^{DBD} > EGFP	w^- ; $\frac{20xUAS-6xGFP}{+}$; $\frac{elav-splitGal4^{DBD}}{6xCRE-splitGal4^{AD}}$; +	12B
elav^{AD} ∩ R21B06^{DBD} > EGFP	w^- ; $\frac{2xUAS-EGFP}{+}$; $\frac{elav-splitGal4^{AD}}{R21B06-splitGal4^{DBD}}$; +	12C
6xCRE^{AD} ∩ R21B06^{DBD} > EGFP	w^- ; $\frac{2xUAS-EGFP}{+}$; $\frac{6xCRE-splitGal4^{AD}}{R21B06-splitGal4^{DBD}}$; +	12D, 13-15, 17, 18-20
6xCRE^{AD} ∩ R21B06^{DBD} > Chrimson	w^- ; $\frac{20xUAS-Chrimson^{VENUS}}{+}$; $\frac{6xCRE-splitGal4^{AD}}{R21B06-splitGal4^{DBD}}$; +	16, 17, 23, 26, 27
OK107-Gal4 > MetRS^{L262G}-EGFP	w^- ;+; $\frac{UAS-MetRS^{L262G}-EGFP}{+}$; $\frac{OK107-Gal4}{+}$	21A
elav^{AD} ∩ R21B06^{DBD} > MetRS^{L262G}-EGFP	w^- ; $\frac{2xUAS-EGFP}{+}$; $\frac{elav-splitGal4^{AD}}{R21B06-splitGal4^{DBD},UAS-MetRS^{L262G}-EGFP}$; +	21B
6xCRE^{AD} ∩ R21B06^{DBD} > MetRS^{L262G}-EGFP	w^- ; $\frac{2xUAS-EGFP}{+}$; $\frac{6xCRE-splitGal4^{AD},UAS-MetRS^{L262G}-EGFP}{R21B06-splitGal4^{DBD},UAS-MetRS^{L262G}-EGFP}$; +	22
Gr66a > Chrimson	w^- ; $\frac{20xUAS-Chrimson^{VENUS}}{Gr66a}$; $\frac{+}{+}$; +	24A, 25, 26
MB077B > Chrimson	w^- ; $\frac{20xUAS-Chrimson^{VENUS}}{MB077B}$; $\frac{MB007B}{+}$; +	24B, 25
OK107-Gal4 > mCD8-GFP	w^- ;+; $\frac{10xUAS-mCD8-GFP}{+}$; $\frac{OK107-Gal4}{+}$	28A
OK107-Gal4 > DopR	w^- ;+; $\frac{DopR}{+}$; $\frac{OK107-Gal4}{+}$	28B-C
6xCRE^{AD} $_{VK27}$ ∩ R21B06^{DBD} >myr-tdTomato ∩ DopR	w^- ; $\frac{DopR}{UAS-CD4tdTomato}$; $\frac{6xCRE-splitGal4^{AD}\,VK27}{R21B06-splitGal4^{DBD}}$; +	29
OK107-Gal4 ∩ tub-Gal80^{ts} > wild type	w^- ;+; $\frac{+}{tub-Gal80^{ts}}$; $\frac{OK107-Gal4}{+}$	30B-C
wild type > D1R1-RNA$_i$	w^- ;+; $\frac{D1R1-RNAi}{tub-Gal80^{ts}}$; $\frac{OK107-Gal4}{+}$	30B
OK107-Gal4 ∩ tub-Gal80^{ts} > D1R1-RNA$_i$	w^- ;+; $\frac{D1R1-RNAi}{tub-Gal80^{ts}}$; $\frac{OK107-Gal4}{+}$	30B
wild type > Dop1R1-V2	w^- ;+; $\frac{UAS-D1R1-V2}{+}$; +	30C
OK107-Gal4 ∩ tub-Gal80^{ts} > Dop1R1-V2	w^- ;+; $\frac{UAS-D1R1-V2}{tub-Gal80^{ts}}$; $\frac{OK107-Gal4}{+}$	30C, 31

4.2.2 ANL feeding

FUNCAT experiments required ANL feeding, it serves as an unnatural amino acid that is incorporated into newly synthesized proteins instead of methionine (supplied by the Dieterich lab, Institute of pharmacology and toxicology, Otto-von-Guericke-Universität, Magdeburg). A 100 mM stock solution of ANL in distilled water was prepared and stored at 4 °C for up to ten days. A 10 mM solution was prepared by dilution from this stock solution and mixed into a yeast paste made from dry yeast. For the application of the yeast paste, a Whatman paper was placed on top of the food within a standard food vial. 72 h before the experiment, a small amount of yeast paste was spread on the Whatman paper, allowing flies to ingest the ANL.

4.3 Immunohistochemistry

During this work, the immunohistochemical labeling protocol for adult brain dissections was improved, resulting in different protocols being used at the beginning and end of this thesis. Which protocol was used in each experiment is indicated in the results section. The antibodies and their dilutions did not change and are listed in Table 3.

Table 3: List of antibodies.
Listed are the used primary and secondary antibodies used, their manufacturer, and their dilution.

antibody	manufacturer	dilution
rabbit anti Dlg	Pielage Lab	1:30,000
rabbit anti DsRed	Takara Bio Inc.	1:2,000
rabbit anti-GFP	Thermo Fisher	1:2,000
mouse anti-Brp (nc82)	Developmental Studies Hybridoma Bank	1:200
mouse anti Rhodopsin	Thermo Fisher	1:1,000
mouse anti TAMRA	Thermo Fisher	1:1,000
guineapig anti Dlg	Davids Biotechnologie GmbH	1:1,000
goat anti guineapig Alexa 647	Thermo Fisher	1:1,000
goat anti-mous Alexa 488	Thermo Fisher	1:1,000
goat anti-mouse Alexa 568	Thermo Fisher	1:1,000
goat anti-rabbit Alexa 488	Thermo Fisher	1:1,000
goat anti rabbit Alexa 594	Thermo Fisher	1:1,000

4.3.1 Old immunohistochemical labeling protocol

Male flies were fixed at 4 °C in 4 % PFA + 0.2 % Triton X-100 for 3.5 h. To remove the fixative, flies were washed three times for 30 min with 0.2 % PBST. The brains were dissected in 0.2 % PBST and up to 20 brains were transferred into one 0.5 ml reaction tube. Subsequently, the brains were blocked in 10 NGS for 15 min at RT. The brains were incubated with primary antibodies in 1 % NGS at 4 °C for at least two days. Excess antibody was washed out at RT with 0.2 % PBST six times for 30 min each. Next, secondary antibodies were applied in 0.2 % PBST in the dark at 4 °C for two days. After incubation, the remaining secondary antibodies were again washed out six times for 30 min at RT before the brains were mounted in Vectashield (Vector Laboratories).

4.3.2 Improved immunohistochemical labeling protocol

The following labeling protocol was established in collaboration with Nina Wilhelmy by combining different protocols from the Janelia Research Campus (IHC – double-label protocol, 2% PFA fixation protocol and dibutylphthalate polystyrene xylene (DPX) mounting protocol: https://www.janelia.org/project-team/flylight/protocols) to improve the quality of immunohistochemical labeling.

Since the flies were dissected unfixed, both the forceps and the dissecting solution (HL3) were kept on ice. In addition, three block dishes, one filled with 70 % ethanol and two filled with HL3, were placed on ice. Flies were first immersed in ethanol and then in HL3 before dissection.

A 20 min alarm was started with the beginning of the first immersion. After 20 min, all dissected brains (up to a maximum of 20) were transferred to a 1.5 ml low-binding reaction tube. The brains were immediately fixed with 2 % PFA for 1 h at RT. PFA was removed by washing four times for 10 min with 0.5 % PBST at RT. If necessary, brains could be stored at 4 °C in 0.5 % PBST for up to 3 days. Brains were blocked with 5 % NGS on a horizontal shaker (200 rpm) for 1.5 h. Next, brains were incubated in primary antibodies for 4 h at RT. Afterwards the brains were shifted to 7-8 °C, where they remained for 2-3 nights. Unbound antibodies were removed by washing three times for 30 min with 0.5 % PBST. Secondary antibodies were also diluted in 5 % NGS and incubated for 4 h at RT followed by 2-3 nights at 7-8 °C. Excess antibodies were removed by washing three times for 30 min in 0.5 % PBST at RT. Afterwards, the brains could either be directly mounted in Vectashield, or, to improve the quality of the labeling, be dehydrated in an ascending ethanol series and cleared in xylene. This step can be performed up to three days after removal of the secondary antibody solution, by storing the brains at 4 °C in 0.5 % PBST. Before dehydration, the brains were fixed a second time for 4 h at RT in 4 % PFA. Residues of the fixative were removed by washing four times in 0.5 % PBST at RT. If necessary, the brains could be stored in 0.5 % PBST at 4 °C for up to three days.

Afterwards, the brains were washed in 1x PBS for 10 min and mounted on PLL-coated coverslips. Next, the coverslips were immersed in fresh milliQ water. Then, the coverslips were incubated in the ascending ethanol series (15 %, 30 %, 50 %, 75 %, 95 %, 100 %, 100 %, and 100 %) for 10 min each. The last step in 100 % ethanol could be extended up to 30 min. Dehydration was followed by clearing under the fume hood using xylene. The coverslips were incubated sequentially in three containers with xylene for 5 min each. Then, approximately five drops of DPX (Sigma-Aldrich) were applied to the coverslip and, after 30 s, placed upside down on a microscope slide with spacers. After another 30 s, the coverslip was pressed down gently. To dry out, the slides were kept in the fume hood for one day. The DPX must be allowed to dehumidify for at least 48 h before microscopy.

4.3.3 FUNCAT labeling protocol

The FUNCAT technique has already been used to visualize newly synthesized proteins in mammalian cells (Dieck et al., 2012; Du et al., 2021; Hinz et al., 2013). The method has also been established in *Drosophila* (Erdmann et al., 2015; Marter et al., 2019; Niehues et al., 2015) however, thus far no reports of a labeling protocol in adult flies have been reported. I visited the Dieterich lab at the Institute of Pharmacology and Toxicology at the Otto-von-Guericke University in Magdeburg to learn the larval FUNCAT protocol and to apply it to adult brain dissections. In collaboration with Nina Wilhelmy, we developed the following protocol in our laboratory. Unfixed brains were dissected in PBS (pH 7.4). Using a brush, up to four brains were transferred into one PBS-containing well of a well-plate (Nunc MicroWell MiniTrays containing 60 wells, Thermo Fisher). After all brains had been dissected, the labeling protocol was carried out in the well plate. For this purpose, 20 µl of the required solution was transferred into the next well and the brains were transferred into the well with a brush. All incubation steps were performed in a darkened box with water-soaked cloths at RT to prevent evaporation of the small volume of solution. A horizontal shaker (100 rpm) was used to ensure uniform exposure of the brains to the solutions. As a first step, the brains were fixed in PLP-fix for 20 min. Then, the fixative was removed by washing twice in PBS with Tween-20 for 5 min followed by three 5 min washes in PBS-DTT. After that, the brains were blocked in B-Block for 3 h. This was followed by three 10 min washing steps with 0.1 % PBST. Next, freshly prepared FUNCAT solution was applied and incubated overnight. The next morning, the residual FUNCAT solution was removed by washing four times for 20 min with FUNCAT wash buffer. Two additional 10 min washes with PBS containing Tween-20 followed before the primary antibodies were incubated in B-Block at 4 °C overnight. The residues of the antibodies were removed by washing three times in PBS with Tween-20 for 15 min. Subsequently, the secondary antibodies were incubated in B-Block for 1 h. This was followed by washing 3 times

for 15 min in PBS containing Tween-20. Two additional 10 min washes with PBS (pH 7.4) followed. Finally, the brains were embedded in Vectashield.

4.3.4 Quantification and microscopy

Immunohistochemical labeling was used to determine the number of CAMEL-positive KCs in different experiments. A Leica TCS SPE laser scanning confocal microscope with a 20x (NA 0.7) oil-immersion objective was used for quantification. Additionally, DopR localization was analyzed and newly synthesized proteins in KCs were visualized using FUNCAT. Images were acquired on Zeiss LSM 700 laser scanning confocal microscope with a 25x (NA 0.8) oil-immersion and with a 40x (NA 1.3) oi-immersion objective and on Stellaris 8 STED microscope with 20x (0.75 NA) glycerol-immersion and 93x (1.3 NA) glycerol-immersion objective. Images were processed using Fiji (Fiji is just imageJ). All schematics were created with BioRender (www.app.biorender.com) and Blender (www.blender.org). Individual illustration elements were aligned using PowerPoint 365 (Microsoft Corporation).

4.4 Behavior

4.4.1 Regulation of environmental influences

To investigate the effects of environmental influences on CAMEL tool activity, a protocol was devised to control environmental inputs. For the analysis of labeled cells, pupae were removed from the wall of the food bottles with a brush and washed in water to remove debris. They were then sorted by sex and placed in fresh food vials according to the protocols. As a control, 20 male and 20 female pupae were placed together in a food vial and reared without any other treatment. Four days after hatching, only the brains of the male flies were dissected and stained with antibodies.

To examine the number of CAMEL-positive cells in pupae, male pupae were collected (Figure 6B) and their cocoons were opened at the anterior end. Then, pupae were fixed in 4 % PFA + 0.2 % Triton X-100 at RT for 45 min. The remnants of the fixative were washed out with 0.2 % PBST three times for 30 min.

To analyze the effects of isolation, one single male pupa was placed in a small food vial (Figure 6C). Four days after hatching, the males were dissected.

To test the regulated increase of environmental influences, 20 male and 20 female pupae were placed in one food vial. One day after hatching, the flies were exposed to a protocol of elevated environmental conditions. For three consecutive days, flies were exposed to the stimulus for

15 min in the morning (8 am), noon (1 pm), and evening (4 pm). On the fourth day after hatching, male flies were dissected (Figure 6A).

One of the enriched environmental conditions was based on a mechanical stimulus. Flies were flipped into a fresh food vial and after 15 min, the flies were transferred back into the original vial (Figure 6D).

Next, the mechanical stimulus was combined with an olfactory stimulus. 4-ethylguaiacol (4-EG, Roth) was diluted 1:1,000 in mineral oil. The mixture was applied to a piece of Whatman paper and placed in the food vial. The flies were transferred on the food vial containing the odor for 15 min and then placed back into the original vial (Figure 6E).

Finally, a pheromone stimulus was added to the mechanical and olfactory stimuli. The procedure was the same as described, and additionally, five female virgins per day (after 4 pm treatment) were placed in the food vial (Figure 6F).

To evaluate the effects of environmental influences on a behavioral level, the CAMEL-tool was coupled to the light-activatable Chrimson channel (Figure 6G-J). In contrast to the protocols described above (Figure 6D-F), no defined number of pupae was used, but a large cohort of adult flies of both sexes. Flies were collected in bottles containing retinal food up to one day after they hatched. On the following day, they were exposed to the enriched environment protocol. Both the effects of an individual sensory stimulus and a combination of two stimuli were examined. After the flies were subjected to the sensory influence protocol for three days, the protocol-related behavior was recalled in the arena using the light preference test (see section 4.4.6 for details). Subsequently, male flies were dissected and their brains were immunohistochemically labeled.

First, the influence of an olfactory stimulus alone was investigated. To avoid mechanical treatment during the protocol, the transfer procedure described above had to be modified. The natural tendency of flies to climb upwards against gravity (negative geotaxis) was exploited. 4-EG was diluted in the food (1:1,000). Then, the odor-containing bottle was placed on top of the fly-containing bottle, so the flies moved upwards. After 15 min, the procedure was reversed and the flies ran from the odor-containing bottle to the original food bottle (Figure 6G).

Second, the behavioral effects of a mechanical stimulus were studied. The flies were flipped into a fresh food container and transferred back to the original food container after 15 min (Figure 6H).

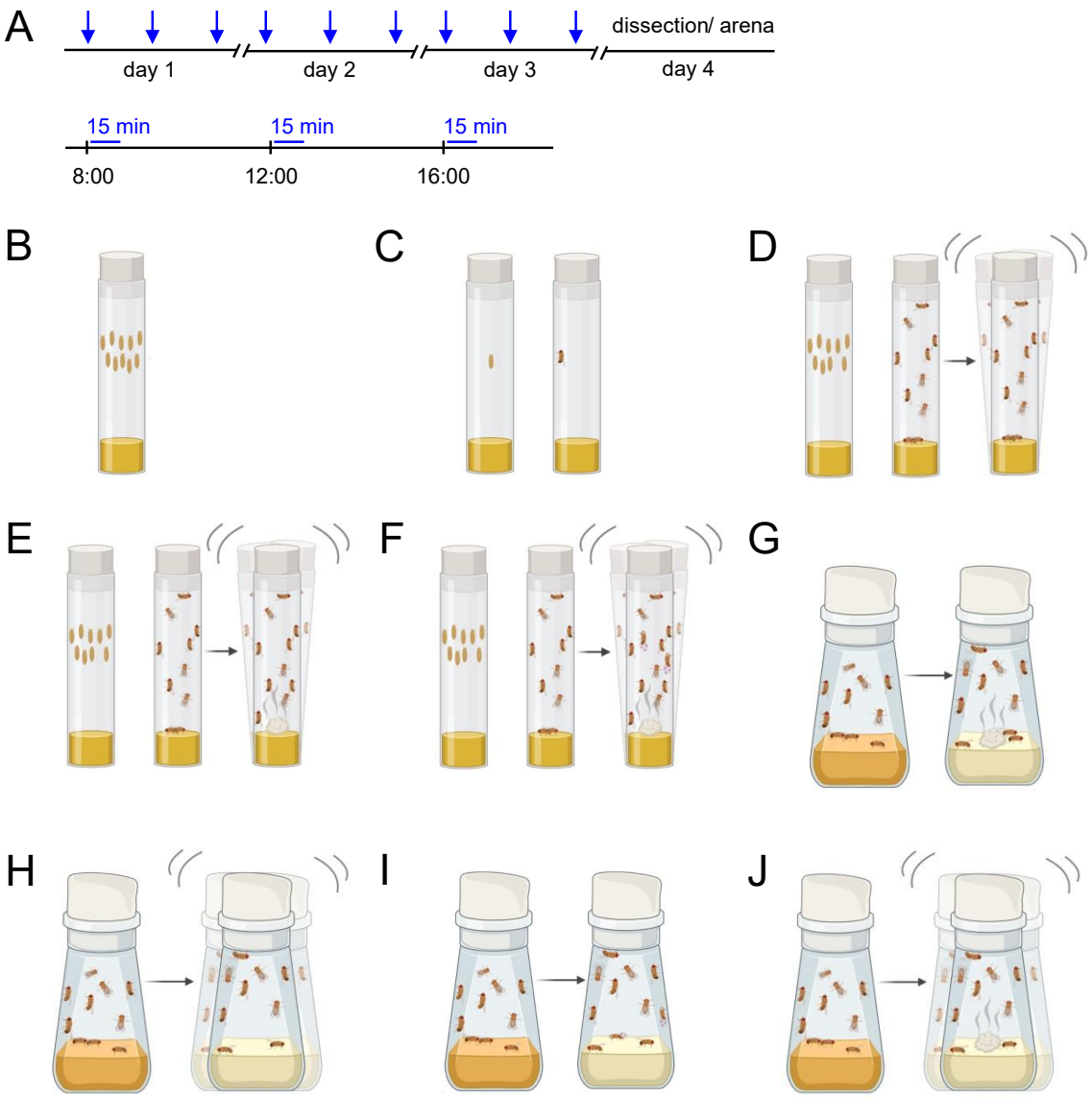


Figure 6: Experimental setup for controlled environmental influences.
(A)Timeline of the experimental protocol. The upper panel shows the three-day protocol with the subsequent dissection and immunohistochemical labeling on day four. The blue arrows indicate the presentation of environmental stimuli. The lower panel shows an example day of the protocol, where the 15 min presentation of the stimuli is shown in blue. (B-J) Schematic drawing of the experimental protocol. (B) Male pupae were collected and dissected. (C) Male pupae were cleaned and transferred as individuals to separate food vials. (D-F) Pupae were washed and 20 male and 20 female pupae each were each placed in food vials. (D) Flies were flipped into a fresh food vial. After 15 min, the flies were transferred back to their original food vial. (E) Additionally, to the mechanical stimulus, the flies were exposed to an olfactory stimulus by transferring the flies to an odor containing food vial. (F) In this experiment, five anesthetized virgin females were added to the original food vial once a day in addition to the mechanical and olfactory treatments. (G-J) In these settings, the number of flies and the size of the food container increased. Furthermore, no pupae were collected but freshly hatched flies were used. (G) Flies were exposed to the odor in a fresh food container. (H) Flies were flipped into a fresh food container and transferred back into their original food bottle. (I) Three times a day, five anesthetized flies were transferred to the container. (J) A combination of mechanical and olfactory stimuli was applied. The flies were transferred into a food bottle with an odor, after 15 min the flies were returned to the original container.

Third, the influence of pheromones was investigated by transferring five anesthetized virgins into the bottle in the morning, at noon and in the evening. The virgins were wild type flies and could be sorted out based on their eye color before the light preference test, so they did not influence the results (Figure 6I).

Fourth, the flies were exposed to a combination of olfactory and mechanical stimuli. The procedure was the same as described above, the only difference was the use of food bottles instead of food vials (Figure 6J).

4.4.2 Appetitive olfactory conditioning

The appetitive olfactory conditioning protocol is based on the protocol of Keene et al., 2006. Flies were starved at 25 °C for 48 h prior to training in vials containing a water-soaked Kimwipe. Groups of approximately 100 flies of both sexes were conditioned together. Experiments were performed in a T-maze with a constant temperature of 20 °C ± 2 °C and constant humidity of 75 % ± 5 %. To odorize the air in the T-maze, a constant airflow of 750 ml/min was generated by a vacuum pump, which sucked through odor-containing mineral oil (Figure 7). The odors used in this thesis were 3-octanol (OCT, Merck, 1:667) and 4-methyl-cyclohexanol (MCH, Merck, 1:1,000).

For paired conditioning, the flies were first transferred into a tube containing blank Whatman paper. In this tube, the flies were exposed to airflow for 30 s, then to the first odor (CS^-) for 90 s, and to airflow again for 45 s. The flies were then transferred to a tube containing sucrose-coated Whatman paper. In this tube, the flies were simultaneously exposed to sucrose and the second odor (CS^+) for 90 s and afterwards to the airflow for 45 s.

During mock conditioning, both odors were presented in the tube without sugar. However, the duration of the air and odor exposure, as well as their order did not change.

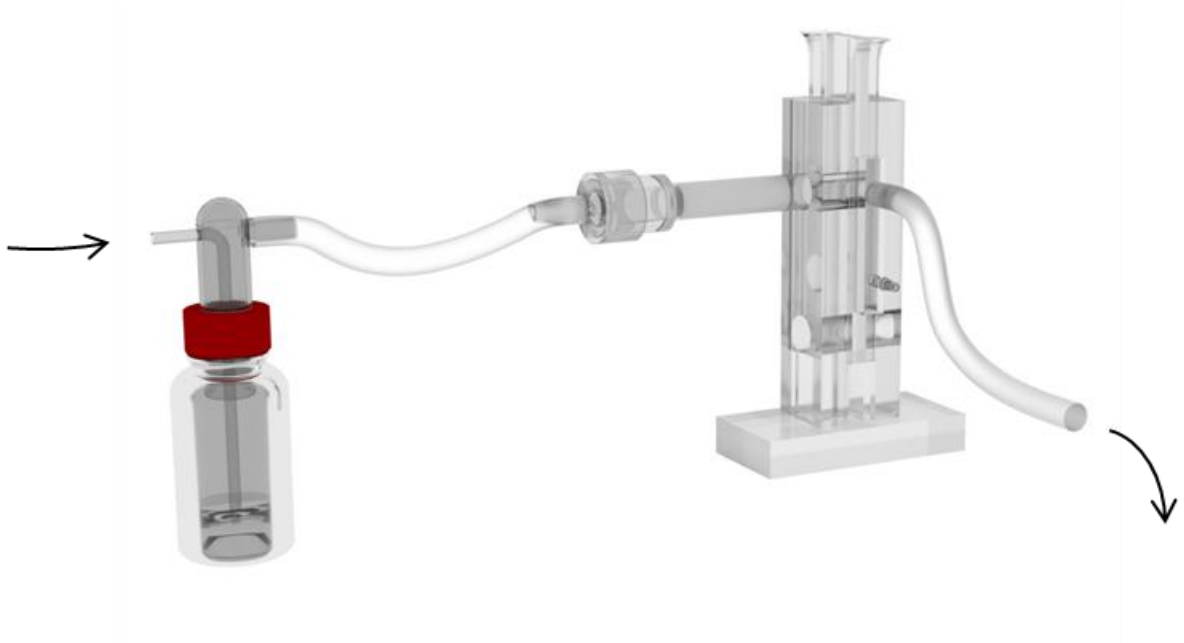


Figure 7: Experimental setup for appetitive olfactory conditioning.
For conditioning, flies were transferred into a vial containing a Whatman paper. The vial was plugged into the upper position of the T-maze. A vacuum pump was used to generate air suction in the T-maze. To expose flies to different odors, the air was transferred through a L-shaped glass tube inserted into the odor-oil mixture bottle. This odorized the air. To expose flies simultaneously to odor and sugar, flies were transferred into a vial containing sugar-coated Whatman paper. The black arrows indicate the direction of the airflow.

For a single sample, one group of flies was conditioned with MCH as CS^+, and another group with OCT as CS^+. A single paired training cycle is sufficient for the flies to learn and memorize the association of CS^+ with the reward. To analyze learning, the flies were tested (see section 4.4.5 for details) after conditioning. To examine memory, the flies were re-starved at 22 °C for 24 h before testing.

4.4.3 Aversive olfactory conditioning

In accordance with the approach published by Tully et al., 1994, aversive olfactory conditioning was performed. During the experiments, constant conditions of 20 °C ± 2 °C, 75 % ± 5 % humidity prevailed. Unlike appetitive conditioning, aversive conditioning did not use a T-maze but a custom-built device that allowed simultaneous conditioning of eight groups (Figure 8). A constant airflow of 750 ml/min was applied which sucked air through the mineral oil mixture (MCH 1:250, OCT 1:167) and allowed odorization of the air. Groups of approximately 100 flies were transferred into copper-coiled tubes each.

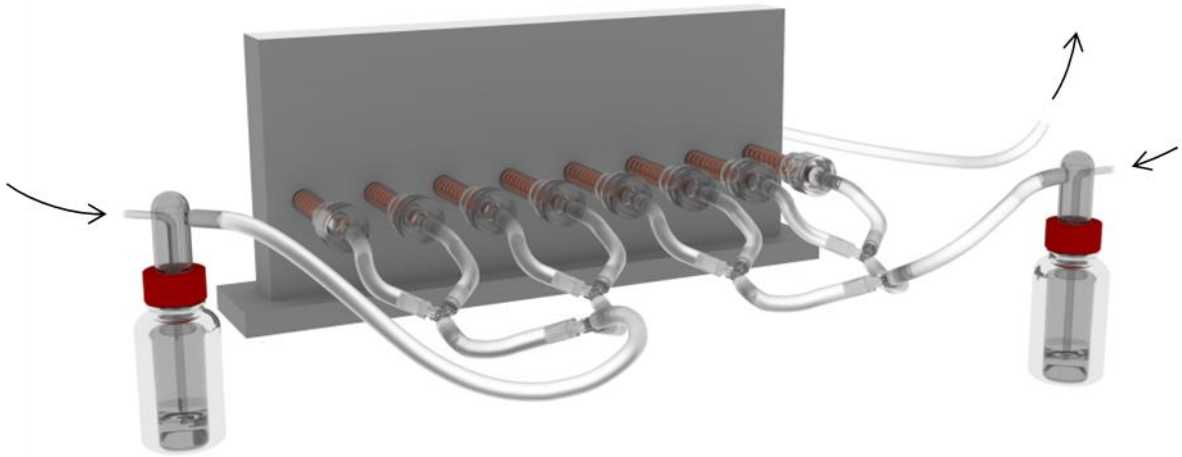


Figure 8: Experimental setup for aversive olfactory conditioning.
For aversive conditioning, flies were transferred into copper-coiled vials. The vials were screwed into the apparatus and connected to the Y-shaped tubes. A vacuum pump was used to generate constant airflow in all eight tubes. To expose flies to the odor, odor-oil-containing bottles were connected to the Y pieces. This allowed four vials to be conditioned with one odor and the other four with a different odor. A custom-made control panel was used to apply electric shocks at the copper-coiled vials. The black arrows indicate the direction of the airflow.

For spaced paired training, flies received air for 2 min to acclimate. Thereafter, flies were simultaneously exposed to the first odor (CS^+) and electrical shocks (twelve 1.5 s pulses of 90 V with 3.5 s pause intervals) simultaneously for 60 s. Followed by 45 s of air and 60 s of the second odor without shocks (CS^-). For spaced training, this cycle was repeated five times at 15 min intervals.

The spaced unpaired training protocols also began with a 2 min pause (air only). Next, the flies were exposed exclusively to electrical shocks (twelve 1.5 s 90 V shocks at 3.5 s intervals) for 60 s. Afterwards, the flies were exposed to the airflow for 5 min. Next, the first odor was presented without shocks for 60 s. Followed by another 45 s of airflow and finally exposure to the second odor without shocks for 60 s. This cycle was repeated five times at 9 min intervals.

For each conditioning experiment, two groups were conditioned (one group conditioned with MCH and one group conditioned with OCT) and the mean was calculated.

4.4.4 Artificial aversive conditioning

For artificial conditioning, the odor presentation was replaced by red light pulses. Odor stimulation was mimicked by activating a random subset of Chrimson-expressing MB neurons using optogenetics. For this purpose, the setup described in 4.4.3 was adapted. The electronic workshop II of the TU Kaiserslautern provided customized aluminum caps for the copper coil tubes. One red light-emitting diode (LED, 625 nm) was attached per cap, ensuring that a constant airflow of 750 ml/min could still be applied (Figure 9). The LEDs were used with an intensity of 100 %, which corresponds to an average value of 0.345 µW/mm^2. Benjamin Escribano used an Arduino UNO Rev3 (Arduino) and a self-written MATLAB script to automate the artificial conditioning.

Two to four days prior to conditioning, flies were fed all-trans retinal food and protected from light. Control groups without retinal were also flipped onto fresh food vials and kept in the dark. During conditioning, darkness, a constant temperature of 20 °C ± 2 °C, and 75 % ± 5 % humidity were maintained. Groups of ~100 flies were loaded into the copper coil vials and the appropriate conditioning protocol was started.

The spaced paired training began with 2 min of airflow to allow the flies to acclimate. Then, the flies were simultaneously exposed to electrical shocks (twelve 1.5 s pulses of 90 V with 3.5 s pause intervals) and 4 Hz red-light pulses (0.125 s on and 0.125 s off) for 60 s, followed by a 15 min pause with airflow only. This cycle was repeated five or ten times depending on the experiment.

Spaced unpaired training started with 2 min of air only for the recovery of the flies. Thereafter, the flies received the electric shocks (twelve 1.5 s pulses of 90 V with 3.5 s pause intervals) for 60 s, followed by 5 min airflow. Subsequently, they were exposed to the red-light pulses (4 Hz, 0.125 s on and 0.125 s off) for 60 s. This cycle was repeated five times with 9 min intervals.

After conditioning, the flies were placed on fresh all-trans retinal food for one to two days before memory was tested (see section 4.4.6 for details).

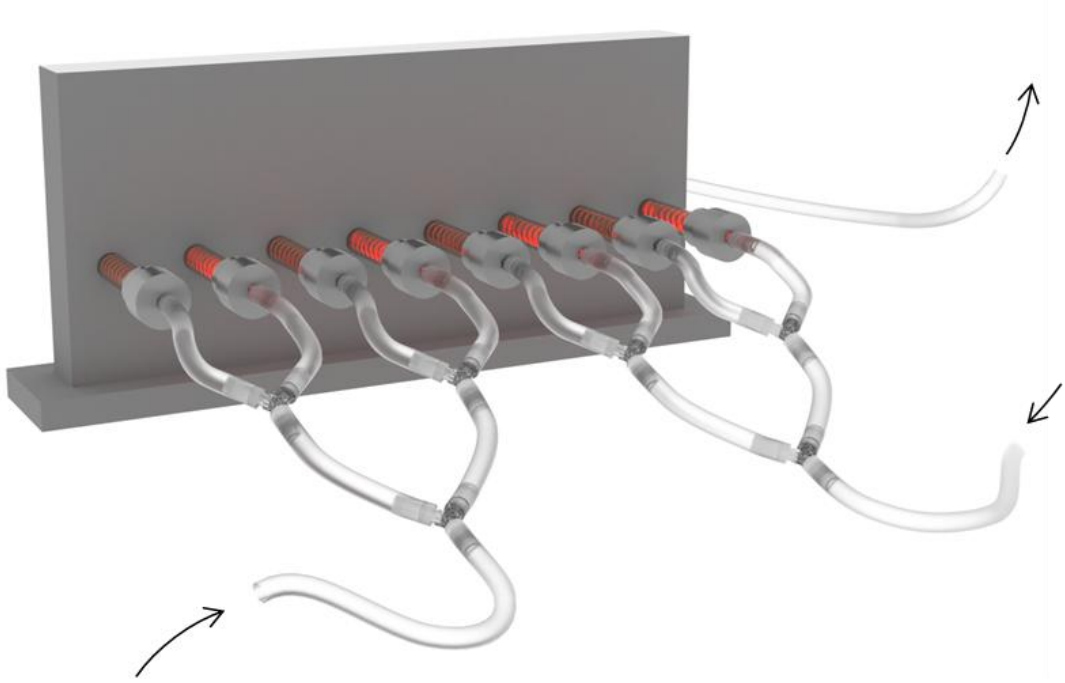


Figure 9: Experimental setup for artificial aversive conditioning.
For artificial conditioning, flies were transferred into copper coiled vials. The vials were screwed into the apparatus and connected to the Y-shaped tubes. A vacuum pump was used to generate constant airflow in all eight tubes. To apply electric shocks at the copper coil, a custom-made control panel was used. In this setup, the plastic caps of the copper coiled vials were replaced by heat-dissipating aluminum caps. These caps contained red high-power LEDs (625 nm). Using a custom MATLAB script, light pulses could be applied in addition to the electric shocks. The black arrows indicate the direction of the airflow.

After the first data sets were completed with this setup, we started to improve the process and found that the maximum intensity of the red LEDs was far below that of our arena. We then decided to continue working with high-power LEDs. The electrical workshop of the TU Kaiserslautern built new heat-dissipating caps with both green and red high-power LEDs. The red high-power LEDs (625 nm) averaged 84.25 µW/mm^2 at 100 %, while the green LEDs (525 nm) averaged 36.57 µW/mm^2 at 100 %. The values of the individual LEDs differed slightly.

The new LEDs allowed us to work optogenetically with the DopR D1R1, which could be activated using green light. For these experiments, flies were fed with 9-cis-retinal 48 h before conditioning and then subjected to different conditioning protocols. All protocols are based on aversive olfactory spaced paired training (4.4.3). For the first protocol, shock and odor presentation were additionally paired with pulsed green light (4 Hz). In the second conditioning protocol, continuous green light was added to odor and shock. The third protocol corresponds exactly to the spaced paired training described in 4.4.3. In protocol four, only the two odors were presented without shock or light. In protocol five, the shock was replaced by 60 s continuous green light, resulting in a simultaneous stimulation with light and odor.

4.4.5 Odor preference test

After both, appetitive and aversive olfactory conditioning, an odor preference test was performed in the T-maze (Figure 10). The temperature was set at 20 °C ± 2 °C, the humidity at 75 % ± 5 %, and the airflow at 750 ml/min. The test tubes used did not contain any Whatman paper. In addition, it was ensured that the tubes were only ever used for the same odor to prevent mixing of the odors. One arm of the T-maze was connected to the CS^+ and the other to the CS^-, thus presenting both odors at the same time.

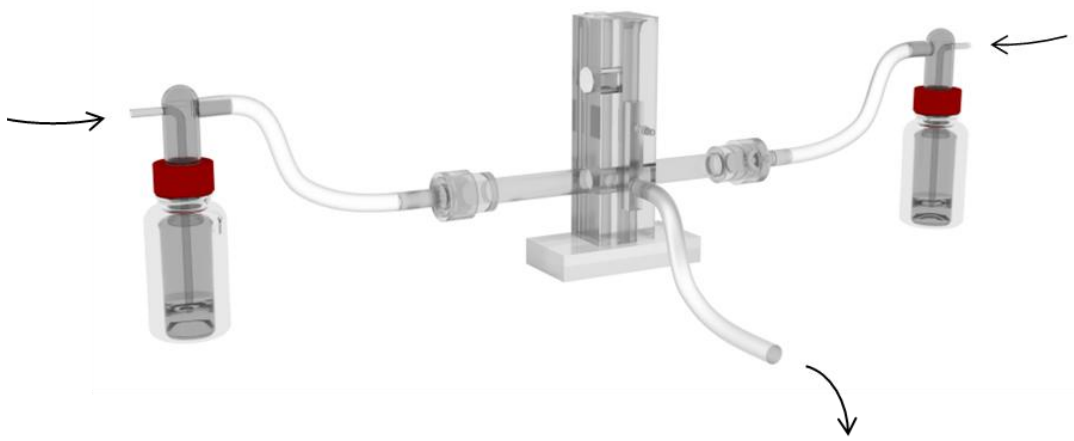


Figure 10: Experimental setup for odor preference test.
Previously conditioned flies were loaded into the elevator of the T-maze. A vacuum pump was used to generate constant airflow. Two empty test tubes were plugged into the T-maze and connected to bottles containing different odor-oil mixtures. Then, the flies were moved down to the decision point with the elevator, where they could freely choose between the two arms of the T-maze. After 2 min, the flies were removed from the respective test tube and counted. The black arrows indicate the direction of the airflow.

During the test, all flies were between four and seven days old. The previously conditioned flies were placed in the elevator of the T-maze and carried to the decision point. There they could freely move between the two arms for 2 min and choose their preferred odor. Flies in the respective arm were counted and the performance index was calculated as follows.

$$\frac{\text{number of flies } CS^+ \; - \; \text{number of flies } CS^-}{\text{total number of flies}} * 100$$

For each experiment, the averaged performance index was calculated from values of the two groups: Flies conditioned with MCH as CS^+ and flies conditioned with OCT as CS^+.

4.4.6 Light preference test

For optogenetic behavioral experiments, a custom-made circular arena was used (Figure 11), adapted from a previously published setup (Aso et al., 2014b; Klapoetke et al., 2014). The red LEDs at the bottom of the arena could be controlled quadrant-specifically by using an Arduino UNO and MATLAB software. The arena was covered with a glass plate, which allowed the flies to move freely, but not to fly. Since the experiments were carried out in the dark, infrared light LEDs and an infrared camera (Raspberry Pi Camera V2.1) were installed above the arena to monitor the flies' movements. With the help of a vacuum pump, a constant airflow of 150 ml/min was applied. During the experiments, the temperature was set at 20 °C ± 2 °C and the humidity was set at 75 % ± 5 %. Groups of approximately 20 flies were loaded into the arena, all flies were between four and seven days old. To artificially activate Chrimson-expressing cells, flies were exposed to the following light illumination protocol: 30 s without light, 30 s illumination of 2 opposite quadrants, 30 s without light, and 30 s illumination in the other two quadrants. An intensity of 40 % red light was used, corresponding to 20 µW/mm^2.

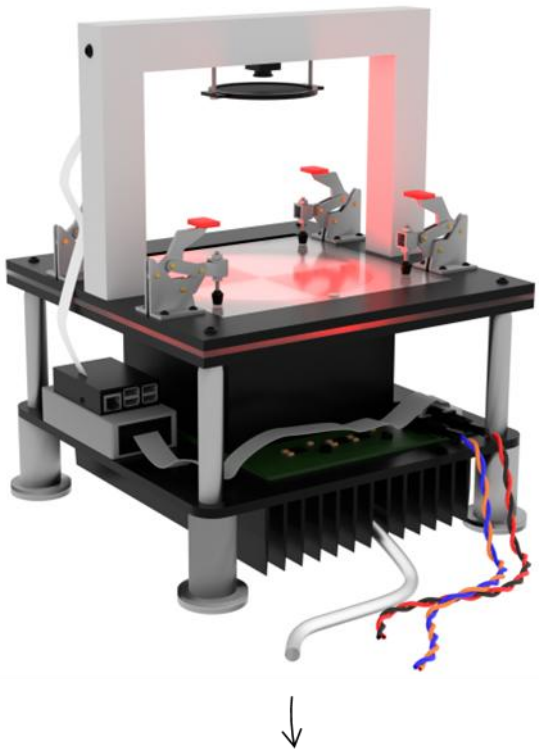


Figure 11: Experimental setup for light preference test.
Flies were tested in the circular arena for their light preference. The glass plate on top of the arena is moveable, allowing flies to be loaded into the arena. After adding the flies, the arena was closed with the glass plate and locked by four clamps. A constant airflow of 150 ml/min was applied to the arena by a vacuum pump. Infra-red LEDs and red LEDs (627 nm) are installed at the bottom of the arena and controlled by an Arduino UNO and MATLAB software. The movement of flies was recorded by a Raspberry Pi and an infrared camera (Raspberry Pi Camera V2.1). The filter in front of the camera prevented the image from being overexposed by the red LEDs. The Raspberry Pi was used to create a web interface that could be accessed from other devices using browsers. This enabled watching and downloading videos from the arena on a laptop. The black arrows indicate the direction of the airflow.

Flies were counted in the illuminated and dark quadrants; afterwards the light preference index was calculated as follows:

$$\frac{\text{number of flies in illuminated quadrants} - \text{number of flies in dark quadrants}}{\text{total number of flies}} * 100$$

For each experiment, the total light preference index was averaged from 10 indices of the last 5 s of the respective illumination phase (55-60 s and 115-120 s).

Counting the flies in their quadrants was initially done by hand and was very time-consuming. During his research practical, Hannes Euler established an improved evaluation method. He used the semi-automatic tracking software TREX (Walter and Couzin, 2021) and a self-written MATLAB script. This script allows not only a faster calculation of the light preference index described above, but also the possibility to extract more information from the data. For example, it could be checked whether the last 5 s of the illumination phase correctly reflects the light preference index, or whether another time interval would be more suitable.

In addition to the well-established cell activation using optogenetics in the arena, I tested artificial activation with red light in the T-maze. Therefore, the T-maze setup described in section 4.4.5 was adapted by a customized cap of one test tube, developed by the electronic workshop II of the TU Kaiserslautern. One red LED (625 nm) was attached to the cap, ensuring that a constant airflow of 750 ml/min could still be applied. As previously described, the flies could freely move between the two arms of the T-maze for 2 min during testing. The LED illuminated one arm of the T-mazes with red light, while the other arm remained in darkness. The light preference index was calculated according to the performance index.

4.5 Statistical analysis

Statistical analyses were carried out with GraphPad Prism 9 (GraphPad Software). Normal distribution of data was tested analytically using the Shapiro-Wilk test. Normally distributed data were analyzed using a parametric t-test (unpaired and two-tailed). If one of the two data sets was not normally distributed, a non-parametric Mann-Whitney test (unpaired two-tailed) was performed. For multiple comparisons a parametric ordinary one-way ANOVA or a non-parametric Kruskal-Wallis test was used. Tukey's (ordinary one-way ANOVA) or Dunn's test (Kruskal-Wallis test) was used to adjust for multiple comparisons (see Table 4 for details).

5. Results

5.1 Natural experiences modulate CAMEL-tool activity

First, I re-evaluated the CAMEL-tool (Figure 12A), which allows the labeling and manipulation of putative memory engram cells (Siegenthaler et al., 2019). Since the goal was to specifically label memory engram cells, the CRE was used to control expression of the AD. As previously demonstrated the CRE protein is required for memory consolidation (Miyashita et al., 2018; Widmer et al., 2018; Yin et al., 1994). In combination with elav^{DBD}, the 6xCRE^{AD} enhancer limited EGFP labeling to cells with an active cAMP/CREB pathway (Figure 12B). The R21B06^{DBD} enhancer restricts expression of EGFP to αβ surface and γ neurons. Together with the pan-neuronal elav^{AD}, the specific expression pattern of R21B06^{DBD} becomes apparent (Figure 12C). The combination of MB specificity and cAMP/CREB pathway activity creates the CAMEL-tool. CAMEL-tool activity leads to sparse labeling of KCs, which encode potentially for individual memories (Figure 12D). In this work, the CAMEL-tool provides the basis to address open questions of memory formation within the *Drosophila* neuronal network.

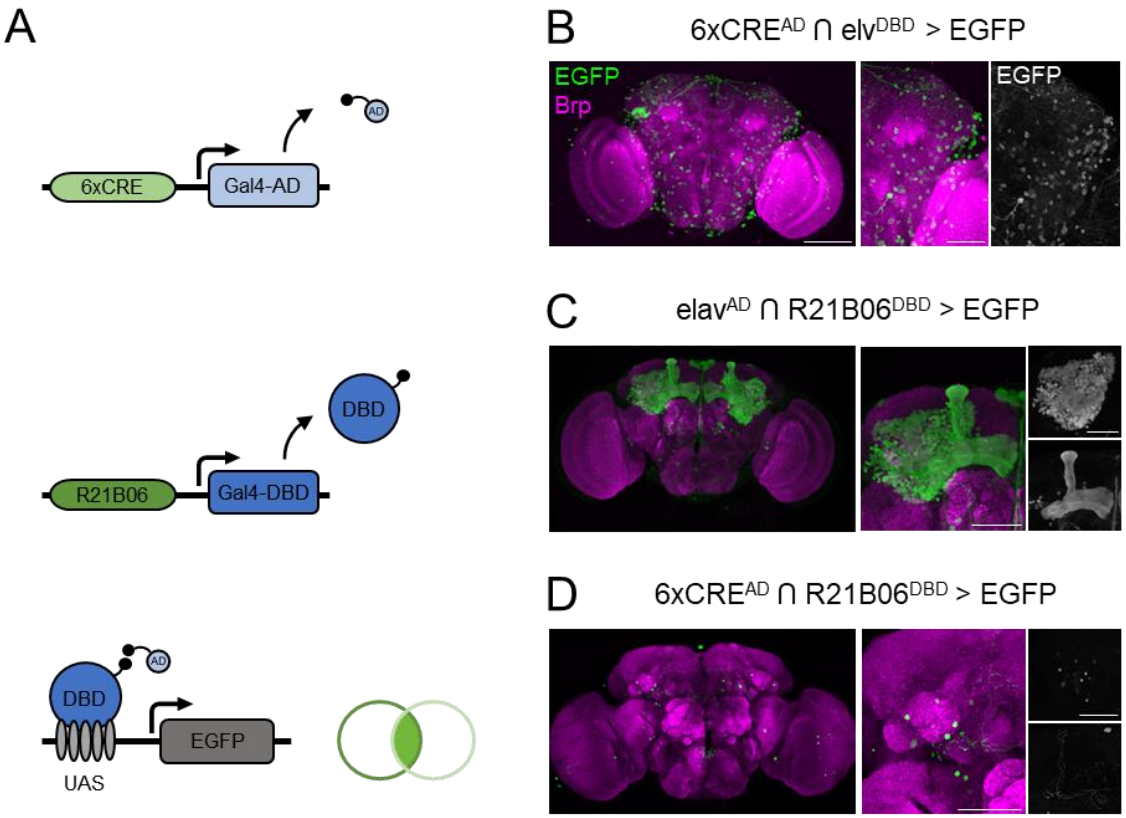


Figure 12: Schematic of the CAMEL-tool.
(A) Model of the split-Gal4 system and CAMEL-tool principle. The specificity of the Gal4 system can be improved by using two independent enhancers to control the expression of the DBD and AD domains of Gal4. Only in cells where both parts of the Gal4 transcription factor are present, a functional Gal4 transcription factor can be reconstituted and bind to the UAS elements to activate the expression of EGFP. (B) The CRE reporter 6xCRE^{AD} in combination with the pan-neuronal elav^{DBD} leads to EGFP expression only in cells with CREB activity. (C) In combination with the pan-neuronal elav^{AD}, the R21B06^{DBD} enhancer labels αβ and γ neurons. (D) CAMEL-tool activation results in a sparse labeling of KCs. Scale bars correspond to 100 µm (left panel) and 50 µm (zoom-in).

5.1.1 Experience-dependent labeling of CAMEL-cells

In accordance with Macpherson et al. (2015), we demonstrated that flies which were raised on odor-free food, show a significantly reduced number of EGFP-expressing CAMEL-neurons compared to flies raised on standard fly food. We therefore concluded that CAMEL-activity depends on olfactory sensory experiences and likely reflects natural memory formation (Siegenthaler et al., 2019).

To further investigate the environmental-dependent activity of the CAMEL-tool, I developed an assay to control different sensory inputs. Therefore, EGFP was expressed under the control of the CAMEL-tool ($6xCRE^{AD} \cap R21B06^{DBD}$ > EGFP). Flies were subjected to the following five protocols: In the first experiment, brains of male pupae were dissected and immunohistochemically labeled (Figure 13A1). In a second trial, male pupae were collected and washed. Then, a single pupa was placed in each food vial. Four days after hatching, brains of the adult flies were prepared and labeled with antibodies (Figure 13A2). For all following experiments, groups of 20 male and female pupae were collected, washed, and transferred into fresh food vials. The treatments began one day after hatching. In the third attempt flies were transferred into fresh food vials in the morning, at noon, and in the evening. The cohorts remained in the vials for 15 min until they were returned to the original ones. This procedure was repeated on the following two days, resulting in a total of three transfers on three consecutive days. On the fourth day of the protocol, the brains of male flies were dissected and stained with antibodies (Figure 14A). The fourth protocol was the same as the third protocol, except that the food vial, in which the flies remained for 15 min also contained the odor 4EG (1:1,000; Figure 14B2). In the last protocol, the flies were again transferred three times a day on three consecutive days into food vials containing 4-EG (1:1,000). In addition to this treatment, five female virgins were added to the food vials on each evening (Figure 14B3). Control flies were not subjected to any experimental manipulations. The controls were always bred and dissected in parallel with the experimental flies.

As olfactory restriction was shown to have a significant impact on CAMEL activity (Siegenthaler et al., 2019), I first tested the consequences of a complete deprivation of sensory inputs. We suspected that this minor sensory input most likely occurs within the first day of adult life or in late pupal development. In collaboration with Saskia Zeilfelder, I adapted the fixation protocol for pupae, stained the brains with antibodies, and quantified the number of EGFP-expressing cells (Figure 13A1-D1). On average, only one labeled CAMEL neuron could be detected in pupal brains. In comparison, the number of CAMEL-positive cells in four-day old flies (control) was significantly higher. These findings could indicate that there is little sensory input to the pupa or that CAMEL tool activity does not begin until the end of the pupal stage.

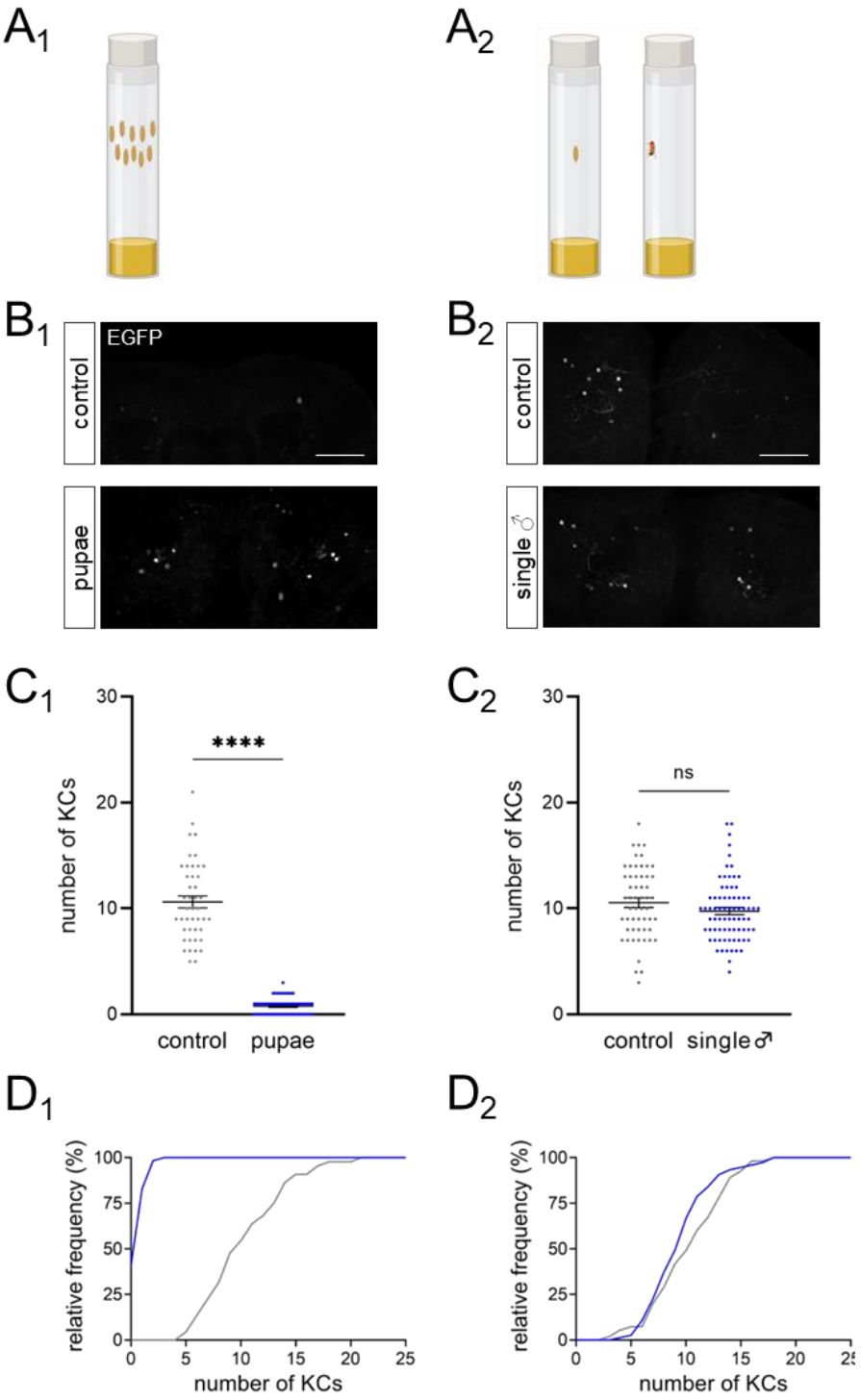


Figure 13: Sensory deprivation minimizes number of labeled CAMEL-cells.
(A1-D1) Dissection of pupal brains revealed a low level of CAMEL specific EGFP-expression in brains compared to four-day old flies (control). (A2-D2) Isolation of male pupae did not result in a significant decrease in the number of CAMEL-positive cells compared to flies that grew up with conspecifics of both sexes (control). (A) Schematic drawing of the experimental protocol, to restrict environmental influences. (A1) Male pupae were collected, dissected, and analyzed for CAMEL expression. (A2) Male pupae were cleaned and transferred as individuals to separate food vials. Four days after hatching, the flies were dissected and stained. (B) Representative microscopic images of the CAMEL-cells. The number of CAMEL-cells marked in pupae (C1 and D1) or individual males (C2 and D2) versus the control groups (grey) is shown in scatterplots (C) and as cumulative frequency distributions (D). Scale bars correspond to 50 µm. Scatter plots show single data points; the horizontal lines represent mean ± standard error of the mean (SEM). Asterisks indicate significant differences between the tested groups.

Next, I tested the effects of isolation. This aspect was particularly interesting because previous reports have shown that social isolation affects both the behavior (Li et al., 2021; Zhou et al., 2008) and the neuronal structure of insects (Maleszka et al., 2009; Technau, 2007). To analyze the effects of isolation on CAMEL-activity, single male pupae were placed into a small food vial and raised without any conspecifics. Four days after hatching, the brains of the male flies were analyzed. The number of CAMEL-positive cells was slightly reduced compared to flies kept under control conditions, but the difference did not reach significance (Figure 13A2-D2). This suggests that fly-fly interactions do not significantly contribute to natural memory formation in a cohort of 40 animals. In summary, the reduction in CAMEL-activity by sensory restriction supports the hypothesis that endogenous CAMEL-labeling is a consequence of experience and potentially reflects natural memory formation.

Enriched environments are a well-established approach to study the relation of sensory experiences and neuronal alterations in mice or rats (Delanogare et al., 2020; Kempermann, 2019; Rosenzweig and Bennett, 1996). Therefore, I also aimed to analyze the effect of increased sensory exposure in *Drosophila*. To control environmental inputs, I set up a four-day protocol for the controlled increase of environmental inputs (Figure 14A). One day after hatching, flies were exposed to different sensory inputs for three consecutive days. To ensure comparability of data, a fixed schedule was used and all animals were exposed to different stimuli for 15 min three times a day.

First, I wanted to investigate the influence of a mechanical stimulus on CAMEL-activity. For this purpose, flies were transferred from one food vial to another, where they remained for 15 min and were then transferred back to the original vial. (Figure 14B1). This mechanical stimulus alone did not result in a significant increase in the number of labeled CAMEL-cells compared to the control (Figure 14C1-E1). Next, the effect on CAMEL activity resulting from the combination of mechanical and olfactory stimuli was analyzed. Flies were transferred into a food vial containing Whatman paper with the odor 4-EG (1:1,000) in mineral oil (Figure 14B2). This treatment resulted in a significant increase in the number of EGFP-expressing cells (Figure 14C2-E2). To determine whether the number of CAMEL-positive cells could be further increased, flies were exposed to pheromones in addition to mechanical and olfactory stimuli (Figure 14B3). For this purpose, five virgin females (as a potential pheromone source) were added to the food vials once a day. Interestingly, the addition of pheromones resulted in a significantly higher number of CAMEL-cells compared to the control (Figure 14C3-E3).

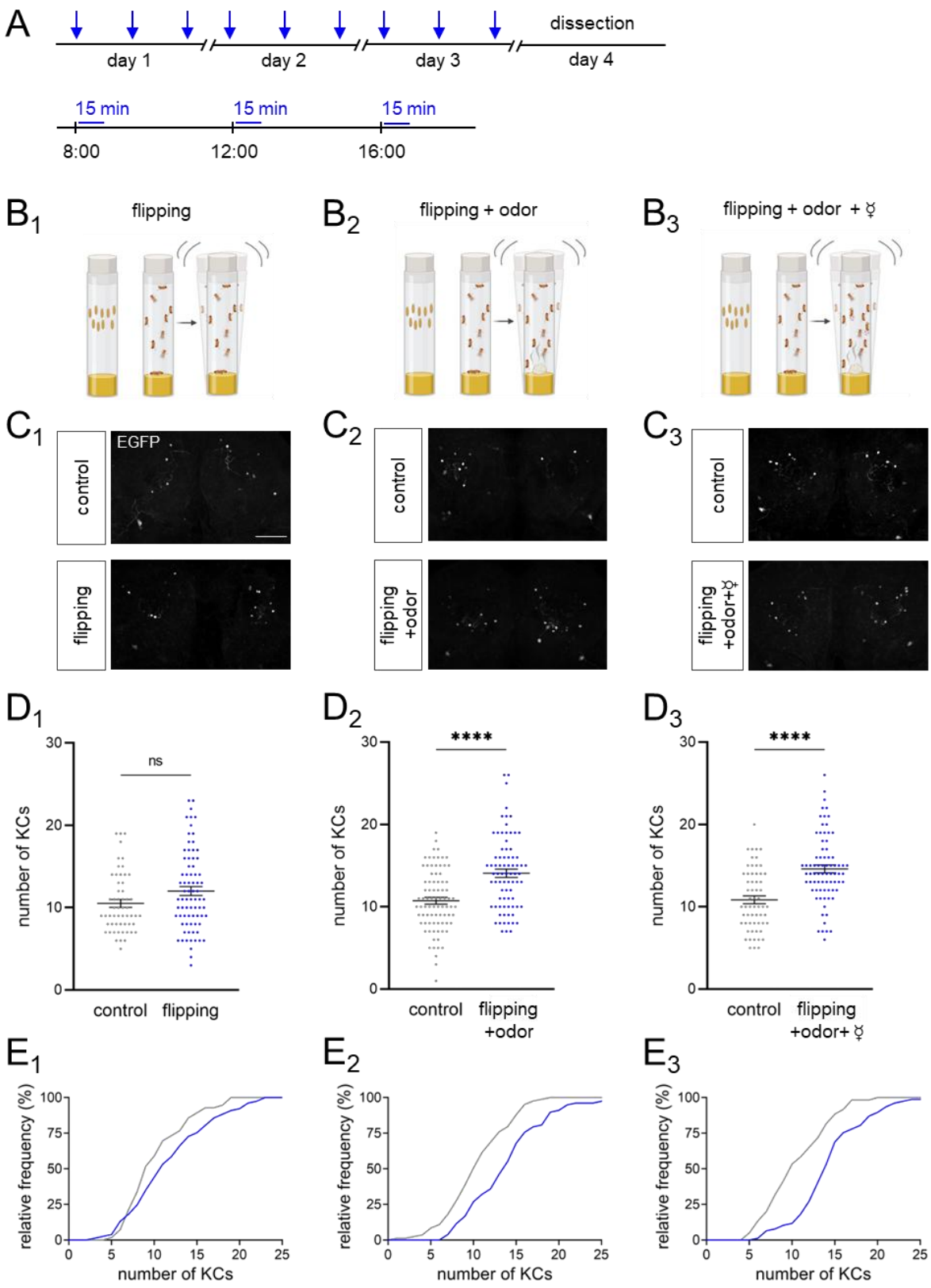


Figure 14: Successive increase of environmental inputs leads to an increasing number of labeled CAMEL-cells.

(A) Timeline of the experimental protocol. The upper panel shows the three-day protocol with the subsequent dissection of the flies on day four. The blue arrows indicate the presentation of environmental stimuli. The lower panel shows an exemplary day of the protocol, where the 15 min long presentation of the stimuli is shown in blue. (B) Schematic drawing of the experimental protocol. Pupae were washed and 20 male and 20 female pupae each were placed in food vials. (B1) Flies were flipped into a fresh food vial at the beginning of the protocol. After 15 min, the flies were transferred back to their original food vial. (B2) In the second setting the vial contained a Whatman

paper with an odor (4-EG 1:1000) in addition to the fly food. (B3) In the third setting odor plus five anesthetized virgins were added to the original food vial after the 4:00 pm stimulus. (C) Representative microscopic images of CAMEL cell bodies. (D-E) The number of labeled CAMEL-cells of flies that experienced more sensory stimuli (blue) was plotted against control flies (gray) as scatterplots (D) and cumulative frequency distributions (E). Scale bars correspond to 50 µm. Scatter plots show single data points; the horizontal lines represent mean ± SEM. Asterisks indicate significant differences between the tested groups.

To summarize the findings of the individual treatments, all data from Figures 13 and 14 are presented within one figure (Figure 15). The number of labelled KCs in control animals is shown in gray. These animals were not subjected to any treatment, and the average number of naturally labeled CAMEL-cells was eleven. Although no statistical analysis was performed, the summary of the data highlights that CAMEL-activity is gradually enhanced with increasing sensory inputs. The observation in isolated males is analogous; reduction of stimuli results in decreased CAMEL activity. The results of the pupae analysis are striking in the overview, approximately half of the animals showed no CAMEL activity at all. Together, these results confirm that CAMEL-activity depends on the experience of the fly and most likely reflects natural memory formation.

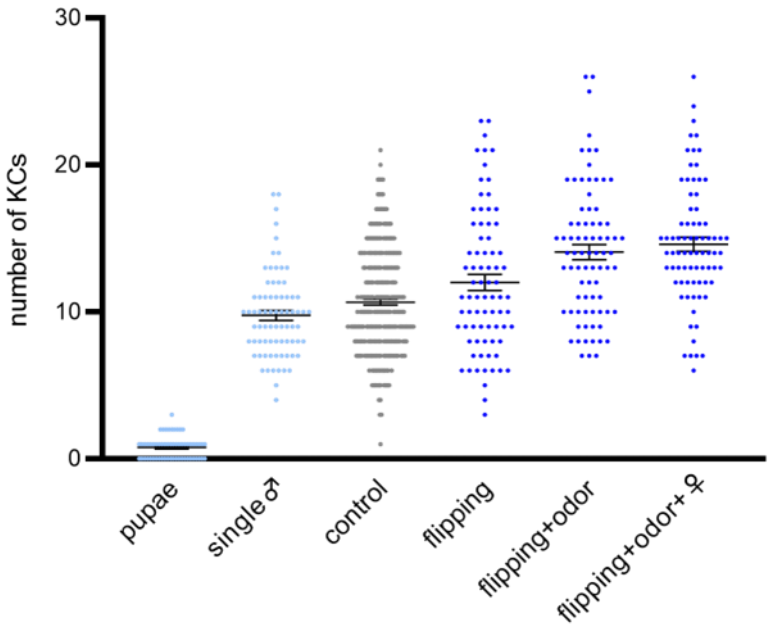


Figure 15: Summary of the number of positive CAMEL-cells in relation to different environmental inputs. The summary of the data from Figure 13 and Figure 14 shows that the CAMEL-tool can be pushed in both directions. Deprivation of environmental influences resulted in a reduced number of labeled CAMEL-cells, whereas presentation of various stimuli resulted in an increased number of EGFP-expressing cells.

5.1.2 Optogenetic reactivation of CAMEL-cells encoding natural memories

The previous experiments shed light onto structural changes at the cellular level. Next, I evaluated the effects of natural memory formation at the behavioral level. Therefore, the CAMEL-tool was used to express the light activatable Chrimson-channel ($6xCRE^{AD}$ ∩ $R21B06^{DBD}$ > Chrimson). Since Chrimson requires the cofactor all-trans retinal for optogenetic activation, all flies were transferred to bottles containing retinal. Experimental flies were exposed to increased sensory stimuli. In the first trial, I used 4-EG (1:1,100) as an olfactory stimulus (Figure 16B). In the second experiment, the flies were transferred between food containers, resulting in a mechanical stimulus (Figure 16C). Third, I investigated the influence of female virgins on male behavior by adding fresh virgins to the food container once a day (Figure 16D). In a final experiment, I combined the olfactory stimulus with the mechanical stimulus (Figure 16E). Flies were exposed to the respective stimuli three times a day for 15 min in all protocols. The exposure to the protocols took place on three consecutive days (Figure 16A). Control animals were also fed with retinal but were not subjected to any experimental manipulations. To assess the behavioral valence of putative natural memory traits induced by the different sensory experiences, the engram cells were artificially reactivated using optogenetics in the circular arena (Figure 16A). The light preference test in the arena is an established assay that allows activation of Chrimson expressing cells via red light exposure. Previous studies have shown that the optogenetic activation of MBONs can elicit either approach or avoidance behavior (Aso et al., 2014b). The light preference test lasted for 2 min, during which the flies could move freely within the arena. After 30 s of darkness, two opposite quadrants were illuminated for 30 s by red light, followed by another 30 s of darkness, and finally, the other two quadrants were illuminated. The position of the flies within the arena was used to calculate the light preference index which reports avoidance or attraction towards light. Afterwards, the brains were dissected and stained with antibodies, to determine whether altered behavior correlated with the number of labeled CAMEL-cells.

First, I investigated the influence of individual sensory stimuli on fly behavior. In the first setting, I analyzed the effects of three exposures to the odor 4-EG. The odor was dissolved in the fly food in one bottle. This bottle was placed upside down on the bottle containing the flies. The negative geotaxis caused all flies to climb into the upper bottle, where they remained for 15 min. Afterwards, the flies were transferred to the original food bottle in the same manner. The recall of experience-dependent CAMEL-cells resulted in a slightly negative light preference index compared to the control group (Figure 16B). In a second setting, the flies were exposed to a mechanical stimulus (flipping). The reactivation of Chrimson expressing CAMEL-cells in the arena caused almost identical values in experimental and control flies (Figure 16C). In the third setting flies were exposed to a chemosensory stimulus by repeated exposure to virgin females. The optogenetic assay indicated a slight, but not significant, light

avoidance after pheromonal exposure compared to the control group. Since the individual stimuli did not show a significant change in light preference compared to the controls, olfactory and mechanical stimuli were combined in a fourth assay (Figure 16E). Here, the reactivation of memory cells resulted in a significant avoidance of red light compared to the control. After the light preference test, male flies were collected from the arena, brains were dissected and immunohistochemically analyzed. Quantification of the labeled CAMEL-cells showed a significantly increased cell number compared to the control group.

The optogenetic experiments suggest that altered sensory experiences are likely to induce a memory trait that can be artificially recalled. Exposure to individual sensory stimuli did not alter behavior, however a combination of stimuli induced a behavioral change. Thus, multiple sensory stimuli or specific combinations of sensory stimuli are required to induce sufficient and meaningful engram cells. To further investigate this aspect, flies could be exposed to two different or all environmental influences and then be tested in the arena. It is noticeable that the memory trait of control flies already has a slightly negative valence. Exposure to several environmental stimuli likely increased the number of memory cells and enhanced light avoidance. Therefore, experience-dependent memory cells in these settings likely encode aversive behavior.

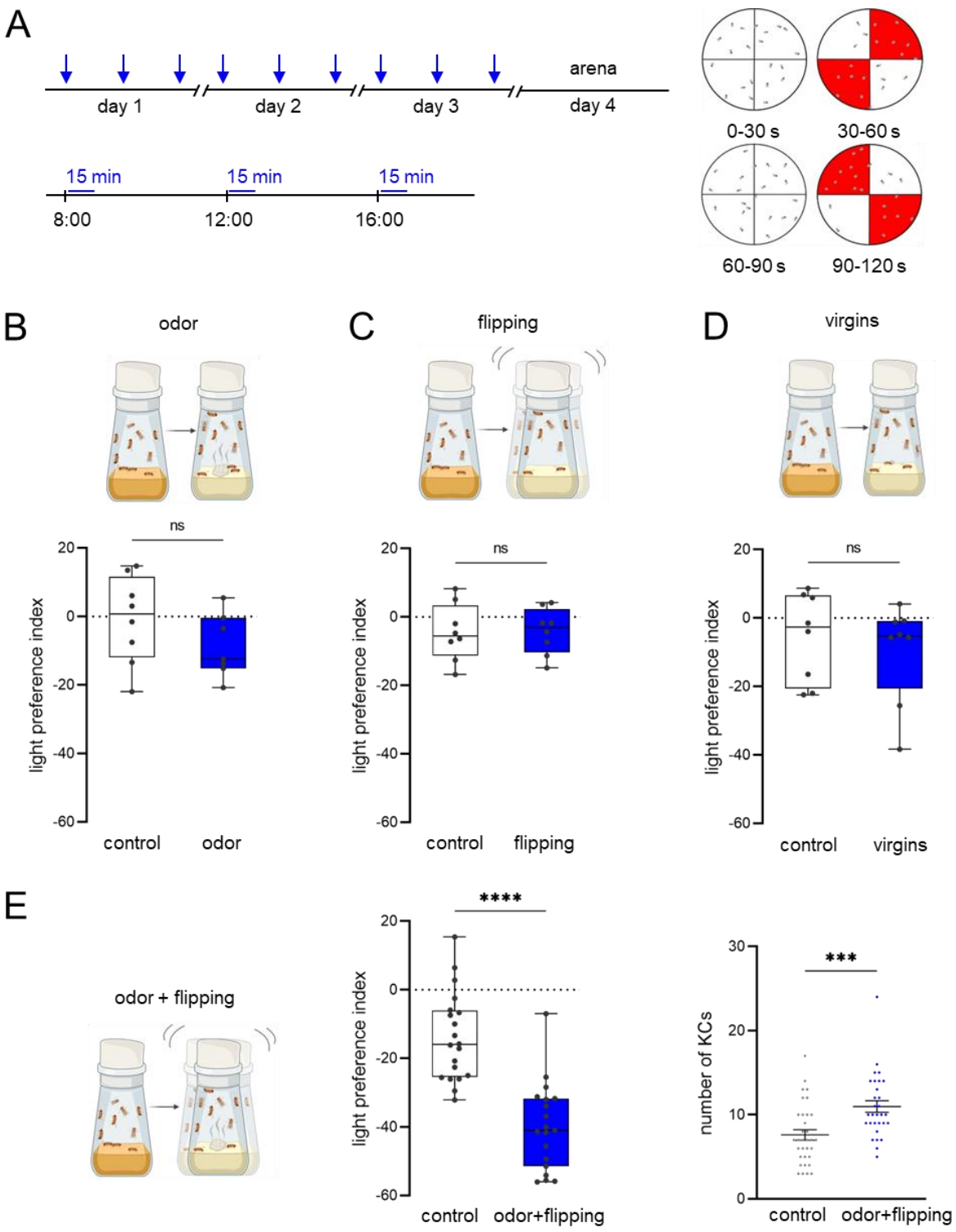


Figure 16: Artificial recall of natural memory requires a combination of environmental inputs.
(A) Timeline of the experimental protocol. The upper panel shows the three-day protocol with subsequent light preference test on day four. The blue arrows indicate the presentation of different environmental stimuli. The lower panel shows an exemplary day of the protocol. The illumination protocol of the circular arena is shown on the right. (B-D) Compared to the control, the stimulation protocols with only one environmental influence did not lead to any significant difference in behavior upon reactivation of CAMEL-positive cells. (E) The combination of olfactory and mechanical stimuli resulted in a significantly stronger light avoidance compared to the control. This difference is also reflected on a cellular level. Flies exposed to increased environmental inputs showed a significantly increased number of EGFP-expressing cells. Scatter plots show single data points, the horizontal lines represent mean ± SEM. Boxplots show the individual data points, the median is indicated by the central line, the box extends the 25th to the 75th percentile, the whiskers correspond to minimum and maximum. Asterisks indicate significant differences between the tested groups.

5.2 Establishment of an improved immunohistochemical labeling protocol

The quantification of experience-dependent memory cells revealed a discrepancy in cell number depending on the reporter used. In control groups, the number of EGFP-expressing cells (Figure 13-Figure 15) was higher than the number of Chrimson-expressing cells (Figure 16). To investigate the cause of this difference more closely, male flies of both genotypes were dissected and stained with antibodies. Examining the microscopic images, it is noticeable that, as expected, Venus-tagged Chrimson-channels are located within the neuronal membrane (Figure 17A) whereas the EGFP signal is cytosolic (Figure 17B). Cytosolic labeling allowed clear identification of the soma of positive CAMEL-cells. Visualizing only the membrane entails the following difficulties for quantification: On the one hand, the contrast between specific and background signal is lower compared to EGFP-expressing cells. On the other hand, it is difficult to detect the somata as the dendritic signal interferes and the axons can also form loops that resemble cell bodies. Quantification revealed a significantly higher number of EGFP-expressing cells compared to Chrimson expressing cells (Figure 17C-D). To ensure an accurate quantification of CAMEL positive cells, independent of the reporter, I established an improved immunohistochemical labeling protocol based on Janelia Research Campus (https://www.janelia.org/project-team/flylight/protocols) in collaboration with Nina Wilhelmy.

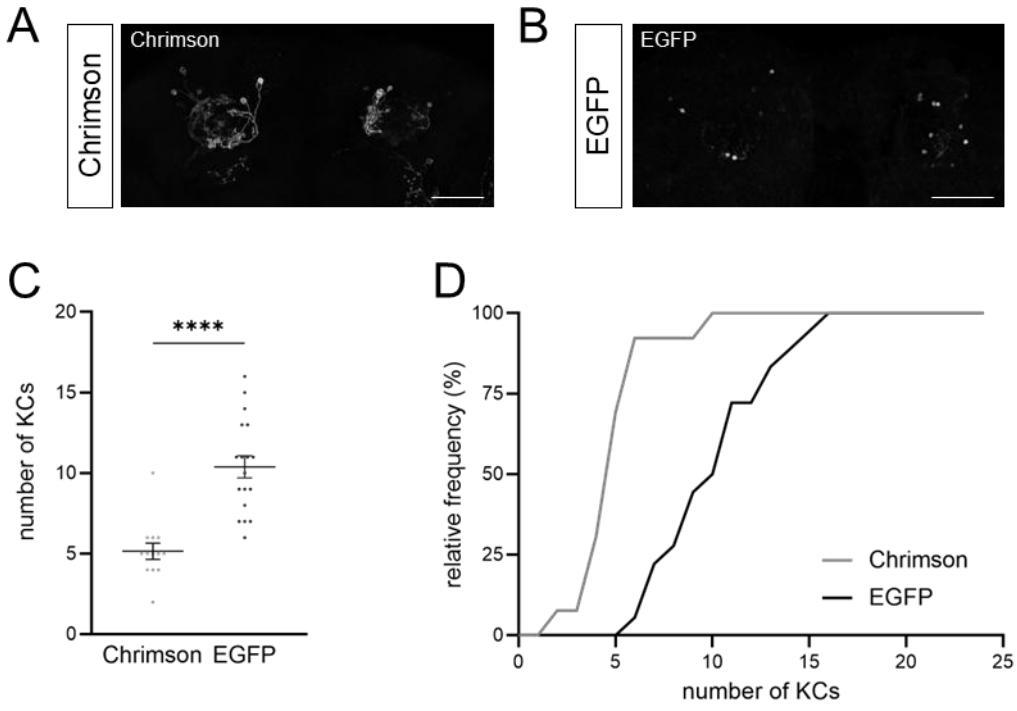


Figure 17: The number of CAMEL-cells depends on the reporter gene expressed.
(A) Representative microscopic images of two reporter genes expressed under the control of the CAMEL-tool. The soma region of Chrimson (left) and EGFP (right) expressing CAMEL-cells is shown. (B) Scatterplot (left) and a cumulative frequency distribution (right) showed a significantly higher cell number of EGFP-expressing CAMEL-neurons (black) compared to Chrimson (gray). Scale bars correspond to 50 µm. Scatter plots show single data points, the horizontal lines represent mean ± SEM. Asterisks indicate significant differences between the tested groups.

To establish the new labeling protocol, we used 6xCRE^{AD} ∩ R21B06^{DBD} > EGFP flies. The microscopic images were acquired with identical settings for the different protocols to enable a direct comparison of the labeling quality. Starting from the existing labeling protocol (Figure 18A), one parameter at a time was adjusted until the new labeling protocol was successfully established (Figure 18C). The following factors were adjusted: Blocking medium, triton concentration, duration of antibody incubation, and mounting medium (data not shown). Comparing the new protocol with the old one, the background signal was decreased, and the labeled cell bodies were outlined more clearly. To further improve the quality of the staining, brains were cleared in an ethanol and xylene series after the secondary antibody labelling. The clearing resulted in an improved quality of the immunohistochemical staining in combination with both the old (Figure 18B) and the new labelling protocol (Figure 18D).

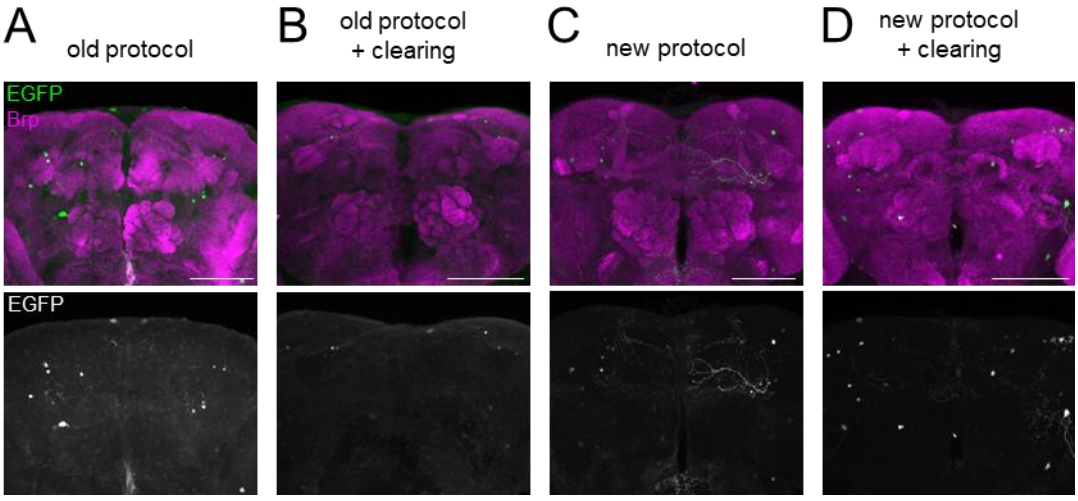


Figure 18: The new protocol improves the quality of antibody labeling.
Representative images of CAMEL-positive cells of 6xCRE^{AD} ∩ R21B06^{DBD} > EGFP flies were acquired with the same settings to evaluate the EGFP signal quality. (A) The old labeling protocol reveals a strong background signal in the GFP channel. (B) Subsequent clearing reduced the background signal and thereby improved the contrast. (C) The new labeling protocol showed hardly any background signal. (D) When the new staining protocol was combined with clearing of the tissue, background staining was barely detectable. Scale bars correspond to 50 µm.

A major difference between the two staining protocols was the preparation of the brains. In the old protocol, whole flies were fixed followed by the dissection of the fixed brains. In contrast, in the new protocol, the brains were first dissected and fixed afterwards. To determine the influence of the fixation time point, the dissected brains were all stained following the new labeling protocol and the resulting fluorescence labeling was compared (Figure 19). Brains fixated after dissection (Figure 19A) showed a higher contrast in EGFP signal and therefore a better labelling quality compared to previously fixated brains (Figure 19B). The improved labeling quality in the new protocol allowed the detection of finer structures such as individual axons. However, the amount of non-specific background signal was similar in both microscopic images. Thus, the dissection of non-fixed brains, followed by fixation and subsequent labelling according to the new protocol represents a simple way to improve the antibody staining.

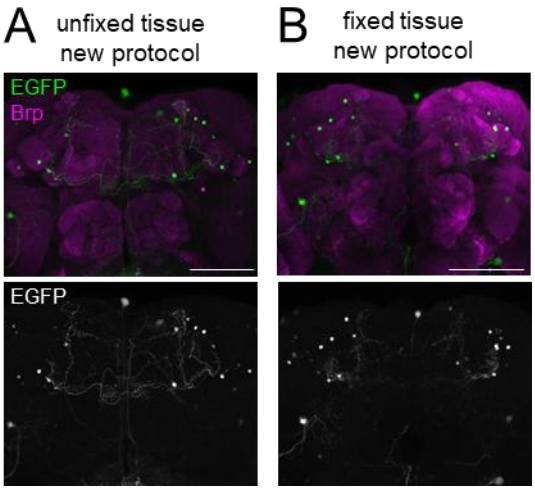


Figure 19: The time point of fixation has a minor influence on the quality of the labeling.
Representative images of CAMEL-positive cells of 6xCRE^{AD} ∩ R21B06^{DBD} > EGFP flies were acquired with the same settings to evaluate the EGFP signal quality. (A) The brains were dissected and afterwards fixed. (B) Flies were fixed before preparation. After the brains were dissected, they were stained according to the new protocol. The two procedures lead to comparable quality of the staining. Scale bars correspond to 50 µm.

5.3 LTM-dependent CAMEL-tool activity

5.3.1 Conditioning-dependent labeling of CAMEL-cells

In a previous study, we used aversive olfactory conditioning to investigate the CAMEL-tool in LTM formation (Siegenthaler et al., 2019). We could show that paired conditioning resulted in an increased number of positive CAMEL-cells 48 h after training. Following aversive conditioning artificial reactivation of these labelled CAMEL-cells using red light was sufficient to recall the formed associative memory. Since we limited our approach to aversive conditioning, one goal of this thesis was to test memory recall after appetitive conditioning.

To investigate the conditioning-dependent CAMEL-activity, EGFP was expressed under the control of the CAMEL-tool. 6xCRE^{AD} ∩ R21B06^{DBD} > EGFP flies were exposed to either paired or mock training (Figure 20A) and tested in an olfactory preference assay. Afterwards the number of positive CAMEL-cells was determined. Paired but not mock conditioning elicited a positive learning index (Figure 20B). Consistent with previous reports (Y.-C. Kim et al., 2007; Krashes and Waddell, 2008; Schwaerzel et al., 2003), a single cycle of training was sufficient to induce protein-synthesis-dependent memory formation in paired- but not in mock-conditioned flies (Figure 20C).

Quantification of EGFP-expressing cells 48 h after training revealed a significantly increased number of labelled cells in paired-conditioned flies compared to control (Figure 20D-E). This data suggests that the CAMEL-tool labels memory engram cells after both aversive and appetitive conditioning.

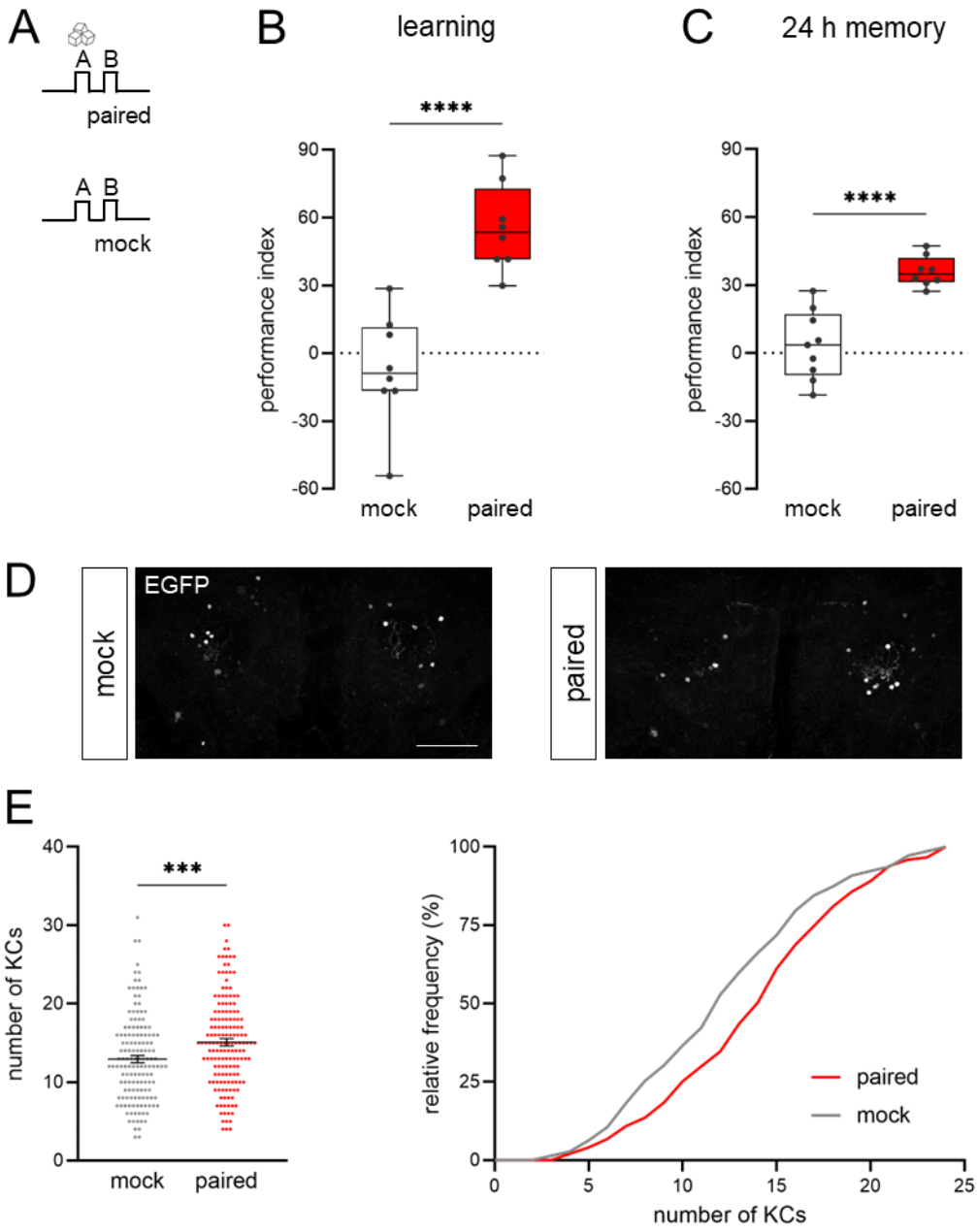


Figure 20: Appetitive memory formation increases the number of CAMEL positive cells.
(A) Appetitive conditioning protocols with five cycles and 15 min pauses in between. For paired conditioning, odor A was combined with a sucrose stimulus (upper panel). For mock conditioning, odor A and B were presented without sucrose (lower panel). (B-C) Flies showed increased learning (B) and memory (C) performance after paired conditioning (red) compared to the mock control (white). (D) Representative images of EGFP-positive cells after conditioning. (E) The number of labeled CAMEL-cells after paired conditioning (red) was plotted against the mock conditioned (gray) flies as a scatterplot and cumulative frequency distribution. The number of CAMEL-cells was significantly higher after paired conditioning compared to the mock control. Scale bars correspond to 50 µm. Scatter plots show single data points, the horizontal lines represent mean ± SEM. Boxplots show the individual data points, the median is indicated by the central line, the box extends the 25th to the 75th percentile, the whiskers correspond to minimum and maximum. Asterisks indicate significant differences between the tested groups.

5.3.2 Visualization of newly synthesized LTM proteins

The CAMEL-tool allows visualization of LTM formation on a cellular level, but it does not provide insights into the molecular changes underlying LTM formation. For this reason, we used FUNCAT to study the dynamics of protein synthesis in different cell types. FUNCAT depends on fluorescent tagging of methionine analogs in newly synthesized proteins. Therefore, we expressed a mutant form of $MetRS^{L262G}$ only in the MB. The flies were fed with a 10 mM ANL 72 h prior to dissection. Only the mutant enzyme, but not the endogenous one, can incorporate ANL instead of methionine during protein synthesis. Thus, newly synthesized proteins can then be visualized using the ANL-binding fluorophore TAMRA.

In collaboration with Nina Wilhelmy, I established the FUNCAT-technique in our laboratory (Wilhelmy, 2020). We restricted the expression of $MetRS^{L262G}$ to the MB using the MB specific enhancer OK107 (Figure 21A). EGFP-tagged $MetRS^{L262G}$ could be visualized by antibody staining, which revealed its localization in the axons and cell bodies of the KCs. The signal of the red-fluorescent dye TAMRA was also visible in all MB neurons. In a second step, the R21B06 enhancer was used that allows to limit the expression of $MetRS^{L262G}$ and therefore newly synthesized proteins to α/β and γ KCs. Specific EGFP and TAMRA signal was evident in the somata and the α/β and γ lobes (Figure 21B). In summary, it was possible to limit the expression of $MetRS^{L262G}$ to a defined subset of cells to label newly synthesized proteins in selective MB cells.

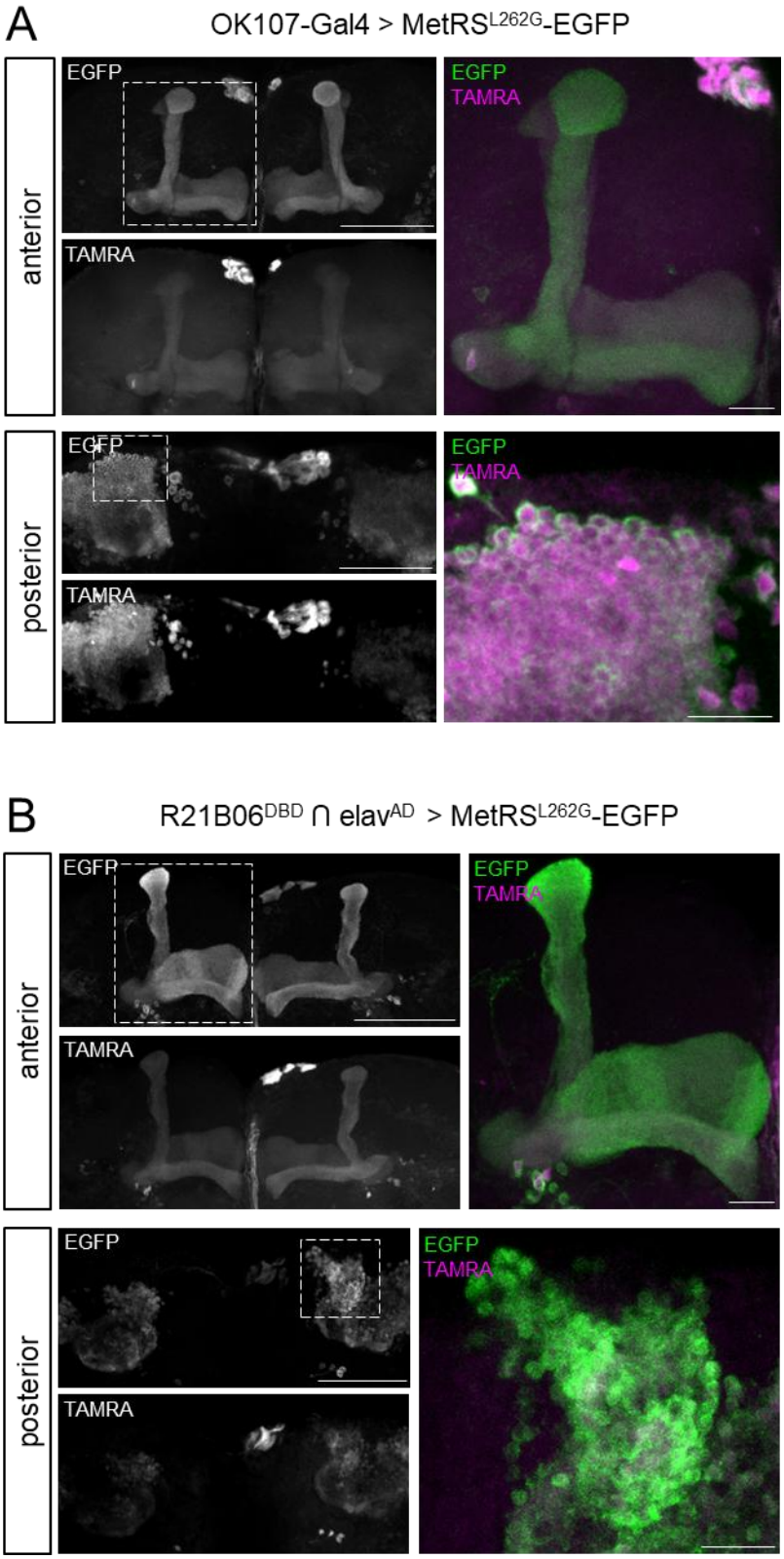


Figure 21: Visualization of EGFP-tagged MetRS^{L262G} and newly synthesized proteins.
MetRS^{L262G} was expressed under the control of a MB specific enhancer (A) and the α/β and γ specific R21B06^{DBD} enhancer (B). MetRS^{L262G} is tagged with EGFP and can be visualized by immunohistochemistry. This enzyme incorporates previously fed ANL (10 mM ANL for 72 h) into newly synthesized proteins. Proteins that incorporated ANL can be visualized by the ANL-binding fluorophore TAMRA. (A) Colocalization of EGFP and TAMRA is visible in all MB lobes (anterior) and cell bodies (posterior). (B) EGFP and TAMRA signals are limited to α/β and γ neurons. The magnification regions are marked by a white dashed square (left). Scale bars correspond to 50 µm (left) and 10 µm in the magnification (right).

Next, we combined the CAMEL-tool and the FUNCAT-technique to visualize newly synthesized proteins specifically in LTM engram cells. CAMEL-dependent expression of $MetRS^{L262G}$ enabled to restrict the labeling of newly synthesized proteins to CAMEL-cells (Figure 22). The EGFP-tagged enzyme was only expressed in α/β and γ neurons with an active cAMP/CREB signaling pathway (CAMEL-cells), resulting in a sparse subset of labeled cells. Microscopic images revealed a punctuated signal in the axons, whereas the cell bodies were quite uniformly labeled with EGFP. Although $MetRS^{L262G}$ was present throughout the axons, detection of newly synthesized proteins in the axons via TAMRA was not possible.

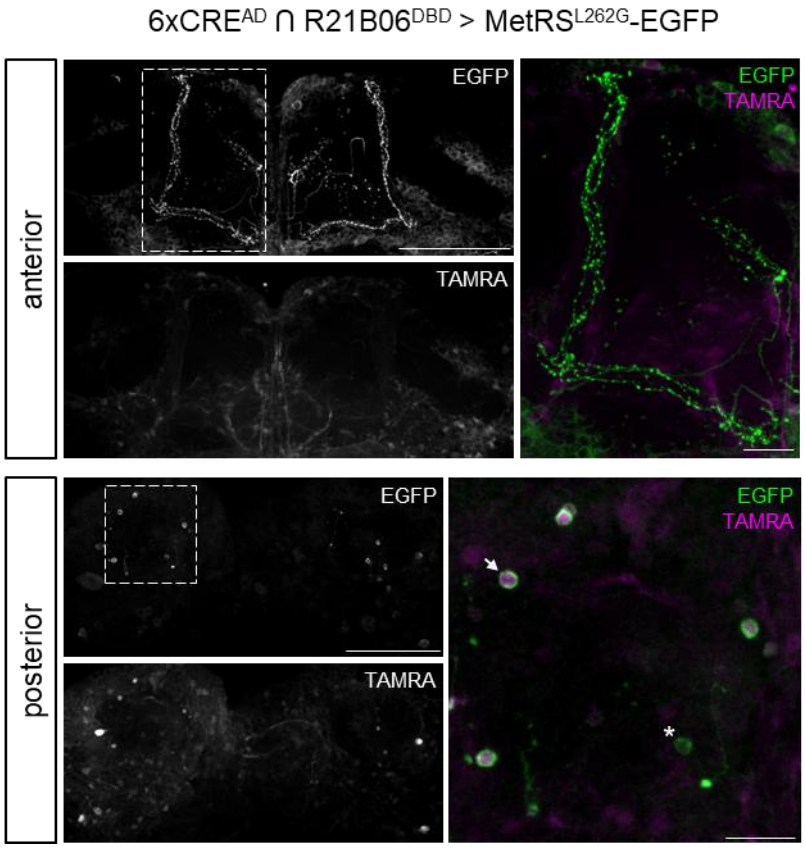


Figure 22: Visualization of protein synthesis in CAMEL-somata.
CAMEL-dependent expression of EGFP-tagged $MetRS^{L262G}$ revealed sparse labeling of KCs. 72 h before dissection, the flies were fed with 10 mM ANL. The ANL was incorporated into newly synthesized proteins and labeled via TAMRA. The anterior region of the brain (upper panel) shows specific punctuated EGFP signal in the axons, but no specific TAMRA signal. In the posterior region, specific TAMRA signaling could be detected in addition to EGFP. The magnification shows cell bodies only positive for EGFP (asterisk) and positive for EGFP and TAMRA (arrow). The magnified regions are marked by a white dashed square (left). Scale bars correspond to 50 µm (left) and 10 µm in the magnification (right).

Examining the microscopic images of the posterior brain region, a small subset of KCs was EGFP labeled. In most cell bodies, a co-labeling with TAMRA was observed (white arrow), yet there were also cells that only showed an EGFP but no TAMRA signal (white asterisk). However, in principle the FUNCAT-technique labeled all newly synthesized proteins. Using the current experimental approach, it was not possible to distinguish whether the tagged proteins were LTM-dependent proteins or, for example, housekeeping proteins.

5.3.3 Recall of conditioning-dependent appetitive memories

Since previous experiments demonstrated a conditioning-dependent increase of labeled CAMEL-cells, the next goal was to retrieve appetitive memory optogenetically (Figure 23). In this experiment, the CAMEL-tool was used to drive the expression of Chrimson. Flies were conditioned (Figure 23A, upper panel) and for efficient retrieval of appetitive memory flies were restarved (Krashes and Waddell, 2008; Tempel et al., 1983) with retinal water prior to the memory recall. After 24 h, the light preference index was determined in the arena (Figure 23A, lower panel) after reactivating memory-dependent CAMEL-cells with red light. Conditioning with OCT as CS^+ (Figure 23B) resulted in a light preference index close to zero for the non retinal control group. For flies that received the cofactor retinal required for the activation of Chrimson, appetitive conditioning caused a significant avoidance of red light compared to the control. Using MCH as a CS^+ (Figure 23C), slightly aversive behavior was observed for flies with and without retinal exposure, even though the two values were not significantly different. Thus, in contrast to aversive-conditioned flies (Siegenthaler et al., 2019), appetitive-conditioning did not enable an efficient memory recall in the optogenetic arena. To ensure that this effect was not due to any technical errors, I analyzed the uptake efficiency of retinal.

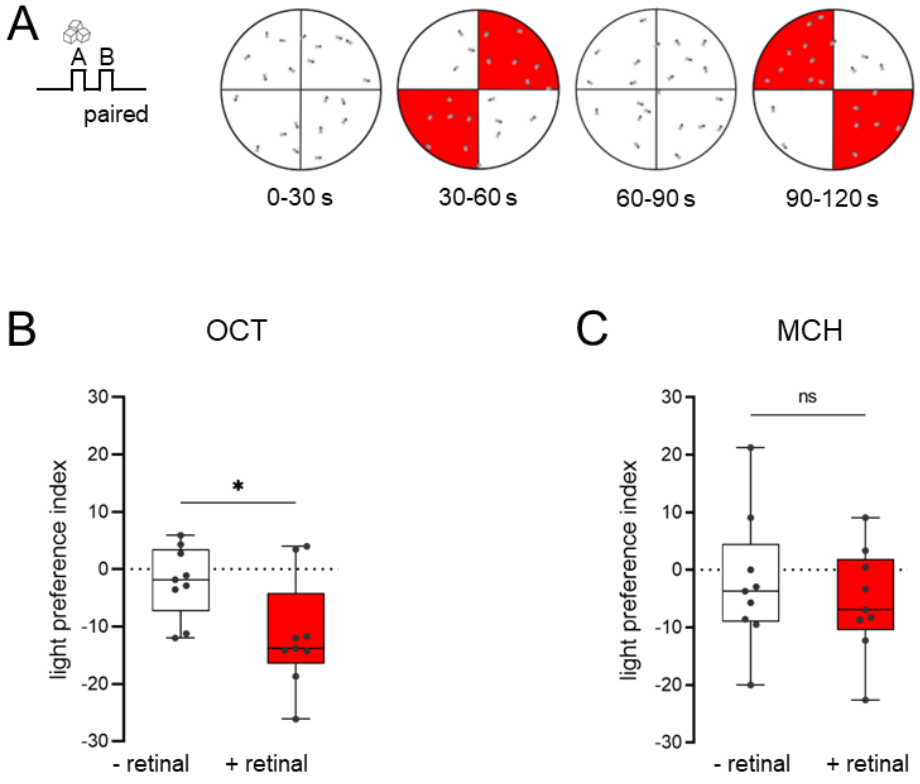


Figure 23: Optogenetic reactivation of conditioning-dependent CAMEL-cells.
(A) Appetitive paired conditioning protocol and light illumination protocol of the circular arena. (B-C) All flies were paired conditioned. The control group (white) did not receive retinal, whereas the experimental flies (red) were provided with retinal diluted in water for 24 h after conditioning. (B) After OCT conditioning, recall of appetitive memory resulted in significantly stronger avoidance of red light for experimental flies compared to the control group. (C) After conditioning with MCH, reactivation of CAMEL-neurons elicited no significant difference between control and retinal fed flies. Boxplots show the individual data points, the median is indicated by the central line, the box extends from the 25th to the 75th percentile, the whiskers correspond to minimum and maximum. Asterisks indicate significant differences between the tested groups.

Previous studies showed that retinal feeding in normal fly food is sufficient to activate Chrimson via red light exposure (Honjo et al., 2012). However, for the retrieval of appetitive memory, it is necessary that the flies are starved between conditioning and testing. Therefore, the retinal had to be ingested with water and not food. In addition, the duration of retinal feeding was reduced to 24 h in the experiment (Figure 23B-C), because flies could not survive prolonged starvation. Therefore, it was also not possible to analyze 48 h memory as we did for shock-trained flies (Siegenthaler et al., 2019). To verify the sufficient uptake of retinal, I used the Gal4-driver line Gr66a, which limits Chrimson-expression to bitter-sensing gustatory receptor neurons. Activation of these neurons leads to a negative light preference index (Marella et al., 2006; Figure 24A). Furthermore, I used the driver MB077B-Gal4 which limits expression of Chrimson to a single neuron per hemisphere, the MBONγ2α'1. In accordance with Aso et al. (2014b), it was shown that activation of this MBON results in red light preference (Figure 24B). Quantification of behavioral data after feeding retinal in normal fly food showed no significant difference between feeding the cofactor for 24 h or 48 h for both tested genotypes. When retinal was fed in water, again no difference in light preference was detected between 24 h and 48 h retinal feeding in both genotypes. Comparing the feeding of retinal in water and normal fly food, no significant difference could be observed regardless of the feeding duration. Together, these results demonstrate that feeding retinal for 24 h enables adequate uptake of retinal independent of the dilution media and is therefore sufficient to ensure neuronal activation using red light.

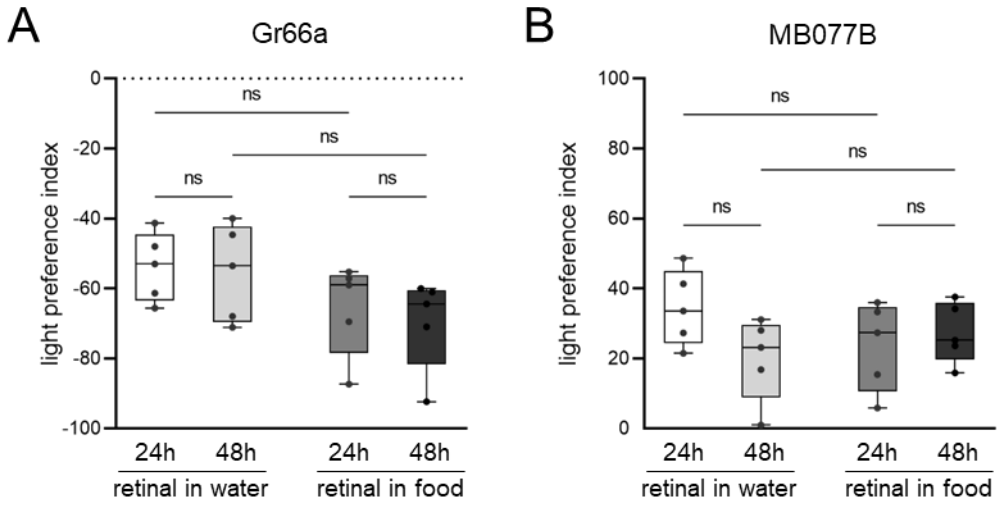


Figure 24: Retinal feeding test.
(A) The Gr66a driver limits the expression of the red light-sensitive Chrimson-channel to gustatory receptor neurons required for bitter tasting. Optogenetic activation of Gr66a neurons leads to light avoidance behavior. (B) MB077B limits the expression of Chrimson to the appetitive MBONγ2α'1, whose activation leads to light-approach behavior. The behavior of both genotypes depends on the Chrimson co-factor all-trans retinal. Feeding the cofactor for 24 h was sufficient to induce Chrimson-dependent activation and thereby elicit avoidance as well as approach behavior. Retinal uptake was sufficient to elicit both behaviors, regardless of whether retinal was mixed into food or added to water.

For this thesis, I used the circular light arena in several attempts to optogenetically activate a defined subset of neurons, resulting in a large collection of arena videos. I initially evaluated these videos manually by first determining the total number of flies in the arena. Then, for seconds 56-60 and 116-120, I counted a still frame of the video and determined the number of flies in illuminated and non-illuminated quadrants. Finally, the light preference index was calculated for each time point and these values were averaged. This manual evaluation is time-consuming and might contain human bias. For this reason, an automatic data analysis tool was developed by Hannes Euler, a master student in our group (Figure 25). Automated data analysis offers several advantages: On the one hand it eliminates human bias, on the other hand, it enabled a more detailed data analysis in a shorter time. I used the previously described drivers Gr66a (Figure 25A, upper panel) and MB077B (Figure 25A, lower panel) to restrict the expression of the light-activatable Chrimson channel to bitter sensing neurons and the MBONγ2α'1. The behavior induced by optogenetic cell activation was evaluated manually (Figure 25C) and automatically, the values determined were then compared with each other (Figure 25D1 and D2). The individual values of the optogenetically activated bitter sensing neurons were almost identical for manual and automatic evaluation (Figure 25D1). The values of the Chrimson-expressing MBONγ2α'1 differed only slightly, and the difference was not significant (Figure 25D2). These results demonstrate the accuracy of the automated evaluation tool.

Next, I used the automated evaluation to extract additional information from the videos. The tool allowed to change the analysis intervals (Figure 25E1 and E2). In accordance with Aso et al. (2014b) for manual analysis the last 5 s of each illumination phase were evaluated. I applied automated data analysis to investigate shortened (0.04 s, 0.4 s, 1 s, 2 s, 3 s and 4 s) and extended (10 s and 15 s) intervals in addition to the already used 5 s analysis interval. The changed analysis intervals were always based on the end point of the illumination phase, only the duration of the analyzed period changed. Plotting the analysis intervals of the Gr66a driver line showed that the light preference indices vary strongly for a duration of up to 1 s (Figure 25E1). The collected data between the last 2 and 5s were almost equal and showed the most aversive PIs for GR66a (Figure 25E1). The same was observed for MB077B, reaching the highest scores within this time period. (Figure 25E2). Extending the analysis interval further to the last 10 or 15 s of the illumination phase, resulted in a reduced avoidance or approach index for Gr66a (Figure 25E1) and MB077B (Figure 25E2), respectively. These results demonstrate that evaluation of the last 5 s of the illumination phases, as it was also done manually on all previous experiments, represents a good choice for data analysis. The duration was long enough to limit the variance and short enough to adequately reveal the light preference.

The automated evaluation not only allows the length of the analysis interval to be varied, but also the time point of data analysis (0 s, 5 s, 10 s and 15 s after light onset) to be shifted within

the illumination phase (Figure 25F1 and F2). In the dark phase of the illumination protocol (Figure 25B), no optogenetic cell activation takes place. Thus, flies of both genotypes are randomly distributed in the arena at the time of light onset (0 s), which was reflected in an almost neutral light preference. The longer the illumination with red light lasts, the stronger the light avoidance in Gr66a (Figure 25F1) and the light preference in MB077B (Figure 25F1). Apparently, most flies reach their final position 10 s after light onset, so the behavioral values changed only slightly after this time point. Thus, the analysis of the last 5 s during illumination phases represents a reasonable choice.

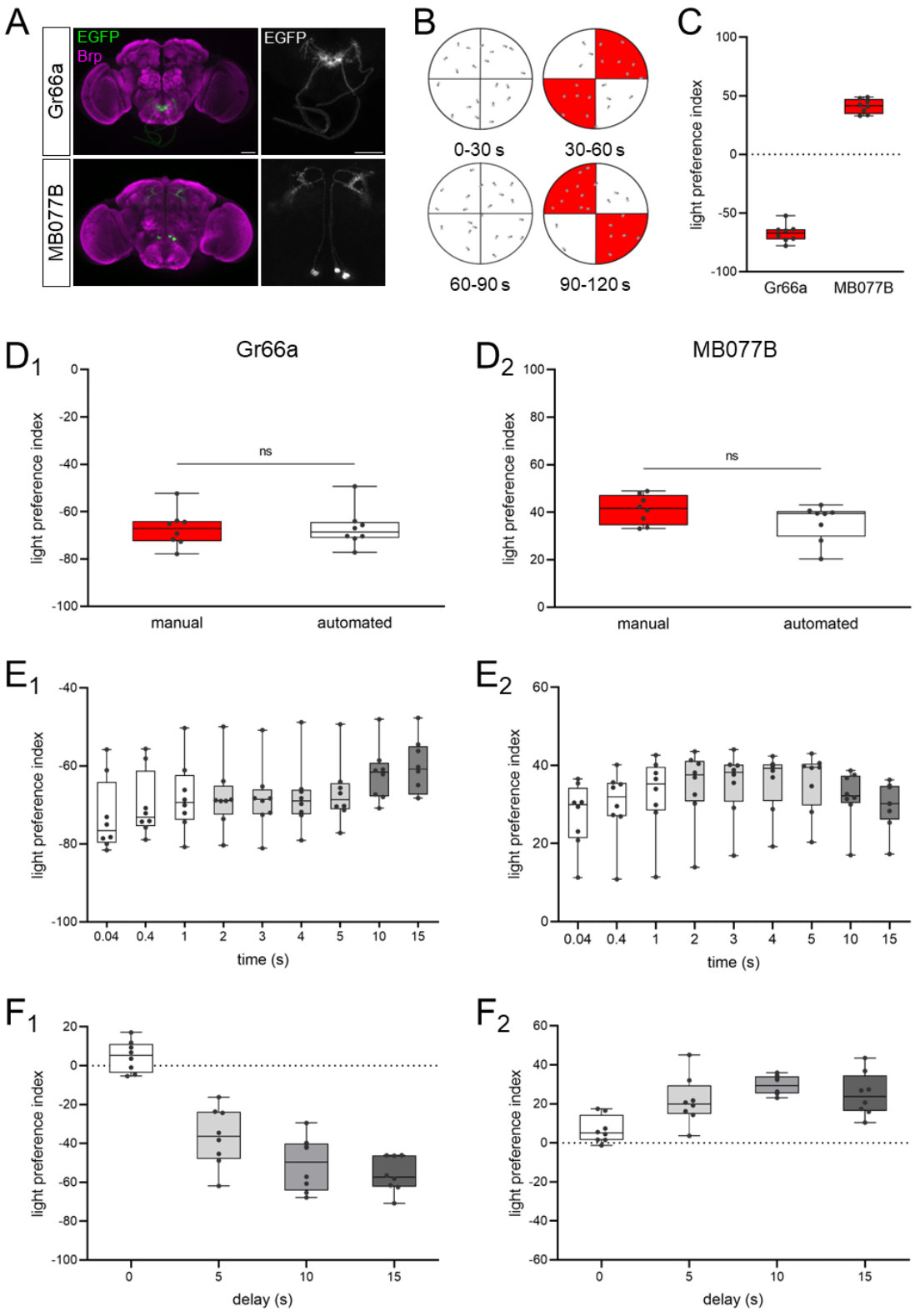


Figure 25: Automated data analysis of arena videos.
(A) The displayed driver lines were used to limit expression of light activatable Chrimson-channels to bitter-sensing gustatory neurons (upper panel) or to restrict expression to the MBONγ2α'1 (lower panel). (B) Light illumination protocol of the circular arena. (C) The activation of Gr66a neurons led to avoidance behavior, the activation of MBONγ2α'1 to approach behavior. To calculate the light preference index, recorded videos were manually evaluated. (D) Comparison of the mean values generated manually (red) and automatically (white) from the last 5 s of each illumination phase. The manual data corresponds to the data from C. The automated data corresponds to the data from E1 and E2 at the time of 5 s. The data sets of the Gr66a driver are almost identical, those of the MB077B driver differed only slightly. (E) The light preference indices were plotted for different analysis intervals. For all calculations, the end of the illumination phase was used as the starting point. If the examined interval was

1 s or shorter (white), the values varied strongly. Between a duration of 2 s and 5 s of video analysis (light gray), the values are largely the same. At a duration of 10 s and 15 s (dark gray), the values fluctuate again. (F) Plotted are automatically calculated light preference indices at different times after illumination. At the time of illumination (white), the flies were evenly distributed in the arena. After 5 s of light exposure (light gray), a directed movement towards dark quadrants (F1) or towards illuminated quadrants (F2) occurred. After 15 s (dark gray), most flies moved to their preferred quadrant. Scale bars correspond to 50 µm. Boxplots show the individual data points, the median is indicated by the central line, the box extends from the 25th to the 75th percentile, the whiskers correspond to minimum and maximum. Asterisks indicate significant differences between the tested groups.

After insufficient retinal uptake was ruled out as a cause of memory retrieval failure, the experimental setup was examined. Our data showed that the setup is very well suited for the analysis of aversive behavior. The expression of Chrimson in bitter receptive neurons (Gr66a) established represents a very reliable positive control for assays resulting in light avoidance. The strong light avoidance of the flies was already observable during the experiment. Recall of appetitive behavior was also possible, but the light preference was usually not strong enough to be observable by eye during illumination phases. For this reason, the T-maze was tested as an alternative setup for optogenetic experiments. The T-maze was modified by attaching a red LED at the end of one arm of the T-maze. This allowed the flies to choose between the illuminated and non-illuminated arm at the decision point.

To investigate the functionality of the new experimental setup, three genotypes were analyzed in both arena and T-maze (Figure 26). In the first control group (wild type flies), no red light-sensitive Channelrhodopsin was expressed. Therefore, these flies should not show any specific behavior to red light illumination. Because activation of Chrimson in bitter tasting receptor neurons led to robust avoidance of red light in previous experiments (Figure 24 and Figure 25), this genotype was used as a positive control. Further, Chrimson was expressed under the control of the CAMEL-tool. These flies were aversively conditioned and subjected to the light preference test 48 h after training. In the arena (Figure 26A), wild type flies displayed a light preference index around zero. Flies expressing Chrimson under the control of Gr66a showed strong avoidance of red light. Compared to the wild type control, the preference index was significantly lower. Reactivation of the conditioning-dependent memory cells resulted in a slight avoidance of red light, but the difference was not significant compared to the control groups. Interestingly, T-maze data (Figure 26B) showed clear differences compared to arena-based data. Wild type flies and Gr66a-control showed similar light avoidance behavior. The artificial recall of the aversive memory in the T-maze lead to light preference behavior. This value was significantly increased compared to both controls. These results showed that the LED setup in the T-maze is likely not ideal yet. It was noticeable that the highest intensity of the red LEDs in the T-maze setup was significantly weaker than the light intensity used in the arena. Furthermore, the distribution of the red light within the tube was not uniform. Looking at a cross section through the vial the light intensity was strongest in the center and decreased

towards the outside. A decrease in light intensity from the LED to the decision point was also observed.

For future experiments the setup needs to be improved further. An even distribution of the red light within the arm of the T-maze is necessary to enable a reliable activation of neurons. For future experiments, an LED strip could offer a good solution for evenly distributed red light. For stronger light intensity, high-power LEDs could be used.

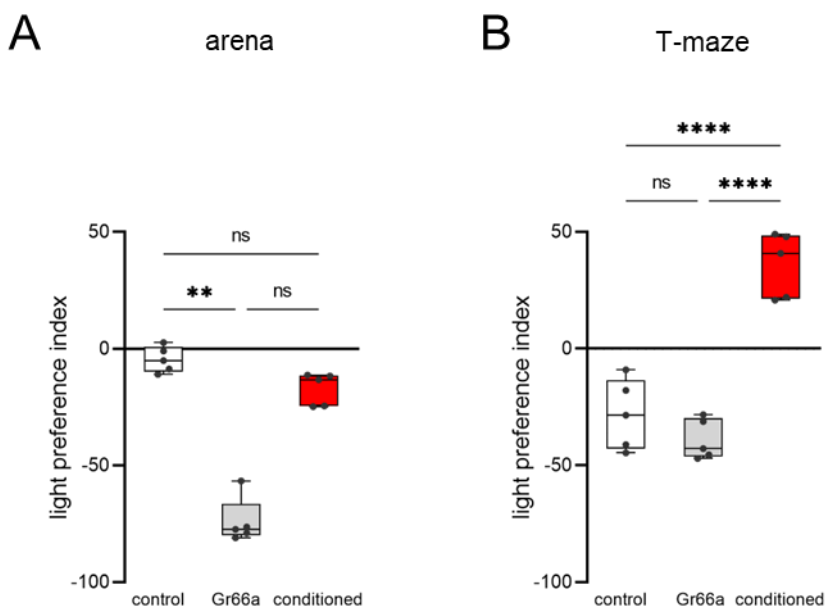


Figure 26: Comparison of memory recall in the circular arena and the T-maze.
The light preference test was performed in the arena (A) and the T-maze (B). In the arena, the control (white) showed no targeted movement towards red light. In the T-maze, red light led to avoidance behavior in the control group. The optogenetic activation of the gustatory receptor neurons required for bitter tasting (Gr66a, shown in gray) led to avoidance behavior, which was stronger in the arena than in the T-maze. The reactivation of CAMEL-cells in aversive conditioned flies (red) elicited slight light avoidance in the arena, whereas the flies preferred the illuminated arm of the T-maze upon reactivation of Chrimson-expressing neurons.

5.4 Artificial aversive conditioning

In a next step, I aimed to artificially induce the formation of an associative olfactory memory in collaboration with Benjamin Escribano. Artificial CAMEL-cell activity was supposed to be achieved using optogenetic activation. Chrimson-expressing CAMEL flies (6xCRE^{AD} ∩ R21B06^{DBD} > Chrimson) were used for these experiments. For this approach, odor exposure was replaced by red light pulses, thereby activating a random subset of Chrimson-expressing MB neurons. As mentioned before, optogenetic activation of Chrimson requires retinal as a cofactor. Flies were subjected to different retinal feeding protocols: 48 h before conditioning, 48 h before testing, or 96 h before testing (Figure 27A, upper panel). Retinal feeding of the animals is indicated by colored dots below the graphs. Two different protocols were used for conditioning (Figure 27A, middle panel). During the spaced paired protocol, flies were exposed to pulsed red light and electrical shocks simultaneously for 1 min, followed by a 15 min rest. This cycle was repeated either five or ten times. In unpaired conditioning, the electric shocks and red-light pulses were presented 5 min apart. The cycle was repeated five times with a 9 min interval. Subsequently, all flies were subjected to a light preference test (Figure 27A, lower panel). First, we aimed to identify the training protocol with the strongest light avoidance to subsequently use this protocol for the additional experiments (Figure 27B-D). In each case, non-retinal fed flies (white) served as controls. For all control groups, the value of the light preference index was around 0. Recalling 24 h memory after 5 conditioning cycles (Figure 27B) resulted in significantly increased red light avoidance compared to the control. After five cycles of conditioning, the avoidance of red light was also significantly higher compared to controls when testing 48 h memory (Figure 27C). Retrieval of 48 h memory after ten conditioning cycles (Figure 27D) showed a significantly decreased light preference index compared to the control. The difference between control and retinal-fed flies was strongest after five cycles of conditioning and 48 h delayed testing. In addition, the values in this data set showed the fewest variation. Therefore, we decided to conduct further studies with this conditioning protocol.

Testing untrained flies with different retinal treatments (Figure 27E) showed that reactivation of natural memory cells already resulted in a negative light preference index. Next, paired-conditioned flies (red) were compared with unpaired-conditioned flies (white) (Figure 27F). Optogenetic reactivation caused a slight but not significant increase in aversive behavior after paired conditioning compared to the control. We next extended the duration of retinal feeding to determine whether the light avoidance effect could be enhanced even further, (Figure 27G). However, the light preference index again showed no significant difference between paired- (red) and unpaired- (white) conditioned flies.

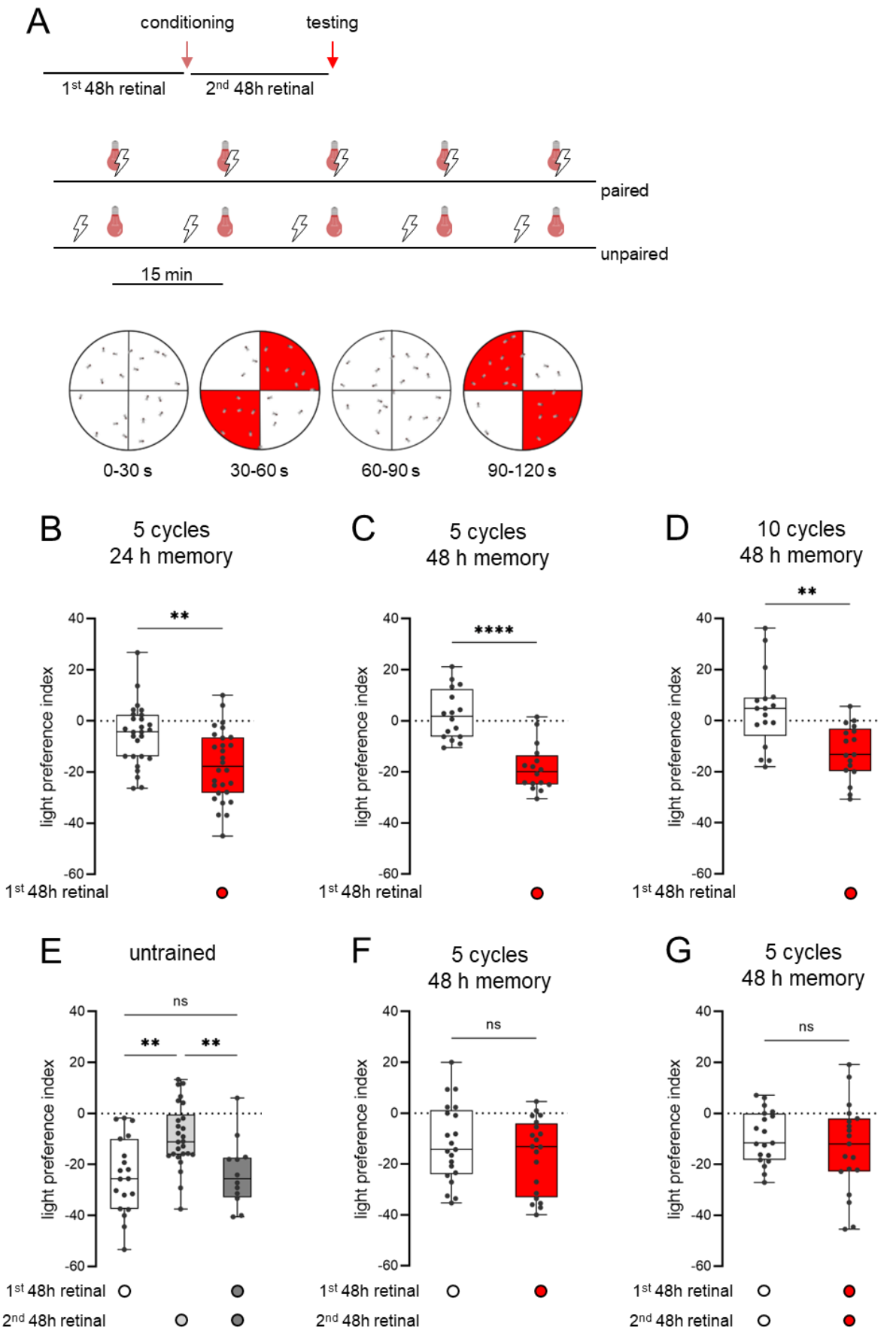


Figure 27: Artificial aversive conditioning of CAMEL-cells using red LEDs.
(A) Timeline of retinal feeding (top panel) and schematic of artificial aversive conditioning protocols with 15 min resting interval between cycles. For paired conditioning, red light was combined with an electric shock (middle

panel). During unpaired conditioning, the red light and the electric shock were presented consecutively (bottom panel). The light illumination protocol of the circular arena was used for memory recall. (B-D) Flies were either fed with retinal (dots) or not fed with retinal (missing dots) before conditioning. Flies not fed with retinal served as control (white), experimental flies (red) were fed with retinal 48 h before conditioning. The flies were subjected to five conditioning cycles and tested after 24 h (B) and 48 h (D) in the arena. (E) 48 h memory was additionally examined after ten cycles of aversive conditioning. (E) Untrained flies were exposed to different feeding protocols of retinal and tested afterwards. (F-G) Flies were conditioned in an unpaired (white, control) or paired paradigm (red) and subjected to retinal for a period of 48 h (F) and 96 h, respectively (G). Boxplots show the individual data points, the median is indicated by the central line, the box extends from the 25th to the 75th percentile, the whiskers correspond to minimum and maximum. Asterisks indicate significant differences between the tested groups.

5.5 Characterization of light activatable DopRs

5.5.1 Light activatable DopRs are incorporated into neuronal membranes

In collaboration with Nina Wilhelmy, light-activatable DopRs (provided by the Soba laboratory as part of a collaboration, Life & Medical Sciences Institute, Bonn) were characterized. The Soba laboratory generated modified versions of two different DopRs (D1R1 and D1R2) that have the potential to be activated by green light independent of the natural ligand dopamine. These receptors were under the control of the UAS element and allowed targeted expression in different tissues. The aim of our project was to determine the localization and function of these modified DopRs in cells that endogenously express DopR.

First, we used the MB specific OK107-Gal4 line to express mCD8-GFP (control) and the light-activatable DopRs in all KCs. The mCD8-GFP labeling (Figure 28A) provides an overview of MB morphology as OK107-Gal4 is expressed in all KCs. The cell bodies of the KCs are in the posterior region of the brain. Anteriorly, the axons of the KCs form the typical L-shaped MBs with the different lobes. Based on the projection pattern, three main subtypes of KCs (αβ, α'β' and γ neurons) could be identified (Crittenden et al., 1998; Lee et al., 1999). Single confocal sections of the MB lobes (Figure 23 A-C 2nd, 3rd row anterior) showed the vertical MB lobes (α and α' neurons, 2nd row), and the horizontal MB lobes (β,β', and γ, 3rd row). Expression of D1R1-V2 (Figure 28B) revealed high levels of expression of D1R1 at the soma region and within the α/β lobes. In the maximum intensity projection of the anterior section, a weak signal in α'/β' and γ lobes can also be detected. However, the α'/β' and γ signal is not evident within individual z-sections (white arrows). In contrast, expression of D1R2-V2 (Figure 28C) resulted in a much higher signal in α'/β' and γ neurons compared to D1R1-V2 with similar levels in the somata and α/β lobes. Nevertheless, the signal in the α'/β' and γ neurons (white arrows) was still much weaker than in α/β neurons.

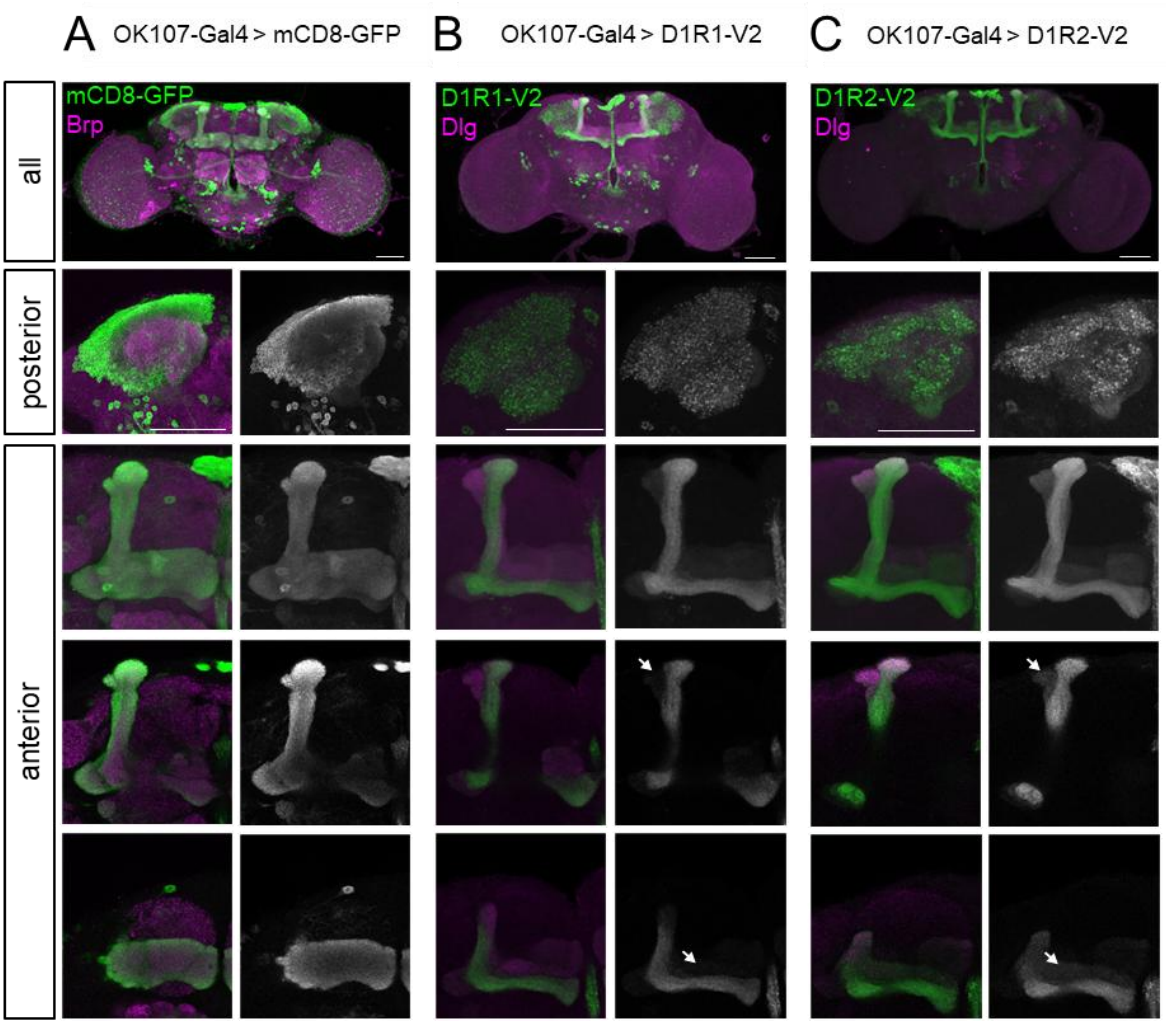


Figure 28: Subcellular localization of light activatable DopRs.
(A-C) OK107-Gal4 was used to express mCD8-GFP (A, control) and light-activatable DopRs (B, C) in all KCs to analyze their localization. Illustrated are the maximum intensity projections of the whole brain, the posterior and the anterior region (first row). The anterior region additionally contains single confocal sections of the vertical (second row) and horizontal (third row) lobes. (A) High levels of mCD8-GFP are present in all lobes and the somata of the MB. Anterior single sections reveal a punctuated mCD8-GFP signal. (B) High D1R1-V2 expression was present in the somata and α/β lobes. A weak signal was also detected in the maximum projection image of α'/β' and γ neurons but not in the single sections (white arrows). (C) D1R2-V2 signal is present in somata and all MB lobes. The receptor is mainly present in α/β neurons but can also be detected at higher levels in α'/β' and γ neurons compared to D1R1-V2 (B, white arrows). All scale bars represent 50 µm and apply to all images within the panels.

The expression of the DopR versions in the entire MB allowed us to determine the localization within the lobes, but the distribution within individual neurons remained unclear. To analyze this, we used the CAMEL-tool inserted at a different chromosomal location (VK27). The standard CAMEL-tool (attP40) marks about eleven KCs (memory engram cells) per brain likely activated through natural memory formation. The VK27 variant is only expressed at very low levels resulting in specific labeling in just about one-third of the brains and the number of labeled CAMEL-neurons is very low (1-3 neurons). This allowed the analysis of receptor distribution within individual neurons (Figure 29). To facilitate the analysis, we co-expressed myr-tdTomato with the light-activatable DopR to mark the cell membrane. In Figure 29A, two α/β neurons and one γ neuron are marked by membrane-targeted myr-tdTomato. In the three

cell bodies (left column, white arrows), D1R1-V2 was highly expressed. While only low levels of the receptor could be detected in the dendrites (left column), D1R1-V2 was clearly visible in a dotted pattern throughout the axons in the MB lobes (right column). In Figure 29B, a single α/β neuron was labeled by the CAMEL-tool. D1R2-V2 also accumulated in the cell body (left column, white arrow) and weak signals could be detected in the dendrites (left column, lower panel). Within axons (right column) only very few dots of D1R2-V2 could be identified.

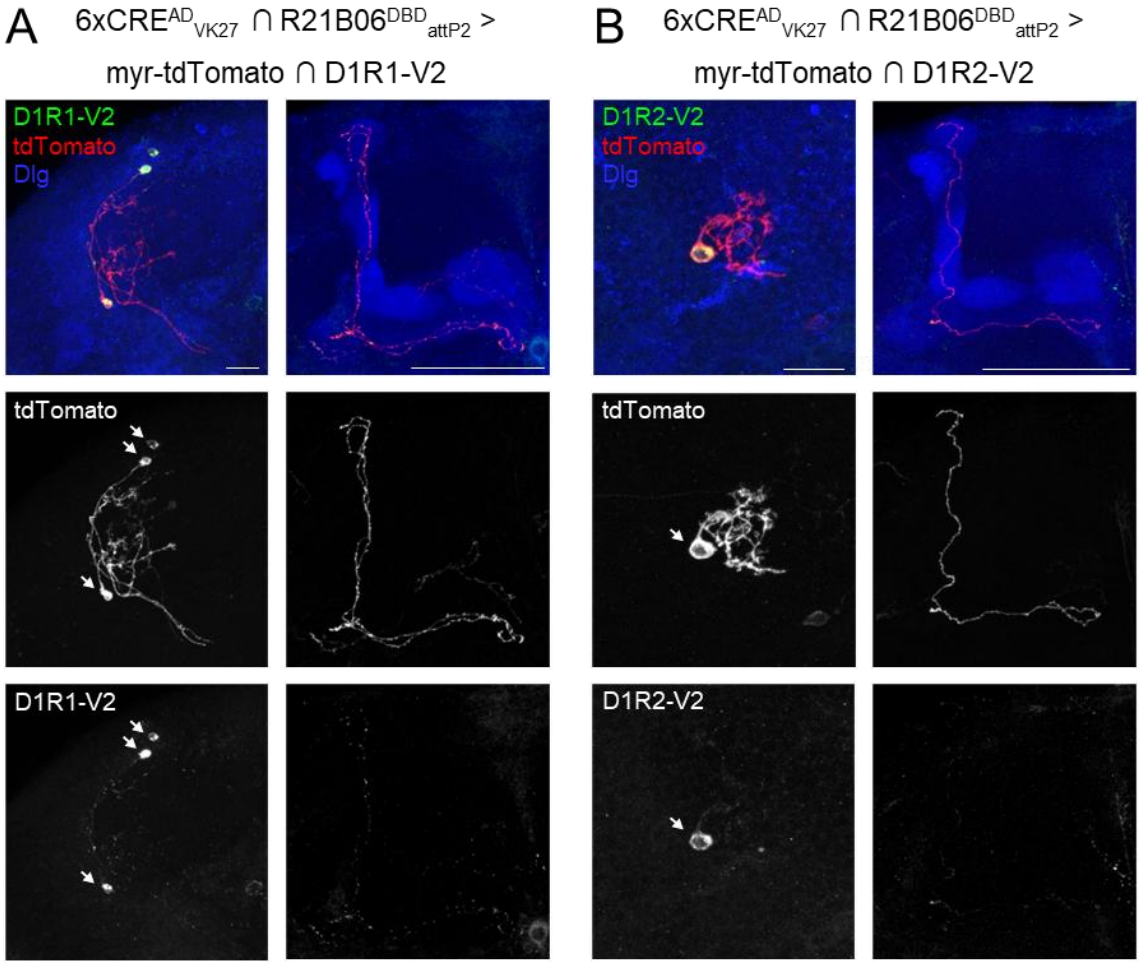


Figure 29: Localization of light activatable DopR in single neurons.
(A-B) DopR (green) expression was limited to a small subset of MB neurons using the CAMEL-tool. Expression of myr-tdTomato (red) in CAMEL-neurons allowed visualization of the entire neuron (middle panels) thereby facilitating the analysis of the DopR localization (lower panels). (A) Three neurons were labeled by tdTomato; their somata are indicated by white arrows. D1R1-V2 accumulated strongly in the somata and weakly in the dendrites (lower left panel). The merge of Dlg (blue) and tdTomato signals (upper, right panel) revealed that two α/β neurons and one γ neuron were labeled in this brain. A weak, punctuated D1R1-V2 signal was present in the axons (lower right panel). (B) A single α/β neuron was positive for tdTomato (upper panels). D1R2-V2 signal was strong in the soma (white arrow). Only low levels of D1R2-V2 were present in dendrites (lower left panel) and D1R2-V2 was only present at very low levels in the axon. Scale bars correspond to 10 µm (left panels) and 50 µm (right panels).

5.5.2 DopR activity in KCs is required but not sufficient for learning

We next investigated the role of the DopRs for learning. First, the necessity of the endogenous D1R1 for learning was analyzed (Figure 30B). We used a temperature-sensitive Gal80 to block Gal4-mediated RNA-interference (RNAi) expression in a temperature-dependent manner during development (Lee and Luo, 1999). The flies were raised at the restrictive temperature 20°C (Gal80 blocks Gal4) to prevent any expression during larval and pupal development. The experimental flies (green in Figure 25) were then shifted to 31 °C to induce RNAi expression one to three days after hatching and four days before conditioning. The parental controls (white and gray) were also subjected to the temperature shift. The flies were trained for five cycles in a custom-made apparatus (Figure 30A, upper panel). Odor A was paired with electrical shocks (negative stimulus) to induce an association of the negative stimulus with the odor. At the cellular level, the electrical shocks lead to an activation of PPL1 neurons (dopaminergic), which innervate the vertical lobes of the MB, and to the release of dopamine (Aso et al., 2012; Mao and Davis, 2009; Figure 30A, MB schematic). Dopamine then binds to the DopRs of the KCs in the vertical lobes and activates downstream G-protein based signaling (Beaulieu et al., 2015; Karam et al., 2020). Conditioning of both parental controls resulted in a strong aversive learning performance. The preference indices of the controls were not significantly different from each other. Compared with both parental controls, RNAi-mediated knockdown of D1R1 in the MB resulted in a significant impairment of learning performance. This indicates that endogenous D1R1 is required for learning in KCs (Figure 30B).

Next, we examined whether ectopic overexpression of the light-activatable D1R1-V2 impaired learning (Figure 30C). Expression of D1R1-V2 was again controlled in a temperature-sensitive manner by Gal80 and active expression was only induced 4 days before conditioning. The overexpression of D1R1-V2 caused a minor decrease in learning performance but did not result in a significant difference to the parental control genotypes (Figure 30C). Based on these results we used D1R1-V2 overexpression for further experiments.

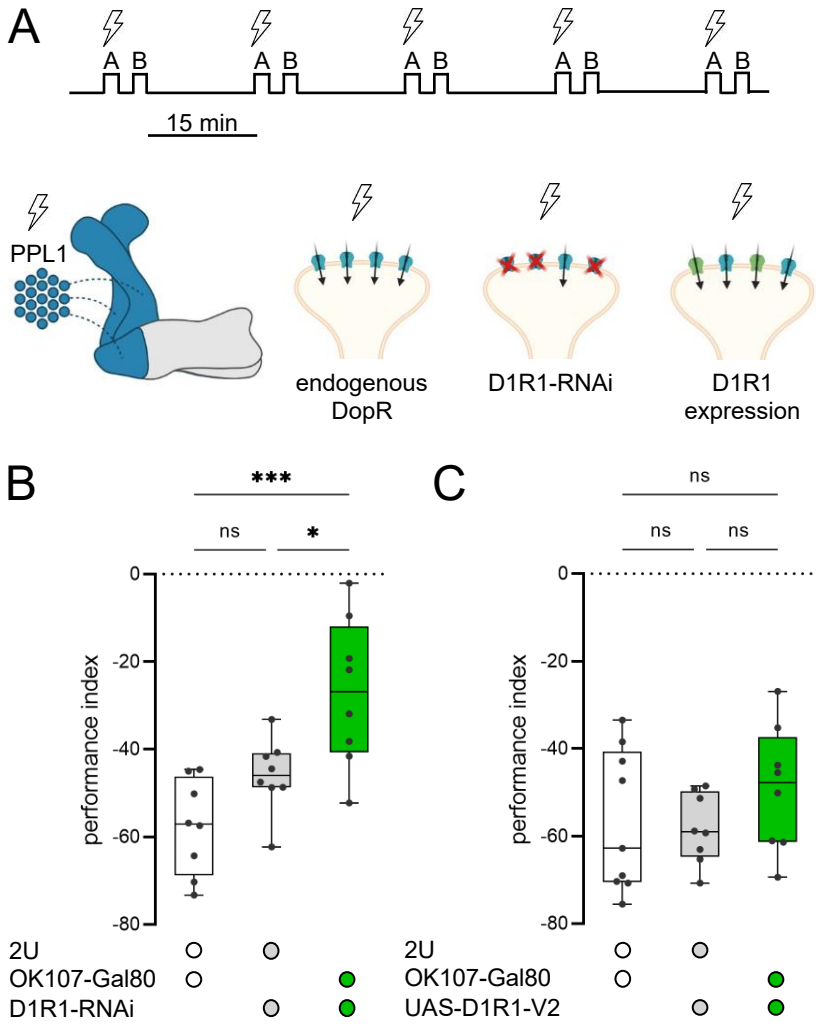


Figure 30: Analysis of DopR knock down and overexpression for learning.
(A) Schematic drawing of the aversive olfactory conditioning protocol and experimental principles. During conditioning, odor A was paired with the electric shock, and odor B was presented shortly afterwards. The cycle was repeated five times with 15 min intervals. This spaced paired training leads to the activation of DANs in the PPL1 cluster that innervates the vertical lobes of the MB (shown in blue in the MB schematic). In wild type flies, dopamine binds to endogenous receptors of the vertical lobes, activating the intracellular signaling cascade (shown in the left scheme). In D1R1-RNAi expressing flies, the number of endogenous DopRs is reduced, resulting in less DopR activation in the vertical lobes. Overexpression of D1R1-V2 results in the presence of both endogenous and light-activatable DopRs. Dopamine released from PPL1 neurons can therefore activate endogenous and D1R1-V2 receptors in the vertical lobes. (B) Learning was significantly reduced in RNAi expressing flies compared to parental controls. (C) Overexpression of D1R1-V2 had no significant effect on learning performance. Boxplots show the individual data points, the median is indicated by the central line, the box extends from the 25th to the 75th percentile, the whiskers correspond to minimum and maximum. Asterisks indicate significant differences between the tested groups.

Next, we wanted to investigate whether optogenetic activation of D1R1-V2 has the potential to influence learning performance. For this purpose, odor A was paired with electric shocks and with green light (Figure 31A, upper panel). In these flies, the shock activates PPL1 neurons, that in turn release dopamine onto the vertical MB lobes. In these lobes, dopamine can activate both endogenous DopRs and D1R1-V2. In contrast, illumination with green light will result in

an activation of D1R1-V2 throughout the entire MB, likely perturbing region-specific KC activation (Figure 31A, MB Scheme).

In the first experiment, we used pulsed green light (Figure 31B). Experimental flies (green) were fed retinal before conditioning and exposed to odor, shock, and light during conditioning. These parameters should result in an activation of endogenous DopRs in the vertical lobes and an activation of D1R1-V2 in all lobes. This learning paradigm resulted in a negative behavioral performance index, but the values were not significantly different from control flies that were not fed the cofactor 9-cis-retinal required for light-activatable DopRs function (white). In the control setting, only the endogenous DopRs in the vertical lobes were activated by dopamine via the PPL1 neurons. Control flies that were exposed to retinal, odor and shock but not light (gray) showed a more negative performance index, but this difference was not significantly different from the other two groups. These results suggest that pulsed green light may interfere with learning independent of D1R1-V2 activation. For this reason, we tried different green light illuminations (data not shown) and decided to continue the experiments with continuous green light exposure.

The only variable that was altered between the first and second attempt (Figure 31C) was the use of continuous green light during conditioning. Conditioning the retinal-free (white) and light-free (gray) controls resulted in comparable aversive performance indices. If flies were fed retinal and exposed to odor, shock, and continuous green light during conditioning (green), there was a trend towards increased avoidance behavior. As the two control groups now showed identical behavior it suggests that the green light stimulus no longer interfered with learning. The trend towards increased learning, though not significant, indicates that the additional activation of D1R1-V2 during conditioning may enhance learning.

In the final experiment (Figure 31D), the electric shock was omitted and replaced by continuous green light. The first control (white) was conditioned with odor and light but was not fed retinal. Consequently, the DopRs were neither activated by light or electrical shocks and no learning was observed. The second control (gray) was fed with retinal and conditioned only with odors. Again, no learning was observed. The experimental flies (green) were fed with retinal and odor exposure was paired with continuous green light during conditioning. This treatment should activate D1R1-V2 in all MB lobes. However, this artificial activation of D1R1-V2 throughout all MB lobes was not sufficient to induce learning.

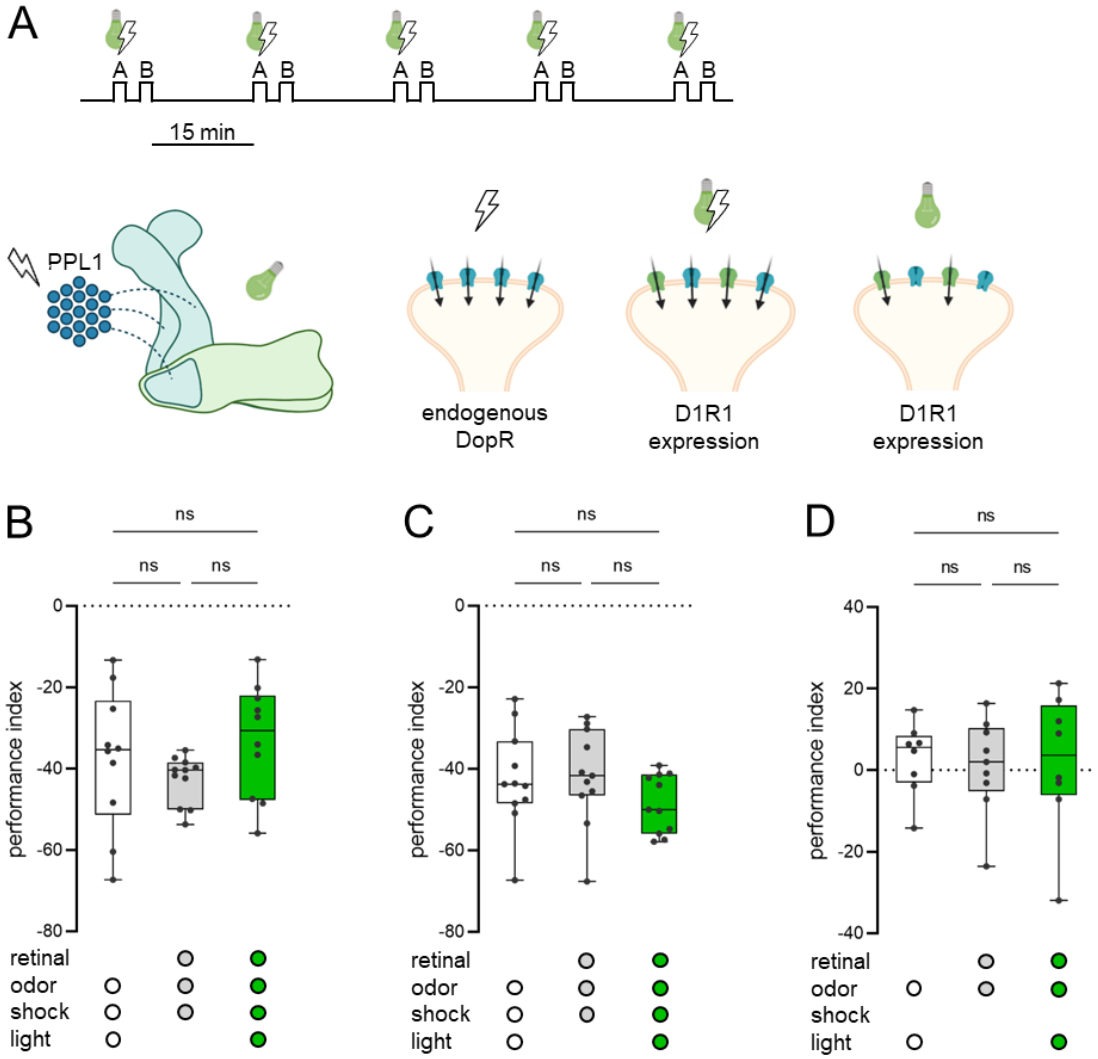


Figure 31: Activation of exogenous D1R1 is not sufficient to induce learning.
(A) Schematic drawing of artificial conditioning protocol and experimental principles. Odor A was paired with pulsed (B) or constant (C-D) green light (225 nm). Odor B was presented after a short time delay. The cycle was repeated five times every 15 mins. The electric shock activated the PPL1 neurons innervating the vertical lobes (shown in blue in the MB schematic). Since D1R1-V2 receptors are located at both horizontal and vertical lobes of the MB, green light exposure should result in receptor activation throughout the MB independent of DAN activity (shown in the MB scheme). All flies (B-D) expressed the D1R1-V2. When the cofactor 9-cis-retinal was not fed only the endogenous DopR were activated by electric shock (first post synapse). Shock exposure should result in an activation of endogenous and exogenous DopRs in the horizontal lobes (second synapse). Simultaneous exposure to electric shocks and green light should lead to the activation of endogenous and exogenous DopRs, as well as D1R1-V2 light-activation in the entire MB (third post synapse). When the electric shock was replaced by green light during conditioning, D1R1-V2 but not endogenous DopRs can be activated by light (fourth post synapse). (B) Pulsed light impaired learning performance independent of 9-cis-retinal feeding (white and green) compared to the conditioning control without light (gray). (C) Learning was not affected by constant green light. No difference was detected between the non-retinal control (white) and the control without light (gray). Conditioning with light, shock, and odor resulted in a non-significant improvement of learning performance. (D) Replacing the shock with light stimulation was not sufficient to induce learning. The mean values of all three conditions were close to 0. Boxplots show the individual data points, the median is indicated by the central line, the box extends from the 25th to the 75th percentile, the whiskers correspond to minimum and maximum. Asterisks indicate significant differences between the tested groups.

6. Discussion

Learning and memory in *Drosophila melanogaster* rely on the associative pairing of sensory stimuli with valence, leading to synaptic plasticity and behavioral adaptation. LTM is formed through structural and molecular changes in the MB and is retrieved by reactivation of sparse engram cells population. In this study, I used the CAMEL-tool to investigate the properties of engram cells at both the molecular and behavioral level.

Taken together, my findings indicate that CAMEL activity is experience-dependent and dynamically reflects changes in environmental stimulation. Both the number of labeled CAMEL-cells and the resulting behavioral output were modulated by sensory context, with multimodal stimulation being required to induce robust and retrievable aversive behavior. Furthermore, CAMEL-labeling was observed in both aversive and appetitive paradigms, highlighting its general applicability for marking memory-related neuronal populations.

In addition, the characterization of the optogenetic DopR variant D1R1 demonstrated that dopaminergic signaling in KCs is required but not sufficient for memory formation, emphasizing the importance of precise spatiotemporal coordination of neuromodulatory input during learning. Together, these results establish CAMEL as a powerful tool to link experience-dependent neuronal activity with behavior and provide a framework for dissecting the cellular and molecular mechanisms underlying memory formation.

6.1 Experience-dependent CAMEL-tool activity

Our environment consists of both inanimate (visual, auditory, olfactory, gustatory and haptic) and social stimuli which are detected and processed in the brain. Enriched environment experiments have become a well-established paradigm in behavioral research, allowing the study of how environmental factors shape neuronal structures (Kempermann, 2019). These experiments are primarily performed in rodents, where animals are housed with conspecifics (social stimulus) in large cages enriched with toys, nesting material and retreat possibilities (inanimate stimulus). The behavioral and neuronal effects of enriched environments are compared with those of animals kept in standard laboratory conditions. Due to the absence of a standardized protocol, experimental designs vary considerably across studies (Fares et al., 2013; Xie et al., 2013). Despite these methodological differences, several consistent findings have emerged, including cortical enlargement (Rosenzweig et al., 1964, 1962), increased hippocampal neurogenesis (Kempermann et al., 1997; Schloesser et al., 2010; Zhang et al., 2018), altered gene expression (Keyvani et al., 2004; Rampon et al., 2000; Rattazzi et al., 2016) and enhanced memory performance in various learning tasks (Garthe et al., 2016; van Praag et al., 2000). In addition to mammals, the effects of environmental enrichment have also been studied in invertebrates such as zebrafish (Volgin et al., 2018), *Drosophila* (Dukas and

Mooers, 2003; Wang et al., 2018), crickets (Judge, 2010; Mallory et al., 2016), and *C. elegans* (Guisnet et al., 2021).

To provide a better understanding of the interaction between environmental stimuli and memory formation in fruit flies, I established a protocol that allows the controlled deprivation or addition of specific cues. I aimed to use the CAMEL tool to label environment-induced engram cells and optogenetically reactivate them, to investigate how environmental factors influence behavior at a neuronal level. This approach would provide a novel framework for investigating the mechanisms by which environmental experiences shape memory traces and behavioral responses in invertebrates.

6.1.1 CAMEL-tool activity in sensory-deprived pupae

We have previously shown that under standard laboratory conditions the CAMEL-tool labels approximately eleven cells, likely representing the natural memory trace in flies (Siegenthaler, 2019; Siegenthaler et al., 2019). By diminishing olfactory input using odor-free food, we were able to significantly reduce the number of CAMEL-positive cells compared to controls. Based on this, I aimed to identify a condition under which CAMEL activity is reduced as much as possible, assuming that minimal environmental stimulation would result in minimal labeling. I therefore focused on the pupal stage, during which flies are naturally isolated from external sensory inputs. On average, these brains contained only a single EGFP expressing cell in the MB (Figure 13A1-D1). These results prove that the CAMEL tool activity relies on sensory input.

During pupal development, sensory-driven activation of the olfactory system is expected to be strongly reduced. Although electrophysiological studies indicate that elements of the olfactory circuit can exhibit spontaneous activity at this stage (Xu et al., 2015) , suggesting that *Drosophila* pupae are capable of odor reception. However, the extent to which odorants penetrate the pupal case remains unknown. While it is well established that insect cocoons are permeable to oxygen and carbon dioxide to ensure gas exchange (Arthur Woods and Lane, 2016; Cavallaro and Hoback, 2014; Hetz and Bradley, 2005), no data exists on their permeability to odorants. More importantly, even if weak sensory stimulation occurred, these stimuli would not acquire valence in the absence of reinforcement such as reward or punishment. As a result, CREB-dependent labeling would not be induced.

In addition, the detectability of CAMEL-labeled cells depends not only on the activity of the Gal4-UAS system but also on the dynamics of EGFP expression. EGFP can be detected within a few hours after induction and has a long half-life, leading to accumulation in labeled cells (Corish and Tyler-Smith, 1999; Hazelrigg et al., 1998). Therefore, if the CAMEL-tool had been

activated during the pupal stage, EGFP fluorescence should have been detectable at the time of dissection. Taken together, in the absence of sensory stimuli paired with valence, the CAMEL tool remains inactive, demonstrating that all observed labeling at later time points arises from experience-dependent, endogenously formed memory traces.

6.1.2 Neural impact of social isolation

Social interactions play a crucial role in shaping behavior, cognition, and neuronal plasticity across species. Social isolation has been shown to affect neural development, stress responses, and learning abilities in mammals (Arakawa, 2018; Einon and Morgan, 1977; Fone and Porkess, 2008; Heidbreder et al., 2000; Serra et al., 2003), birds (Aydinonat et al., 2014; George et al., 2020), fish (Ward et al., 2011), primates (Harlow et al., 1965), and humans (Chappell and Badger, 1989). Although *Drosophila melanogaster* is not eusocial, it exhibits diverse social behaviors (Ferreira and Moita, 2019; Sokolowski, 2010). These behaviors rely on pheromone-based communication for species recognition, mating, and information transfer about food sources (Bartelt et al., 1985; Billeter et al., 2009; Ferveur, 2005; Ramdya et al., 2014; Savarit et al., 1999; Soto-Yéber et al., 2018). Thus, *Drosophila* provides a valuable model to study the neural basis of social experience.

To assess the impact of social isolation on engram cell formation, I reared male flies either in isolation or in a social group consisting of 40 individuals (equal numbers of males and females). I hypothesized that the deprivation of social interactions would lead to a reduction in CAMEL-labeled engram cells. However, while a trend towards fewer labeled cells in isolated flies was observed, the difference was not statistically significant (Figure 13A2-D2). A possible explanation for this result is that the isolation period in my experiment was too short to induce measurable effects. Li et al., (2021) demonstrated that prolonged social isolation in *Drosophila* alters sleep patterns and increases food intake due to stress. However, these effects only emerged after five to seven days of isolation, whereas shorter periods (one to three days) had no significant impact. Since the flies in my experiment were isolated for four days, this duration might have been insufficient to induce substantial neuronal changes. Moreover, environmental conditions have been shown to influence the number of KCs in the MB. It was found that flies reared in isolation for three weeks exhibited a significant reduction in KC numbers compared to socially reared controls (Technau, 1984), A similar effect on MB size has also been observed in honeybees (Maleszka et al., 2009). While my experiment focused on short-term isolation, subtle structural changes in the MBs cannot be ruled out and may have influenced CAMEL labeling.

Furthermore, social isolation itself might act as a stressor, potentially leading to engram cell formation rather than reducing it. Stress is known to influence memory processes across species, including humans (Kim and Diamond, 2002; Kolb and Whishaw, 1998; McEwen and Sapolsky, 1995). In humans, chronic social isolation and loneliness have been associated with cognitive decline, increased susceptibility to mental health disorders, and disrupted sleep patterns (Azizi-Zeinalhajlou et al., 2022; Leigh-Hunt et al., 2017; Pearce et al., 2023; Sachdev, 2022). Given that sleep disturbances are also a key consequence of isolation in *Drosophila* (Li et al., 2021), it is possible that similar mechanisms underlie the neuronal changes observed across species.

Another potential explanation is that memory traces related to social interactions are encoded in a distinct neuronal population that is not captured by the CAMEL-tool. Given that pheromone-based communication plays a central role in *Drosophila* social behavior - including species recognition, foraging, and courtship (Bartelt et al., 1985; Billeter et al., 2009; Ferveur, 2005; Ramdya et al., 2014; Savarit et al., 1999; Soto-Yéber et al., 2018) – it seems unlikely that the absence of conspecifics has no significant effect on memory traces. Therefore, I propose that social experiences are represented in a different subregion of the MB. This would result in no observable difference in the number of CAMEL cells following social isolation.

6.1.3 Increased environmental stimulation enhances CAMEL-activity

6.1.3.1 CAMEL-labeling through mechanical stimulus

After analyzing the effects of reduced environmental influences using CAMEL-dependent EGFP expression, I next focused on the more extensively studied area of increased environmental stimuli. To investigate the impact of mechanical stimulation, I quantified the number of labeled CAMEL-neurons after repeatedly transferring flies into fresh food vials multiple times per day. I observed a trend towards an increased number of labeled cells (Figure 14B1-E1).

Although this effect did not reach statistical significance, it is likely that mechanotransduction was activated during the transfer process. In *Drosophila*, mechanotransduction occurs through the activation of ion channels in response to mechanical stimuli such as stretch or tension, thereby triggering defensive behaviors that promote survival (Hehlert et al., 2021; Kim et al., 2012; Li et al., 2016). Strong mechanical stimuli may also activate nociceptors that mediate the perception of harmful stimuli (He et al., 2022).

Alternatively, the mechanical stimulus or the repeated environmental disturbance may have induced a stress response, leading to increased CAMEL activity. Stress paradigms in

Drosophila have been shown to alter behavior and neurotransmitter systems, including serotonergic signaling in the MB (Neckameyer and Weinstein, 2005; Ries et al., 2017). Given the evolutionary conservation of neurotransmitter systems between vertebrates and *Drosophila*, the fly has emerged as a valuable model to study the neurobiological effects of stress.

As in mammals, stress alters both behavior and neurotransmitter systems in adult flies (Amat et al., 2005; Argue and Neckameyer, 2013; Chadha and Cook, 2014; Ramos-Hryb et al., 2021). The hypothesis that stress induces neurochemical changes within the MBs could explain why mechanic stimulation led to increased CAMEL-activity in my experiments. This idea is supported by studies on cAMP signaling in stress responses. In mice, mutations in the cAMP pathway have been linked to stress-induced behavioral changes (Brewer et al., 2003; Kim and Han, 2009; Razzoli et al., 2010; Schaefer et al., 2000). Similarly, studies in *Drosophila* suggest that cAMP pathway mutants are hypersensitive to aversive stress stimuli (Chadha and Cook, 2014; Préat, 1998).

In addition to molecular analyses, I performed behavioral assays to assess whether mechanical stimulation affects CAMEL-dependent behavior using optogenetic reactivation (Figure 16C). However, contrary to previous reports, I did not observe significant behavioral differences compared to the control. One possible explanation is the short duration of the mechanical stimulus in my experiment: flies were transferred from one vial to another three times per day over the course of three consecutive days and returned to the original vial 15 minutes later. In other studies with adult flies, mechanical stress was applied for 10 h per day (Ries et al., 2017) or even continuously for 24 h (Neckameyer and Weinstein, 2005).

6.1.3.2 Combined Environmental Stimulation Enhances CAMEL-Activity

Since mechanical stimulation alone did not significantly increase CAMEL-labeling, I hypothesized that a combination of environmental stimuli might amplify the effect. To test this, I combined the mechanical stimulus with an olfactory stimulus (presentation of 4-EG at a dilution of 10^{-3}). This approach indeed led to a significant increase in the number of EGFP-labeled CAMEL neurons (Figure 14B2-E2).

This effect is most likely explained by the formation of an associative memory. In a previous study, we demonstrated that aversive olfactory conditioning significantly increased the number of CAMEL-positive cells (Siegenthaler et al., 2019). These conditioning-dependent CAMEL-neurons could be optogenetically reactivated, leading to avoidance behavior. While my experiment does not follow a classical conditioning paradigm, it involved the repeated pairing of a potentially aversive stimulus (mechanical stimulation) with an odor over the course of nine

trials. Possibly, this temporal pairing was sufficient to induce an associative memory trace, resulting in the recruitment of CAMEL-neurons. A purely additive effect of independent sensory inputs cannot be excluded but appears less likely.

To further increase environmental complexity, I introduced virgin females into the cohort (Figure 14B3-E3). The presence of virgin females therefore likely resulted in courtship-related activation of sensory neurons. However, although the number of CAMEL-positive cells was significantly increased compared to the control, the addition of a third stimulus did not lead to a further increase compared to the combined mechanical and olfactory stimulation. This may indicate that courtship-related stimuli do not further enhance CAMEL activity, possibly because the neuronal circuits underlying courtship behavior only partially overlap with the MB neuron population labeled by the CAMEL tool. For example, P1 neurons and other components of the male-specific courtship circuitry are known to be activated by female cues and mediate behavioral output outside the MB (Kohatsu et al., 2011; Liu et al., 2019; Yamamoto and Koganezawa, 2013). The observed CAMEL activity may therefore not fully capture the neuronal representation of courtship behavior in this context.

Taken together, these findings indicate that CAMEL activity is experience-dependent and scales with the number of memory-inducing events. The results suggest that meaningful combinations of sensory stimuli, rather than single stimuli alone, are required to robustly increase CAMEL labelling, emphasizing the importance of identifying behaviorally relevant stimuli when using CAMEL as a proxy for natural memory formation in *Drosophila*. These findings highlight the complexity of social influence on neuronal circuits and points to the need for further investigations. Future experiments could investigate the impact of prolonged social exposure or directly test the influence of different social contexts using alternative tools, such as monitoring specific pheromone-related neuronal subpopulations in the MB. These approaches may provide deeper insights into the role of social experience in shaping memory and behavior in *Drosophila*.

6.1.4 Experience-dependent memory modulates behavior

After demonstrating that increased environmental influences cause structural changes within the MB, I next investigated whether these modulations are linked to experience-dependent memory encoding and are reflected in specific behavioral responses. While I detected an increase in the number of CAMEL-labeled cells, the valence of these additionally labeled neurons remained unclear – specifically, whether they encoded appetitive or aversive memories. To address this, I used the CAMEL-tool to express light-activatable Chrimson channels in the experience-dependent CAMEL-cells. By optogenetically reactivating these cells, I was able to examine whether the experience dependent engram cells do encode an

appetitive or aversive memory observable by the corresponding behavior upon successful recall.

For this purpose, flies were exposed to different sensory stimuli over three consecutive days and tested in a light preference assay on the fourth day. While individual stimuli did not induce significant behavioral changes (Figure 16B-D), the combination of mechanical and olfactory stimulation resulted in a significant increase in light avoidance (Figure 16E). This contrast between the individual and combined stimuli highlights the importance of multisensory integration for memory formation. After successfully retrieving the experience-dependent aversive behavior, I quantified the number of CAMEL-positive neurons within the same flies, allowing a direct correlation between cell count and behavior (Figure 16E). The number of labeled cells significantly increased compared to the control, indicating that the combined stimulation recruited additional engram cells. In line with previous experiments, optogenetic reactivation of these cells induced avoidance behavior, suggesting that this experimental paradigm resulted in aversive memory formation.

Together, these findings suggest that single sensory stimuli alone are not sufficient to induce stable, retrievable memory, but rather require the pairing of multiple sensory cues, consistent with classical conditioning. This is in agreement with previous studies showing that multisensory learning in *Drosophila* enhances memory performance by linking the activity of modality-specific KCs in the MB (Okray et al., 2023). While individual sensory stimuli are often variable in their effects, their combination can evoke enhanced neural activation, which facilitates more stable memory consolidation (Waschke et al., 2025). This explanation helps account for the lack of measurable behavioral change in response to individual stimuli in my experiments, while the combination of mechanical and olfactory stimulation resulted in significant light avoidance.

As suggested by the labeling experiments (see section 6.1.3.2), the most likely explanation is that the mechanical stimulus acted as a stressor, triggering dopaminergic signaling that supported the formation of an aversive associative memory when paired with the olfactory stimulus. In contrast, a simple summation of independent sensory inputs appears unlikely to account for the observed increase in CAMEL labeling. In this context, 4-EG, used at a concentration of 10^{-3}, has been shown to induce aversive behavior (Brown et al., 2017; Dweck et al., 2016), indicating that both stimuli likely carried negative valence. Their combination may therefore have enhanced synaptic depression in the CAMEL-labeled neurons, reinforcing the observed avoidance behavior. It is noteworthy that even control flies displayed a slight light avoidance, suggesting that subtle aversive experiences may already occur under standard housing conditions and contribute to memory formation.

6.2 Appetitive memory formation and engram cell recruitment

We previously demonstrated that the number of labeled CAMEL-cells significantly increased 48 h after aversive conditioning. Moreover, we were able to retrieve the conditioning-dependent behavior through optogenetic activation of CAMEL-positive engram cells (Bräuler, 2019; Siegenthaler et al., 2019). The remarkable aspect of this approach is that it enables artificial reactivation of CAMEL neurons, allowing the associated behavior to be recalled even in the absence of the CS^+.

Since our previously published experiments focused exclusively on aversive memory, I aimed to demonstrate that CAMEL-activity can also reflect successful appetitive memory formation following conditioning. This would highlight the versatility of the CAMEL-tool, as this would enable us to label and manipulate engram cells associated with both positive and negative valences, thereby offering new possibilities for future research into memory mechanisms. First, I performed paired appetitive conditioning and subsequently tested learning and memory performance (Figure 20B-C). I was able to demonstrate that the performance was significantly increased compared to the control in both cases. However, it is important to emphasize that learning and memory performance were assessed using an odor preference test. Therefore, flies were simultaneously exposed to the CS^+ (the odor paired with the US) and the CS^- (the unpaired odor) at the decision point of the T-maze and were free to choose which odor they preferred by choosing the respective arm of the T-maze. Consequently, the presentation of the CS^+ triggered an association with rewarded behavior, causing the flies to move in the corresponding direction. Using an olfactory approach for memory recall does not result in the specific reactivation of CAMEL-positive engram cells, but rather the reactivation of all conditioning-dependent engram cells.

Next, I examined the conditioning-dependent labeling of CAMEL-neurons. I showed that the number of CAMEL-positive cells was significantly higher after paired conditioning compared to the mock-conditioned control (Figure 20D-E). Interestingly, the number of CAMEL-positive cells following aversive (12 cells, Siegenthaler et al., 2019) and appetitive conditioning (13 cells) was comparable, supporting the validity of my experiment. However, it remains uncertain whether all engram cells formed during appetitive conditioning are captured by the CAMEL-tool. Previous studies have shown that 5–10 % of KCs reliably respond to each odor presentation (Honegger et al., 2011; Perez-Orive et al., 2002; Turner et al., 2008), corresponding to approximately 200 to 400 KCs. Importantly, it remains unclear what fraction of these odor-responsive neurons contributes to memory encoding. Thus, I was able to demonstrate that the CAMEL-tool is suitable for labeling and targeting of memory cells following both aversive and appetitive conditioning. However, only a small subset of the potentially odor-responsive KCs was captured using the CAMEL-tool.

To test whether appetitive memories could be retrieved via optogenetic activation of CAMEL-cells, I trained flies that expressed the light-activatable Chrimson channel under the control of the CAMEL-tool. I then subjected them to a light preference test in the arena, where conditioning-dependent CAMEL-cells should be reactivated by red light illumination (Figure 23). However, I was unable to retrieve the associative appetitive memory using this method. To rule out methodological reasons for this failure, I examined several critical aspects of the experiment, starting with retinal uptake. For the recall of appetitive memory, it is necessary that the flies are starved between conditioning and testing. Therefore, the retinal had to be ingested with water and not food. My results confirmed that a 24 h retinal feeding period was sufficient for neuronal activation in the arena, regardless of whether retinal was provided in water or standard fly food (Figure 24). Thus, insufficient retinal uptake was unlikely to be the cause of the unsuccessful memory retrieval.

To eliminate additional potential sources of error, I critically examined the manual data analysis. Initially, I evaluated the videos recorded in the circular light arena by manually counting the number of flies in illuminated and non-illuminated quadrants and calculating the light preference index (Bräuler, 2019; Siegenthaler et al., 2019). However, this approach was time-consuming and susceptible to human bias. To address these limitations, an automated analysis tool was developed by Hannes Euler. A comparison between manual and automated evaluations confirmed the accuracy of the tool, as both methods yielded nearly identical results (Figure 25). This consistency validates the reliability of my previously collected data and indicates that human influence on the analysis can be considered negligible in this case. Nevertheless, in experiments with weaker behavioral responses or more ambiguous movements, observer bias could become more relevant, highlighting the general advantage of automated methods. Moreover, the use of standardized automated analysis allows for improved comparability across datasets and experimental conditions. At the same time, the automated analysis tool proves to be of advantage for future studies, as it enables a more detailed and time-efficient data evaluation. Its functionality could also be expanded in the future to include additional parameters or analysis types, similar to those described in previous studies (Aso et al., 2014b).

The arena is an established method for activating Chrimson-expressing cells and recalling the corresponding behavior. However, since the optogenetic reactivation of conditioning-dependent CAMEL-cells did not induce appetitive behavior, I wanted to test whether an approach in the T-maze would enable a successful memory retrieval. Therefore, a red LED was attached to the end of one arm of the T-maze. I decided to directly compare fly behavior in both setups. Since the recall of aversive behavior proved to be highly stable in my hands, I chose to aversively condition Chrimson-expressing CAMEL flies and test them in both setups (Figure 26). Additionally, as controls I included wild-type flies and used the Gr66a driver line,

to restrict Chrimson expression to bitter-sensing neurons. They served as a positive control, since optogenetic activation of Gr66a neurons was previously shown to reliably induce aversive behavior (Aso et al., 2014b; Bräuler, 2019; Marella et al., 2006). Comparing the two setups revealed clear differences in light-induced behavioral responses. Red light had no effect in the arena on control flies, the light preference index was close to zero. Whereas in the T-maze, control flies avoided the illuminated arm. Optogenetic activation of Gr66a-expressing bitter-sensing neurons induced light avoidance in both setups, but the light preference index was lower in the arena. Reactivation of the CAMEL neurons following aversive conditioning elicited avoidance behavior in the arena, whereas in the T-maze it unexpectedly resulted in light approach behavior. In accordance with previous publications (Aso et al., 2014b; Bräuler, 2019; Siegenthaler, 2019; Siegenthaler et al., 2019), these findings confirm that the arena is a reliable setup for optogenetic experiments. This is due to the robust activation of Chrimson-expressing cells and the absence of behavioral responses to red light alone in control flies, indicating that light stimulation itself does not influence behavior. In contrast, the T-maze results suggest setup-related artifacts, likely due to an uneven distribution of red light and lower light intensity compared to the arena.

In summary, I was able to rule out all methodological errors as potential causes for the unsuccessful memory retrieval following appetitive conditioning. Instead, it seems most likely that optogenetic reactivation of the rather low number of CAMEL cells was insufficient to recall appetitive memories reliably. While 12 CAMEL-positive cells were labeled after aversive conditioning (Siegenthaler et al., 2019) and 13 after appetitive conditioning, the numbers are low compared to the total population of odor-responsive KCs(Honegger et al., 2011; Perez-Orive et al., 2002; Turner et al., 2008), although the exact fraction that contributes to memory encoding remains unknown. Naïve CAMEL flies exhibit mildly aversive behavior in the arena, suggesting a negatively biased baseline. Therefore, it is plausible that the recall of aversive memories is more robust in flies, potentially reflecting their higher relevance for survival.

6.3 Visualization of newly synthesized proteins in engram cells

Understanding the dynamics of protein synthesis at the level of individual neurons is essential to uncover the molecular mechanisms underlying memory formation. In this context, FUNCAT represents a powerful method to investigate the temporal dynamics of protein synthesis following memory formation. In collaboration with Nina Wilhelmy, I established the FUNCAT technique in our laboratory and combined it with the CAMEL-tool to selectively label newly synthesized proteins in sparse neuronal populations resembling individual engram cells (Wilhelmy, 2020).

However, investigating protein dynamics in such sparse neuronal populations poses significant technical challenges, as current imaging resolution primarily permits qualitative spatial analysis. By combining the FUNCAT technique with the CAMEL-tool, the expression of MetRS was restricted to a small subset of KCs resembling engram cells. The number of cells thereby corresponded to the number of CAMEL-cells reflecting natural memory (Siegenthaler et al., 2019). Using MB-specific enhancers, EGFP and TAMRA signals were detected throughout KCs (Figure 21). In contrast, colocalization in CAMEL-cells was restricted to the somata, with only $MetRS^{L262G}$ present in the axons (Figure 22). One technical explanation could be insufficiently specific TAMRA labeling. Despite improved sensitivity, laser scanning microscopy still requires a minimum fluorophore concentration for reliable detection. ANL was not incorporated at every methionine position in newly synthesized proteins. There are two main reasons for this limitation: First, both the mutant $MetRS^{L262G}$ and the endogenous MetRS are expressed in CAMEL-cells and therefore compete for loading the methionine tRNA. Second, ANL and methionine are both present during translation and directly compete for incorporation. A previous study showed that the binding of AHA and HPG to MetRS is slower than that of methionine (Kiick et al., 2002). However, a quantitative comparison of ANL and methionine incorporation efficiency has not yet been performed, complicating assessment. But why can FUNCAT visualize newly synthesized proteins in combination with MB-specific enhancers? The explanation is straightforward. The MB consists of a significantly higher number of KCs, and the axons of the KCs nestle closely together to form the MB lobes. This arrangement improves the contrast, as the laser beam excites multiple fluorescent proteins simultaneously, enhancing the overall signal. This issue could be addressed in future experiments in two ways: First, improvement of ANL uptake and incorporation efficiency. Second, through improved labeling protocols or performance of tissue clearing. Such approaches could enhance the TAMRA signal for individual cells.

Furthermore, a molecular explanation for the absence of TAMRA signal in the axons of CAMEL cells could be related to the spatial regulation of protein synthesis. Translation has been shown to occur not only in the soma but also in dendritic compartments (Cioni et al., 2018; Kim and Jung, 2020; Kos et al., 2016; Yoon et al., 2012), although direct evidence for this process remains technically challenging and is largely derived from non-*Drosophila* model systems. In this context, local translation of synaptic mRNAs plays an important role in synaptic plasticity and memory formation (Jung et al., 2014; Vanderklish and Edelman, 2005; Wang et al., 2009). However, dendritic protein synthesis appears to occur at substantially lower levels compared to somatic translation (Dieterich et al., 2010), which may result in reduced accumulation of newly synthesized proteins in distal neuronal compartments and thereby limit their detectability by TAMRA labeling.

Overall, a limitation of the FUNCAT technique is that the incorporation of ncAAs can potentially affect protein properties, as little is known about the site-dependent incorporation of ncAAs (Saleh et al., 2019). However, the findings of Erdmann et al. (2015) counter these concerns. They showed that the permanent incorporation of ANL into glial and muscle proteins had little effects.

FUNCAT does not provide information on the identity or quantity of newly synthesized proteins. To address this limitation, BONCAT could be combined with mass spectrometric analysis to enable protein identification and quantification. In the context of memory research, however, linking protein identity to function requires cell-type specificity. Combining BONCAT with the CAMEL-tool would therefore allow selective labeling of proteins synthesized in engram cells following defined conditioning protocols. A major limitation of this approach is the requirement for substantial amounts of labeled material, which cannot be achieved with the low number of CAMEL-positive cells under standard conditions. To overcome this, we combined CAMEL with the temperature-sensitive cation channel TrpA1, enabling temporal control of CAMEL activation via heat-induced neuronal depolarization. This strategy increased the number of labeled cells (Wilhelmy, 2020), potentially enabling BONCAT-based mass spectrometry in the future.

6.4 Optogenetic approach to generate an artificial olfactory memory

In collaboration with Benjamin Escribano, I aimed to artificially induce the formation of an associative olfactory memory by replacing the olfactory stimulus with optogenetic activation of CAMEL cells during aversive conditioning (Escribano, 2021). Normally, during paired aversive olfactory conditioning, an odor activates a specific subset of KCs, while an electric shock serves as punishment, triggering the activation of DANs (Turner et al., 2008). Using the CAMEL-tool, an arbitrary target gene can be expressed in an experience-dependent subpopulation of KCs corresponding to engram cells (Bräuler, 2019; Siegenthaler, 2019; Siegenthaler et al., 2019). We aimed to selectively activate a small number of KCs during conditioning, mimicking the natural association process and inducing artificial memory formation. Therefore, we expressed the optogenetic ion channel Chrimson under control of the CAMEL tool, enabling a targeted reactivation of engram cells during artificial conditioning. To subsequently evaluate a potentially formed artificial memory, we used the light preference test in the arena. We performed optogenetics using different time frames. Only a protocol consisting of ten conditioning cycles followed by a 48 h retention interval resulted in a significant behavioral effect (Figure 27).

However, despite this optimization, no consistent difference between control and experimental flies could be observed, as both groups displayed light avoidance. Notably, even naïve flies

showed aversive behavior upon optogenetic activation of CAMEL-cells. This suggests that CAMEL-cells may have a natural predisposition to elicit aversive behavior upon activation This observation is in line with my previous findings(see section 6.1.4 and 6.2), where even control flies exhibited mild light avoidance, indicating that subtle aversive experiences under standard housing conditions may already contribute to memory formation.

These results indicate that this approach was unable to reliably generate or retrieve an artificial aversive memory. A potential explanation for this limitation lies in the technical constraints of the experimental setup. The light intensity may not have been high enough to activate the Chrimson-expressing neurons. Measurements of the arena and T-maze LEDs revealed that, at 20 µW/mm², the Arena LEDs were nearly 60 times brighter than the T-maze LEDs. In collaboration with Nina Wilhelmy and the electrical workshop, we subsequently upgraded our conditioning setup by incorporating red high-power LEDs (625 nm), which can achieve a luminosity of approximately 84 µW/mm².

In my opinion, the frequency of the light pulses (125 ms on, 125 ms off) was not optimized. The Chrimson channel is characterized by rapid activation following red light exposure. In *Drosophila*, it has been shown that even brief illumination durations of 1-2 ms can induce excitatory postsynaptic potentials. Chrimson also generates stable postsynaptic potentials with longer exposure durations (40-160 ms). Since the off-phase between pulses lasted only 125 ms, it may have been too short to allow full deactivation of Chrimson, which has a closure time constant of approximately 200 ms. However, given the fast activation time of 1-2 ms, the CAMEL-cells should still have been activated (Klapoetke et al., 2014). Nonetheless, I would recommend extending the dark phase to account for the slow closure time constant.

Another possible limitation could be the relatively small number of light-activatable neurons. In naïve flies, only a small fraction of KCs is labeled by the CAMEL system. Although natural odor stimulation recruits a larger KC population, it remains unclear how many neurons are required to form a functional memory engram. Therefore, the number of optogenetically activatable cells in this experiment may have been insufficient to reliably induce or retrieve memory-related behavior. To address this, we attempted to increase the population of Chrimson-expressing neurons by co-expressing the heat-sensitive channel TRPA1. While this approach successfully increased the number of labeled cells in a time-dependent manner (Wilhelmy, 2020)., it failed to induce a significant behavioral change in the light preference test (Wilhelmy, 2024). A key limitation of this strategy is that TRPA1 activation likely recruits neurons independently of learning-specific processes. As a result, many of these neurons may not represent true engram cells. Reactivation of such a non-specific neuronal population is therefore unlikely to produce meaningful, memory-related behavioral responses.

Nevertheless, artificial memory formation has been successfully demonstrated in other systems, for example in *Drosophila* larvae, where the reward stimulus was replaced thermogenetically and the odor stimulus optogenetically at the same time (Honda et al., 2016). This suggests that, despite the limitations observed here, the general approach remains promising and should be further refined. Achieving reliable artificial memory formation would open the door for powerful follow-up experiments. For example, identifying the proteomic or transcriptomic signature of engram cells via mass spectrometry or RNA sequencing could shed light on molecular mechanisms underlying memory encoding, consolidation, and maintenance. Furthermore, this method would enable the use of FUNCAT or BONCAT to specifically visualize newly synthesized proteins in memory-encoding neurons at defined time points post-conditioning. Especially BONCAT would require a sufficiently large population of engram cells, which might only be attainable via artificial activation strategies such as TRPA1-enhanced CAMEL-labelling.

6.5 Functional characterization of light-activated DopRs

To specifically investigate the role of dopaminergic signaling pathways during memory formation, two light-activatable DopRs (D1R1-V2 and D1R2-V2) were characterized in collaboration with Nina Wilhelmy, focusing on their localization and function within the MB (Wilhelmy, 2024; Zhou et al., 2023). The goal was to determine whether the receptors are efficiently expressed in KCs, correctly localized to the cell membrane, and whether they are functional *in vivo*.

D1R1-V2 showed strong localization in α/β-neurons, while D1R2-V2 was also present in α'/β'- and γ-neurons (Figure 28). Single-cell analyses revealed that the axonal signal of D1R1-V2 appeared stronger than that of D1R2-V2, which was more weakly detected in axons (Figure 29). This suggests that the subcellular localization of D1R1-V2 to axons is more efficient than that of D1R2-V2. Immunohistochemical studies showed that endogenous D1R1 is expressed in all MB lobes, whereas endogenous D1R2 is exclusively found in α'/β'-KCs(Kondo et al., 2020). Consistent with these results, a single-cell transcriptomic analysis indicated that many KCs express multiple DopRs (Croset et al., 2018). All four DopRs (Dop1R1, Dop1R2, Dop2R, and DopEcR) were detected in KCs, contradicting the immunohistochemical studies that suggest a more selective distribution. The discrepancies between the studies regarding the distribution of DopRs might be attributed to differences in methodological approaches. Immunohistochemistry only detects translated DopRs and is dependent on the quality and binding efficiency of antibodies and fixation. In contrast, single-cell transcriptomics detects mRNA levels, reflecting the transcriptional potential of the cells, which can lead to an overestimation of DopR numbers. Given the subcellular localization patterns, receptor presence in axons is likely essential for their functional role. Both DopRs have been implicated

in memory formation and consolidation (Y. C. Kim et al., 2007; C. Liu et al., 2012; Siju et al., 2021; Sun et al., 2020). While D1R1 is mainly involved in memory acquisition, D1R2 contributes to forgetting (Berry et al., 2012; Himmelreich et al., 2017).

Next, we investigated the *in vivo* functionality of D1R1 and whether its activity in KCs is required and sufficient to mediate associative learning. Using MB-specific RNAi-mediated knockdown of endogenous D1R1, we found that reduced dopamine signaling significantly impaired aversive olfactory learning in adult flies (Figure 30B). This confirms that D1R1 signaling in the MB is essential for memory formation and is consistent with previous findings that D1-like receptors are involved in associative learning processes in *Drosophila* (Y. C. Kim et al., 2007; Qin et al., 2012). Supporting our results, our collaborators demonstrated in larval experiments that D1R1 activity in KCs is likewise required for reward learning. Together, these findings highlight a conserved role of D1R1 across developmental stages and confirm that D1R1 signaling in KCs is a central component of associative memory formation. Interestingly, overexpression of the light-activatable D1R1-V2 in KCs did not impair learning, suggesting that additional receptor copies do not disrupt endogenous signaling under basal conditions (Figure 30C). This supports the notion that D1R1-V2 is not constitutively active and does not interfere with the normal dopaminergic input. Similar observations were made in larvae, where expression of optoDop1R1 alone had no adverse effects on behavior without light activation (Zhou et al., 2023). Based on this, we employed D1R1-V2 in further experiments to assess whether targeted activation is sufficient to modulate or induce memory formation.

We first tested whether light-induced activation of D1R1-V2 during aversive conditioning could enhance learning. Pulsed green light stimulation did not lead to significant differences in behavioral performance compared to controls, regardless of retinal feeding (Figure 31B). Surprisingly, this condition slightly impaired learning even in flies that did not receive retinal and therefore lacked functional activation of D1R1-V2, suggesting that pulsed light might interfere with the conditioning paradigm itself. This nonspecific effect could be due to stress, distraction, or disruption of temporal contingency between the stimuli. To overcome this potential confounding factor, we next employed continuous green light, which no longer impaired learning in retinal-deprived flies (Figure 31C). Under these conditions, simultaneous optogenetic activation of D1R1-V2 and presentation of electric shocks led to a trend towards enhanced learning, although the effect did not reach significance. These findings suggest that artificial activation of D1R1-V2 might support endogenous signaling during learning but is not robustly enhancing memory formation.

To determine whether D1R1 activation can substitute the reinforcement signal, we next tested whether optogenetic activation of D1R1-V2 in the absence of electric shocks was sufficient to induce learning (Figure 31D). Despite broad activation of D1R1-V2 across all MB lobes during odor presentation, no significant behavioral changes were observed. This indicates that

optogenetic activation of D1R1-V2 alone was not sufficient to substitute punishment-induced dopamine signaling or induce learning in this experiment. In contrast to the spatially and temporally precise dopamine release by PPL1 neurons during natural learning, artificial stimulation likely lacks the required specificity and contextual relevance. Moreover, uniform activation of D1R1-V2 across all lobes might interfere with the sparse, compartmentalized coding necessary for effective memory formation.

Taken together, our data demonstrates that D1R1 activity in KCs is necessary, but not sufficient, to drive associative learning. The failure of broad, non-specific activation to induce memory formation highlights the importance of spatially restricted dopamine signaling within the MB and supports the model that learning relies on a precise coincidence of odor-evoked KC activity and dopamine release in defined MB compartments.

Our approach of employing optogenetic activation of D1R1 to directly assess receptor function *in vivo* provides further experimental validation of this hypothesis. Importantly, we demonstrated that receptor activation alone, in the absence of the natural spatial and temporal context of dopaminergic input from PPL1 neurons, is insufficient to induce associative learning. This finding emphasizes the intricate and tightly regulated nature of memory formation and underscores the critical role of precisely coordinated dopamine signaling at specific cellular and subcellular sites.

6.6 Conclusion

In this thesis, I characterized the CAMEL-tool as a reliable method for activity-dependent labeling of memory-encoding neurons and demonstrated its applicability for both aversive and appetitive memory traces in *Drosophila*. These results provide a foundation for future strategies to manipulate engram cells, offering new opportunities to systematically dissect the structure and function of memory-related neuronal networks. I demonstrated that CAMEL-activity reflects changes in environmental stimulus exposure, including stress-related and multimodal sensory input, and enabled the functional retrieval of behavior through optogenetic reactivation. By combining CAMEL with FUNCAT, I visualized newly synthesized proteins in sparse neuronal populations, providing a foundation for future molecular investigations of engram cell dynamics. This opens the possibility to study the temporal sequence of molecular changes that occur during memory consolidation and retrieval. By capturing snapshots of protein synthesis and signaling dynamics at defined time points, stage-specific regulatory mechanisms can be identified. This, in turn, allows for a deeper understanding of how transient molecular events contribute to long-lasting changes in neuronal function and connectivity within engram cells. Importantly, such insights can be the basis of the development of new disease models for memory-related disorders. Dysregulation of these molecular processes is

a hallmark of various neuropsychiatric and neurodegenerative diseases, including Alzheimer's disease or post-traumatic stress disorder. Understanding the underlying molecular timeline in healthy systems therefore provides a crucial reference point to identify pathological deviations and potential therapeutic targets. Furthermore, the characterization of light-activatable DopRs revealed that D1R1 activity in KCs is required but not sufficient for memory formation, underscoring the importance of spatiotemporally precise dopaminergic signaling in the MB. The optogenetic control of specific receptor pathways offers a powerful approach to dissect dopaminergic modulation with unprecedented precision, potentially enabling the development of new tools to manipulate intracellular signaling in a temporally controlled and cell-type-specific manner. Together, these findings emphasize the utility of CAMEL for dissecting the neural and molecular basis of memory formation *in vivo* and they lay the groundwork for future studies aiming to mechanistically unravel the interplay between neuronal activity, neuromodulation, and memory-related protein synthesis.

7. References

Adel, M., Griffith, L.C., 2021. The Role of Dopamine in Associative Learning in Drosophila: An Updated Unified Model. Neurosci. Bull. https://doi.org/10.1007/s12264-021-00665-0

Agard, N.J., Prescher, J.A., Bertozzi, C.R., 2004. A Strain-Promoted [3 + 2] Azide-Alkyne Cycloaddition for Covalent Modification of Biomolecules in Living Systems. J. Am. Chem. Soc. 126, 15046–15047. https://doi.org/10.1021/ja044996f

Akalal, D.-B.G., Yu, D., Davis, R.L., 2010. A Late-Phase, Long-Term Memory Trace Forms in the γ Neurons of *Drosophila* Mushroom Bodies after Olfactory Classical Conditioning. J. Neurosci. 30, 16699–16708. https://doi.org/10.1523/JNEUROSCI.1882-10.2010

Amano, H., Maruyama, I.N., 2011. Aversive olfactory learning and associative long-term memory in Caenorhabditis elegans. Learn. Mem. 18, 654–665. https://doi.org/10.1101/LM.2224411

Amat, J., Baratta, M. V, Paul, E., Bland, S.T., Watkins, L.R., Maier, S.F., 2005. Medial prefrontal cortex determines how stressor controllability affects behavior and dorsal raphe nucleus Nature Neu, 365–371. https://doi.org/10.1038/nn1399

Androschuk, A., Al-Jabri, B., Bolduc, F. V., 2015. From Learning to Memory: What Flies Can Tell Us about Intellectual Disability Treatment. Front. psychiatry 6. https://doi.org/10.3389/FPSYT.2015.00085

Arakawa, H., 2018. Ethological approach to social isolation effects in behavioral studies of laboratory rodents. Behav. Brain Res. 341, 98–108. https://doi.org/10.1016/J.BBR.2017.12.022

Argue, K.J., Neckameyer, W.S., 2013. Sexually dimorphic recruitment of dopamine neurons into the stress response circuitry. Behav. Neurosci. 127, 734–743. https://doi.org/10.1037/A0033807

Arthur Woods, H., Lane, S.J., 2016. Metabolic recovery from drowning by insect pupae. J. Exp. Biol. 219, 3126–3136. https://doi.org/10.1242/JEB.144105

Aso, Y., Grübel, K., Busch, S., Friedrich, A.B., Siwanowicz, I., Tanimoto, H., 2009. The Mushroom Body of Adult *Drosophila* Characterized by GAL4 Drivers. J. Neurogenet. 23, 156–172. https://doi.org/10.1080/01677060802471718

Aso, Y., Hattori, D., Yu, Y., Johnston, R.M., Iyer, N.A., Ngo, T.-T., Dionne, H., Abbott, L., Axel, R., Tanimoto, H., Rubin, G.M., 2014a. The neuronal architecture of the mushroom body provides a logic for associative learning. Elife 3. https://doi.org/10.7554/eLife.04577

Aso, Y., Herb, A., Ogueta, M., Siwanowicz, I., Templier, T., Friedrich, A.B., Ito, K., Scholz, H., Tanimoto, H., 2012. Three Dopamine pathways induce aversive odor memories with different stability. PLoS Genet. 8. https://doi.org/10.1371/journal.pgen.1002768

Aso, Y., Sitaraman, D., Ichinose, T., Kaun, K.R., Vogt, K., Belliart-Guérin, G., Plaçais, P.Y., Robie, A.A., Yamagata, N., Schnaitmann, C., Rowell, W.J., Johnston, R.M., Ngo, T.T.B., Chen, N., Korff, W., Nitabach, M.N., Heberlein, U., Preat, T., Branson, K.M., Tanimoto, H., Rubin, G.M., 2014b. Mushroom body output neurons encode valence and guide memory-based action selection in *Drosophila*. Elife 3, e04580. https://doi.org/10.7554/eLife.04580

Aydinonat, D., Penn, D.J., Smith, S., Moodley, Y., Hoelzl, F., Knauer, F., Schwarzenberger, F., 2014. Social Isolation Shortens Telomeres in African Grey Parrots (Psittacus erithacus erithacus). PLoS One 9, e93839. https://doi.org/10.1371/JOURNAL.PONE.0093839

Azizi-Zeinalhajlou, A., Mirghafourvand, M., Nadrian, H., Samei Sis, S., Matlabi, H., 2022. The contribution of social isolation and loneliness to sleep disturbances among older adults: a systematic review. Sleep Biol. Rhythms 20, 153. https://doi.org/10.1007/S41105-022-00380-X

Baltruschat, L., Prisco, L., Ranft, P., Lauritzen, J.S., Fiala, A., Bock, D.D., Tavosanis, G., 2021. Circuit reorganization in the Drosophila mushroom body calyx accompanies memory consolidation. Cell Rep. 34, 108871. https://doi.org/10.1016/J.CELREP.2021.108871

Bartelt, R.J., Schaner, A.M., Jackson, L.L., 1985. cis-Vaccenyl acetate as an aggregation pheromone inDrosophila melanogaster. J. Chem. Ecol. 11, 1747–1756. https://doi.org/10.1007/BF01012124

Beatty, K.E., Liu, J.C., Xie, F., Dieterich, D.C., Schuman, E.M., Wang, Q., Tirrell, D.A., 2006. Fluorescence Visualization of Newly Synthesized Proteins in Mammalian Cells. Angew. Chemie Int. Ed. 45, 7364–7367. https://doi.org/10.1002/ANIE.200602114

Beatty, K.E., Tirrell, D.A., 2008. Two-color labeling of temporally defined protein populations in mammalian cells. Bioorg. Med. Chem. Lett. 18, 5995–5999. https://doi.org/10.1016/J.BMCL.2008.08.046

Beaulieu, J.M., Espinoza, S., Gainetdinov, R.R., 2015. Dopamine receptors - IUPHAR Review 13. Br. J. Pharmacol. 172, 1–23. https://doi.org/10.1111/BPH.12906

Bennett, J.E.M., Philippides, A., Nowotny, T., 2021. Learning with reinforcement prediction errors in a model of the Drosophila mushroom body. Nat. Commun. 2021 121 12, 1–14.

https://doi.org/10.1038/s41467-021-22592-4

Berry, J.A., Cervantes-Sandoval, I., Nicholas, E.P., Davis, R.L., 2012. Dopamine Is Required for Learning and Forgetting in Drosophila. Neuron 74, 530–542. https://doi.org/10.1016/j.neuron.2012.04.007

Billeter, J.-C., Atallah, J., Krupp, J.J., Millar, J.G., Levine, J.D., 2009. Specialized cells tag sexual and species identity in Drosophila melanogaster. Nature 461, 987–991. https://doi.org/10.1038/nature08495

Bilz, F., Geurten, B.R.H., Hancock, C.E., Widmann, A., Fiala, A., 2020. Visualization of a Distributed Synaptic Memory Code in the Drosophila Brain. Neuron. https://doi.org/10.1016/j.neuron.2020.03.010

Brand, A.H., Perrimon, N., 1993. Targeted gene expression as a means of altering cell fates and generating dominant phenotypes. Development 118, 401–15. https://doi.org/10.1242/dev.118.2.401.

Bräuler, V., 2019. Characterization of memory engram neurons in Drosophila. Technische Universität Kaiserslautern, Germany.

Brewer, J.A., Bethin, K.E., Schaefer, M.L., Muglia, L.M., Vogt, S.K., Weninger, S.C., Majzoub, J.A., Muglia, L.J., 2003. Dissecting adrenal and behavioral responses to stress by targeted gene inactivation in mice. Stress 6, 121–125. https://doi.org/10.1080/1025389031000116460

Brightwell, J.J., Smith, C.A., Countryman, R.A., Neve, R.L., Colombo, P.J., 2005. Hippocampal overexpression of mutant creb blocks long-term, but not short-term memory for a socially transmitted food preference. Learn. Mem. 12, 12–17. https://doi.org/10.1101/LM.85005

Brown, E.B., Patterson, C., Pancoast, R., Rollmann, S.M., 2017. Artificial selection for odor-guided behavior in Drosophila reveals changes in food consumption. BMC Genomics 18. https://doi.org/10.1186/S12864-017-4233-1

Burke, C.J., Huetteroth, W., Owald, D., Perisse, E., Krashes, M.J., Das, G., Gohl, D., Silies, M., Certel, S., Waddell, S., 2012. Layered reward signalling through octopamine and dopamine in *Drosophila*. Nature 492, 433–437. https://doi.org/10.1038/nature11614

Busto, G.U., Cervantes-Sandoval, I., Davis, R.L., 2010. Olfactory Learning in *Drosophila*. Physiology 25, 338–346. https://doi.org/10.1152/physiol.00026.2010

Campbell, R.A.A., Honegger, K.S., Qin, H., Li, W., Demir, E., Turner, G.C., 2013. Imaging a Population Code for Odor Identity in the Drosophila Mushroom Body. J. Neurosci. 33,

10568–10581. https://doi.org/10.1523/JNEUROSCI.0682-12.2013

Castellucci, V.F., Kandel, E.R., Schwartz, J.H., Wilson, F.D., Nairn, A.C., Greengard, P., 1980. Intracellular injection of the catalytic subunit of cyclic AMP-dependent protein kinase simulates facilitation of transmitter release underlying behavioral sensitization in Aplysia. Proc. Natl. Acad. Sci. U. S. A. 77, 7492–6. https://doi.org/10.1073/PNAS.77.12.7492

Cavallaro, M.C., Hoback, W.W., 2014. Hypoxia Tolerance of Larvae and Pupae of the Semi-Terrestrial Caddisfly (Trichoptera: Limnephilidae). Ann. Entomol. Soc. Am. 107, 1081–1085. https://doi.org/10.1603/AN14035

Cervantes-Sandoval, I., Martin-Peña, A., Berry, J.A., Davis, R.L., 2013. System-like consolidation of olfactory memories in *Drosophila*. J. Neurosci. 33, 9846–54. https://doi.org/10.1523/JNEUROSCI.0451-13.2013

Cervantes-Sandoval, I., Phan, A., Chakraborty, M., Davis, R.L., 2017. Reciprocal synapses between mushroom body and dopamine neurons form a positive feedback loop required for learning. Elife 6. https://doi.org/10.7554/ELIFE.23789,

Chadha, A., Cook, B., 2014. The effect of stress on motor function in Drosophila. PLoS One 9. https://doi.org/10.1371/JOURNAL.PONE.0112076

Chappell, N.L., Badger, M., 1989. Social isolation and well-being. J. Gerontol. 44. https://doi.org/10.1093/GERONJ/44.5.S169

Cioni, J.M., Koppers, M., Holt, C.E., 2018. Molecular control of local translation in axon development and maintenance. Curr. Opin. Neurobiol. 51, 86–94. https://doi.org/10.1016/J.CONB.2018.02.025

Claridge-Chang, A., Roorda, R.D., Vrontou, E., Sjulson, L., Li, H., Hirsh, J., Miesenböck, G., 2009. Writing Memories with Light-Addressable Reinforcement Circuitry. Cell 139, 405–415. https://doi.org/10.1016/j.cell.2009.08.034

Cognigni, P., Felsenberg, J., Waddell, S., 2018. Do the right thing: neural network mechanisms of memory formation, expression and update in *Drosophila*. Curr. Opin. Neurobiol. 49, 51–58. https://doi.org/10.1016/j.conb.2017.12.002

Cohn, R., Morantte, I., Ruta, V., 2015. Coordinated and Compartmentalized Neuromodulation Shapes Sensory Processing in Drosophila. Cell 163, 1742–1755. https://doi.org/10.1016/J.CELL.2015.11.019

Corbin, J.D., Krebs, E.G., 1969. A cyclic AMP - stimulated protein kinase in adipose tissue. Biochem. Biophys. Res. Commun. 36, 328–336. https://doi.org/10.1016/0006-

291X(69)90334-9

Corish, P., Tyler-Smith, C., 1999. Attenuation of green fluorescent protein half-life in mammalian cells. Protein Eng. 12, 1035–1040. https://doi.org/10.1093/PROTEIN/12.12.1035

Couto, A., Alenius, M., Dickson, B.J., 2005. Molecular, Anatomical, and Functional Organization of the *Drosophila* Olfactory System. Curr. Biol. 15, 1535–1547. https://doi.org/10.1016/j.cub.2005.07.034

Crittenden, J.R., Skoulakis, E.M., Han, K.A., Kalderon, D., Davis, R.L., 1998. Tripartite mushroom body architecture revealed by antigenic markers. Learn. Mem. 5, 38–51. https://doi.org/10.1101/lm.5.1.38

Croset, V., Treiber, C.D., Waddell, S., 2018. Cellular diversity in the Drosophila midbrain revealed by single-cell transcriptomics. Elife 7. https://doi.org/10.7554/ELIFE.34550

Das Chakraborty, S., Sachse, S., 2021. Olfactory processing in the lateral horn of Drosophila. Cell Tissue Res. 383, 113–123. https://doi.org/10.1007/S00441-020-03392-6

Dash, P.K., Hochner, B., Kandel, E.R., 1990. Injection of the cAMP-responsive element into the nucleus of Aplysia sensory neurons blocks long-term facilitation. Nature 345, 718–721. https://doi.org/10.1038/345718a0

Davis, H.P., Squire, L.R., 1984. Protein synthesis and memory: A review. Psychol. Bull. 96, 518–559. https://doi.org/10.1037/0033-2909.96.3.518

Davis, R.L., 2004. Olfactory learning. Neuron 44, 31–48. https://doi.org/10.1016/J.NEURON.2004.09.008

Davis, R.L., 1993. Mushroom bodies and drosophila learning. Neuron 11, 1–14. https://doi.org/10.1016/0896-6273(93)90266-T

Deal, R.B., Henikoff, J.G., Henikoff, S., 2010. Genome-wide kinetics of nucleosome turnover determined by metabolic labeling of histones. Science 328, 1161. https://doi.org/10.1126/SCIENCE.1186777

Delanogare, E., de Souza, R.M., Rosa, G.K., Guanabara, F.G., Rafacho, A., Moreira, E.L.G., 2020. Enriched environment ameliorates dexamethasone effects on emotional reactivity and metabolic parameters in mice. Stress 23, 466–473. https://doi.org/10.1080/10253890.2020.1735344

DeZazzo, J., Tully, T., 1995. Dissection of memory formation: from behavioral pharmacology to molecular genetics. Trends Neurosci. 18, 212–218. https://doi.org/10.1016/0166-

2236(95)93905-D

Dieck, S.T., Müller, A., Nehring, A., Hinz, F.I., Bartnik, I., Schuman, E.M., Dieterich, D.C., 2012. Metabolic labeling with noncanonical amino acids and visualization by chemoselective fluorescent tagging. Curr. Protoc. Cell Biol. 1, Unit7.11. https://doi.org/10.1002/0471143030.cb0711s56

Dieterich, D.C., Hodas, J.J.L., Gouzer, G., Shadrin, I.Y., Ngo, J.T., Triller, A., Tirrell, D.A., Schuman, E.M., 2010. In situ visualization and dynamics of newly synthesized proteins in rat hippocampal neurons. Nat. Neurosci. 13, 897–905. https://doi.org/10.1038/NN.2580

Dieterich, D.C., Link, A.J., Graumann, J., Tirrell, D.A., Schuman, E.M., 2006. Selective identification of newly synthesized proteins in mammalian cells using bioorthogonal noncanonical amino acid tagging (BONCAT). Proc. Natl. Acad. Sci. U. S. A. 103, 9482–9487. https://doi.org/10.1073/PNAS.0601637103/SUPPL_FILE/01637FIG8.JPG

Dolan, M.-J., Belliart-Guérin, G., Bates, A.S., Frechter, S., Lampin-Saint-Amaux, A., Aso, Y., Roberts, R.J.V., Schlegel, P., Wong, A., Hammad, A., Bock, D., Rubin, G.M., Preat, T., Plaçais, P.-Y., Jefferis, G.S.X.E., 2018. Communication from Learned to Innate Olfactory Processing Centers Is Required for Memory Retrieval in *Drosophila*. Neuron 100, 651-668.e8. https://doi.org/10.1016/j.neuron.2018.08.037

Du, Y., Li, X., Yan, W., Zeng, Z., Han, D., Ouyang, H., Pan, X., Luo, B., Zhou, B., Fu, Q., Lu, D., Huang, Z., Li, Z., 2021. Deciphering the in vivo Dynamic Proteomics of Mesenchymal Stem Cells in Critical Limb Ischemia. Front. Cell Dev. Biol. 9. https://doi.org/10.3389/fcell.2021.682476

Dubnau, J., Tully, T., 1998. GENE DISCOVERY IN *DROSOPHILA* : New Insights for Learning and Memory. Annu. Rev. Neurosci. 21, 407–444. https://doi.org/10.1146/annurev.neuro.21.1.407

Duffy, J.B., 2002. GAL4 system in drosophila: A fly geneticist's swiss army knife. genesis 34, 1–15. https://doi.org/10.1002/GENE.10150

Dukas, R., Mooers, A., 2003. Environmental enrichment improves mating success in fruit flies. Anim. Behav. 66, 741–749. https://doi.org/10.1006/ANBE.2002.2261

Dweck, H.K., Ebrahim, S.A., Khallaf, M.A., Koenig, C., Farhan, A., Stieber, R., Weißflog, J., Svatoš, A., Grosse-Wilde, E., Knaden, M., Hansson, B.S., 2016. Olfactory channels associated with the Drosophila maxillary palp mediate short-and long-range attraction. https://doi.org/10.7554/eLife.14925.001

Einon, D.F., Morgan, M.J., 1977. A critical period for social isolation in the rat. Dev.

Psychobiol. 10, 123–132. https://doi.org/10.1002/DEV.420100205

Erdmann, I., Marter, K., Kobler, O., Niehues, S., Abele, J., Müller, A., Bussmann, J., Storkebaum, E., Ziv, T., Thomas, U., Dieterich, D.C., 2015. Cell-selective labelling of proteomes in Drosophila melanogaster. Nat. Commun. 6. https://doi.org/10.1038/ncomms8521

Eschbach, C., Fushiki, A., Winding, M., Afonso, B., Andrade, I. V., Cocanougher, B.T., Eichler, K., Gepner, R., Si, G., Valdes-Aleman, J., Fetter, R.D., Gershow, M., Jefferis, G.S., Samuel, A.D., Truman, J.W., Cardona, A., Zlatic, M., 2021. Circuits for integrating learned and innate valences in the insect brain. Elife 10. https://doi.org/10.7554/ELIFE.62567,

Escribano, B., 2021. Functional and Structural Analysis of Engram Cells in Drosophila. Technische Universität Kaiserslautern, Germany.

Evans, H.T., Bodea, L.G., Götz, J., 2020. Cell-specific non-canonical amino acid labelling identifies changes in the de novo proteome during memory formation. Elife 9. https://doi.org/10.7554/ELIFE.52990

Fares, R.P., Belmeguenai, A., Sanchez, P.E., Kouchi, H.Y., Bodennec, J., Morales, A., Georges, B., Bonnet, C., Bouvard, S., Sloviter, R.S., Bezin, L., 2013. Standardized environmental enrichment supports enhanced brain plasticity in healthy rats and prevents cognitive impairment in epileptic rats. PLoS One 8. https://doi.org/10.1371/JOURNAL.PONE.0053888

Felsenberg, J., Jacob, P.F., Walker, T., Barnstedt, O., Edmondson-Stait, A.J., Pleijzier, M.W., Otto, N., Schlegel, P., Sharifi, N., Perisse, E., Smith, C.S., Lauritzen, J.S., Costa, M., Jefferis, G.S.X.E., Bock, D.D., Waddell, S., 2018. Integration of Parallel Opposing Memories Underlies Memory Extinction. Cell 175, 709-722.e15. https://doi.org/10.1016/J.CELL.2018.08.021/ATTACHMENT/BC8E2912-3703-4FB1-B10E-73DF91FC9747/MMC1.PDF

Ferreira, C.H., Moita, M.A., 2019. What can a non-eusocial insect tell us about the neural basis of group behaviour? Curr. Opin. insect Sci. 36, 118–124. https://doi.org/10.1016/J.COIS.2019.09.001

Ferveur, J.-F., 2005. Cuticular Hydrocarbons: Their Evolution and Roles in *Drosophila* Pheromonal Communication. Behav. Genet. 35, 279–295. https://doi.org/10.1007/s10519-005-3220-5

Fishilevich, E., Vosshall, L.B., 2005. Genetic and Functional Subdivision of the *Drosophila* Antennal Lobe. Curr. Biol. 15, 1548–1553. https://doi.org/10.1016/j.cub.2005.07.066

Fone, K.C.F., Porkess, M.V., 2008. Behavioural and neurochemical effects of post-weaning social isolation in rodents-relevance to developmental neuropsychiatric disorders. Neurosci. Biobehav. Rev. 32, 1087–1102. https://doi.org/10.1016/J.NEUBIOREV.2008.03.003

Garthe, A., Roeder, I., Kempermann, G., 2016. Mice in an enriched environment learn more flexibly because of adult hippocampal neurogenesis. Hippocampus 26, 261–271. https://doi.org/10.1002/HIPO.22520

Gass, P., Wolfer, D.P., Balschun, D., Rudolph, D., Frey, U., Lipp, H.P., Schütz, G., 1998. Deficits in Memory Tasks of Mice with CREB Mutations Depend on Gene Dosage. Learn. Mem. 5, 274–288. https://doi.org/10.1101/LM.5.4.274

George, J.M., Bell, Z.W., Condliffe, D., Dohrer, K., Abaurrea, T., Spencer, K., Leitão, A., Gahr, M., Hurd, P.J., Clayton, D.F., 2020. Acute social isolation alters neurogenomic state in songbird forebrain. Proc. Natl. Acad. Sci. U. S. A. 117, 23311–23316. https://doi.org/10.1073/PNAS.1820841116

Girbig, M., Misiaszek, A.D., Müller, C.W., 2022. Structural insights into nuclear transcription by eukaryotic DNA-dependent RNA polymerases. https://doi.org/10.1038/s41580-022-00476-9

Gruntman, E., Turner, G.C., 2013. Integration of the olfactory code across dendritic claws of single mushroom body neurons. Nat. Neurosci. 2013 1612 16, 1821–1829. https://doi.org/10.1038/nn.3547

Guan, J.S., Jiang, J., Xie, H., Liu, K.Y., 2016. How does the sparse memory “engram” neurons encode the memory of a spatial–temporal event? Front. Neural Circuits 10. https://doi.org/10.3389/FNCIR.2016.00061/ABSTRACT

Guisnet, A., Maitra, M., Pradhan, S., Hendricks, M., 2021. A three-dimensional habitat for C. elegans environmental enrichment. PLoS One 16. https://doi.org/10.1371/JOURNAL.PONE.0245139

Guven-Ozkan, T., Davis, R.L., 2014. Functional neuroanatomy of *Drosophila* olfactory memory formation. Learn. Mem. 21, 519–526. https://doi.org/10.1101/lm.034363.114

Halfon, M.S., Gisselbrecht, S., Lu, J., Estrada, B., Keshishian, H., Michelson, A.M., 2002. New fluorescent protein reporters for use with the *drosophila* gal4 expression system and for vital detection of balancer chromosomes. genesis 34, 135–138. https://doi.org/10.1002/gene.10136

Harlow, H.F., Dodsworth, R.O., Harlow, M.K., 1965. Total social isolation in monkeys. Proc. Natl. Acad. Sci. U. S. A. 54, 90. https://doi.org/10.1073/PNAS.54.1.90

Hazelrigg, T., Liu, N., Hong, Y., Wang, S., 1998. GFP expression in Drosophila tissues: time requirements for formation of a fluorescent product. Dev. Biol. 199, 245–249. https://doi.org/10.1006/DBIO.1998.8922

He, J., Li, B., Han, S., Zhang, Y., Liu, K., Yi, S., Liu, Y., Xiu, M., 2022. Drosophila as a Model to Study the Mechanism of Nociception. Front. Physiol. 13. https://doi.org/10.3389/FPHYS.2022.854124

Hehlert, P., Zhang, W., Göpfert, M.C., 2021. Drosophila Mechanosensory Transduction. Trends Neurosci. 44, 323–335. https://doi.org/10.1016/J.TINS.2020.11.001

Heidbreder, C.A., Weiss, I.C., Domeney, A.M., Pryce, C., Homberg, J., Hedou, G., Feldon, J., Moran, M.C., Nelson, P., 2000. Behavioral, neurochemical and endocrinological characterization of the early social isolation syndrome. Neuroscience 100, 749–768. https://doi.org/10.1016/S0306-4522(00)00336-5

Heisenberg, M., 2003. Mushroom body memoir: from maps to models. Nat. Rev. Neurosci. 4, 266–275. https://doi.org/10.1038/nrn1074

Heisenberg, M., Borst, A., Wagner, S., Byers, D., 1985. *Drosophila* mushroom body mutants are deficient in olfactory learning. J. Neurogenet. 2, 1–30.

Hetz, S.K., Bradley, T.J., 2005. Insects breathe discontinuously to avoid oxygen toxicity. Nat. 2004 4337025 433, 516–519. https://doi.org/10.1038/nature03106

Hige, T., Aso, Y., Modi, M.N., Rubin, G.M., Turner, G.C., 2015. Heterosynaptic Plasticity Underlies Aversive Olfactory Learning in Drosophila. Neuron 88, 985–998. https://doi.org/10.1016/J.NEURON.2015.11.003

Hige, T., Turner, G., 2015. Learning: The Good, the Bad, and the Fly. Neuron 86, 343–345. https://doi.org/10.1016/J.NEURON.2015.04.012

Himmelreich, S., Masuho, I., Berry, J.A., MacMullen, C., Skamangas, N.K., Martemyanov, K.A., Davis, R.L., 2017. Dopamine Receptor DAMB Signals via Gq to Mediate Forgetting in Drosophila. Cell Rep. 21, 2074–2081. https://doi.org/10.1016/J.CELREP.2017.10.108

Hinz, F.I., Dieterich, D.C., Schuman, E.M., 2013. Teaching old NCATs new tricks: Using non-canonical amino acid tagging to study neuronal plasticity. Curr. Opin. Chem. Biol. https://doi.org/10.1016/j.cbpa.2013.07.021

Hinz, F.I., Dieterich, D.C., Tirrell, D.A., Schuman, E.M., 2012. Noncanonical Amino AcidLabeling in Vivo to Visualizeand Affinity Purify Newly Synthesized Proteins in Larval Zebrafish. ACS Chem. Neurosci. 3, 40. https://doi.org/10.1021/CN2000876

Hirano, Y., Ihara, K., Masuda, T., Yamamoto, T., Iwata, I., Takahashi, A., Awata, H., Nakamura, N., Takakura, M., Suzuki, Y., Horiuchi, J., Okuno, H., Saitoe, M., 2016. Shifting transcriptional machinery is required for long-term memory maintenance and modification in *Drosophila* mushroom bodies. Nat. Commun. 7, 1–14. https://doi.org/10.1038/ncomms13471

Honda, T., Lee, C.Y., Honjo, K., Furukubo-Tokunaga, K., 2016. Artificial induction of associative olfactory memory by optogenetic and thermogenetic activation of olfactory sensory neurons and octopaminergic neurons in drosophila larvae. Front. Behav. Neurosci. 10, 137. https://doi.org/10.3389/FNBEH.2016.00137/BIBTEX

Honegger, K.S., Campbell, R.A.A., Turner, G.C., 2011. Cellular-resolution population imaging reveals robust sparse coding in the Drosophila mushroom body. J. Neurosci. 31, 11772–11785. https://doi.org/10.1523/JNEUROSCI.1099-11.2011

Honjo, K., Hwang, R.Y., Tracey, W.D., 2012. Optogenetic manipulation of neural circuits and behavior in Drosophila larvae. Nat. Protoc. 2012 78 7, 1470–1478. https://doi.org/10.1038/nprot.2012.079

Huang, C., Wang, P., Xie, Z., Wang, L., Zhong, Y., 2013. The differential requirement of mushroom body α/β subdivisions in long-term memory retrieval in *Drosophila*. Protein Cell 4, 512–519. https://doi.org/10.1007/s13238-013-3035-8

Huoviala, P., Dolan, M.-J., Love, F., Frechter, S., Roberts, R.J. V, Mitrevica, Z., Schlegel, P., Bates, A.S.S., Aso, Y., Rodrigues, T., Cornwall, H., Stensmyr, M., Bock, D., Rubin, G.M., Costa, M., Jefferis, G.S.X.E., 2018. Neural circuit basis of aversive odour processing inDrosophilafrom sensory input to descending output. https://doi.org/10.1101/394403

Isabel, G., Pascual, A., Preat, T., 2004. Exclusive Consolidated Memory Phases in *Drosophila*. Science (80-.). 304, 1024–1027. https://doi.org/10.1126/science.1094932

Ito, K., Awano, W., Suzuki, K., Hiromi, Y., Yamamoto, D., 1997. The Drosophila mushroom body is a quadruple structure of clonal units each of which contains a virtually identical set of neurones and glial cells. Development 124, 761–771. https://doi.org/10.1242/DEV.124.4.761,

Jefferis, G.S.X.E., Potter, C.J., Chan, A.M., Marin, E.C., Rohlfing, T., Maurer, C.R., Luo, L., 2007. Comprehensive Maps of *Drosophila* Higher Olfactory Centers: Spatially Segregated Fruit and Pheromone Representation. Cell 128, 1187–1203. https://doi.org/10.1016/j.cell.2007.01.040

Josselyn, S.A., Köhler, S., Frankland, P.W., 2017. Heroes of the Engram. J. Neurosci. 37,

4647–4657. https://doi.org/10.1523/JNEUROSCI.0056-17.2017

Judge, K.A., 2010. Female social experience affects the shape of sexual selection on males. Evol. Ecol. Res. 12, 389–402.

Jung, H., Gkogkas, C.G., Sonenberg, N., Holt, C.E., 2014. Remote control of gene function by local translation. Cell 157, 26–40. https://doi.org/10.1016/J.CELL.2014.03.005

Kandel, E.R., 2012. The molecular biology of memory: cAMP, PKA, CRE, CREB-1, CREB-2, and CPEB. Mol. Brain 5, 14. https://doi.org/10.1186/1756-6606-5-14

Karam, C.S., Jones, S.K., Javitch, J.A., 2020. Come Fly with Me: An overview of dopamine receptors in Drosophila melanogaster. Basic Clin. Pharmacol. Toxicol. https://doi.org/10.1111/bcpt.13277

Kaupp, U.B., 2010. Olfactory signalling in vertebrates and insects: differences and commonalities. Nat. Rev. Neurosci. 2010 113 11, 188–200. https://doi.org/10.1038/nrn2789

Kazama, H., 2015. Systems neuroscience in Drosophila: Conceptual and technical advantages. Neuroscience 296, 3–14. https://doi.org/10.1016/J.NEUROSCIENCE.2014.06.035

Keene, A.C., Krashes, M.J., Leung, B., Bernard, J.A., Waddell, S., 2006. Drosophila Dorsal Paired Medial Neurons Provide a General Mechanism for Memory Consolidation. Curr. Biol. 16, 1524–1530. https://doi.org/10.1016/j.cub.2006.06.022

Keene, A.C., Waddell, S., 2007. *Drosophila* olfactory memory: single genes to complex neural circuits. Nat. Rev. Neurosci. 8, 341–354. https://doi.org/10.1038/nrn2098

Kempermann, G., 2019. Environmental enrichment, new neurons and the neurobiology of individuality. Nat. Rev. Neurosci. 2019 204 20, 235–245. https://doi.org/10.1038/s41583-019-0120-x

Kempermann, G., Kuhn, H.G., Gage, F.H., 1997. More hippocampal neurons in adult mice living in an enriched environment. Nature 386, 493–495. https://doi.org/10.1038/386493a0

Keyvani, K., Sachser, N., Witte, O.W., Paulus, W., 2004. Gene Expression Profiling in the Intact and Injured Brain Following Environmental Enrichment. J. Neuropathol. Exp. Neurol. 63, 598–609. https://doi.org/10.1093/JNEN/63.6.598

Kida, S., Josselyn, S.A., De Ortiz, S.P., Kogan, J.H., Chevere, I., Masushige, S., Silva, A.J., 2002. CREB required for the stability of new and reactivated fear memories. Nat. Neurosci. 5, 348–355. https://doi.org/10.1038/NN819

Kida, S., Serita, T., 2014. Functional roles of CREB as a positive regulator in the formation and enhancement of memory. Brain Res. Bull. 105, 17–24. https://doi.org/10.1016/J.BRAINRESBULL.2014.04.011

Kiick, K.L., Saxon, E., Tirrell, D.A., Bertozzi, C.R., 2002. Incorporation of azides into recombinant proteins for chemoselective modification by the Staudinger ligation. Proc. Natl. Acad. Sci. U. S. A. 99, 19–24. https://doi.org/10.1073/PNAS.012583299/SUPPL_FILE/5832TEXT.PDF

Kim, E., Jung, H., 2020. Local mRNA translation in long-term maintenance of axon health and function. Curr. Opin. Neurobiol. 63, 15–22. https://doi.org/10.1016/J.CONB.2020.01.006

Kim, J.J., Diamond, D.M., 2002. The stressed hippocampus, synaptic plasticity and lost memories. Nat. Rev. Neurosci. 3, 453–462. https://doi.org/10.1038/NRN849

Kim, K.S., Han, P.L., 2009. Mice lacking adenylyl cyclase-5 cope badly with repeated restraint stress. J. Neurosci. Res. 87, 2983–2993. https://doi.org/10.1002/JNR.22119

Kim, S.E., Coste, B., Chadha, A., Cook, B., Patapoutian, A., 2012. The role of Drosophila Piezo in mechanical nociception. Nature 483, 209–212. https://doi.org/10.1038/NATURE10801

Kim, Y.-C., Lee, H.-G., Han, K.-A., 2007. Classical reward conditioning in *Drosophila melanogaster*. Genes, Brain Behav. 6, 201–207. https://doi.org/10.1111/j.1601-183X.2006.00241.x

Kim, Y.C., Lee, H.G., Han, K.A., 2007. D1 dopamine receptor dDA1 is required in the mushroom body neurons for aversive and appetitive learning in Drosophila. J. Neurosci. 27, 7640–7647. https://doi.org/10.1523/JNEUROSCI.1167-07.2007

Klapoetke, N.C., Murata, Y., Kim, S.S., Pulver, S.R., Birdsey-Benson, A., Cho, Y.K., Morimoto, T.K., Chuong, A.S., Carpenter, E.J., Tian, Z., Wang, J., Xie, Y., Yan, Z., Zhang, Y., Chow, B.Y., Surek, B., Melkonian, M., Jayaraman, V., Constantine-Paton, M., Wong, G.K.-S., Boyden, E.S., 2014. Independent optical excitation of distinct neural populations. Nat. Methods 11, 338–346. https://doi.org/10.1038/nmeth.2836

Kobayakawa, K., Kobayakawa, R., Matsumoto, H., Oka, Y., Imai, T., Ikawa, M., Okabe, M., Ikeda, T., Itohara, S., Kikusui, T., Mori, K., Sakano, H., 2007. Innate versus learned odour processing in the mouse olfactory bulb. Nature 450, 503–508. https://doi.org/10.1038/NATURE06281

Kohatsu, S., Koganezawa, M., Yamamoto, D., 2011. Female Contact Activates Male-Specific Interneurons that Trigger Stereotypic Courtship Behavior in Drosophila. Neuron 69,

498–508. https://doi.org/10.1016/j.neuron.2010.12.017

Kolb, B., Whishaw, I.Q., 1998. Brain plasticity and behavior. Annu. Rev. Psychol. 49, 43–64. https://doi.org/10.1146/ANNUREV.PSYCH.49.1.43

Kolb, H.C., Finn, M.G., Sharpless, K.B., 2001. Click Chemistry: Diverse Chemical Function from a Few Good Reactions - Kolb - 2001 - Angewandte Chemie International Edition - Wiley Online Library [WWW Document]. https://doi.org/doi/10.1002/1521-3773(20010601)40:11<2004::AID-ANIE2004>3.0.CO;2-5

Kondo, S., Takahashi, T., Yamagata, N., Imanishi, Y., Katow, H., Hiramatsu, S., Lynn, K., Abe, A., Kumaraswamy, A., Tanimoto, H., 2020. Neurochemical Organization of the Drosophila Brain Visualized by Endogenously Tagged Neurotransmitter Receptors. Cell Rep. 30, 284-297.e5. https://doi.org/10.1016/J.CELREP.2019.12.018/ATTACHMENT/86E2F237-4496-4248-86BE-0974F1ADF270/MMC3.PDF

Kos, A., Wanke, K.A., Gioio, A., Martens, G.J., Kaplan, B.B., Aschrafi, A., 2016. Monitoring mRNA Translation in Neuronal Processes Using Fluorescent Non-Canonical Amino Acid Tagging. J. Histochem. Cytochem. 64, 323–333. https://doi.org/10.1369/0022155416641604

Krashes, M.J., Keene, A.C., Leung, B., Armstrong, J.D., Waddell, S., 2007. Sequential use of mushroom body neuron subsets during Drosophila odor memory processing. Neuron 53, 103–115. https://doi.org/10.1016/j.neuron.2006.11.021.

Krashes, M.J., Waddell, S., 2008. Rapid consolidation to a radish and protein synthesis-dependent long-term memory after single-session appetitive olfactory conditioning in Drosophila. J. Neurosci. 28, 3103–13. https://doi.org/10.1523/JNEUROSCI.5333-07.2008

Kremer, M.C., Christiansen, F., Leiss, F., Paehler, M., Knapek, S., Andlauer, T.F.M., Förstner, F., Kloppenburg, P., Sigrist, S.J., Tavosanis, G., 2010. Structural long-term changes at mushroom body input synapses. Curr. Biol. 20, 1938–1944. https://doi.org/10.1016/j.cub.2010.09.060

Lai, S.L., Lee, T., 2006. Genetic mosaic with dual binary transcriptional systems in Drosophila. Nat. Neurosci. 2006 95 9, 703–709. https://doi.org/10.1038/nn1681

Larsson, M.C., Domingos, A.I., Jones, W.D., Chiappe, M.E., Amrein, H., Vosshall, L.B., 2004. Or83b encodes a broadly expressed odorant receptor essential for Drosophila olfaction. Neuron 43, 703–714. https://doi.org/10.1016/j.neuron.2004.08.019

Lee, T., Lee, A., Luo, L., 1999. Development of the *Drosophila* mushroom bodies: sequential

generation of three distinct types of neurons from a neuroblast. Development 126, 4065–76. https://doi.org/10.1016/j.jes.2015.12.036

Lee, T., Luo, L., 1999. Mosaic analysis with a repressible neurotechnique cell marker for studies of gene function in neuronal morphogenesis. Neuron 22, 451–461. https://doi.org/10.1016/S0896-6273(00)80701-1

Leigh-Hunt, N., Bagguley, D., Bash, K., Turner, V., Turnbull, S., Valtorta, N., Caan, W., 2017. An overview of systematic reviews on the public health consequences of social isolation and loneliness. Public Health 152, 157–171. https://doi.org/10.1016/J.PUHE.2017.07.035

Leiss, F., Groh, C., Butcher, N.J., Meinertzhagen, I.A., Tavosanis, G., 2009. Synaptic organization in the adult Drosophila mushroom body calyx. J. Comp. Neurol. 517, 808–824. https://doi.org/10.1002/CNE.22184,

Levin, L.R., Han, P.L., Hwang, P.M., Feinstein, P.G., Davis, R.L., Reed, R.R., 1992. The Drosophila learning and memory gene rutabaga encodes a Ca2+/Calmodulin-responsive adenylyl cyclase. Cell 68, 479–489. https://doi.org/10.1016/0092-8674(92)90185-F

Li, J., Zhang, W., Guo, Z., Wu, S., Jan, L.Y., Jan, Y.N., 2016. A Defensive Kicking Behavior in Response to Mechanical Stimuli Mediated by Drosophila Wing Margin Bristles. J. Neurosci. 36, 11275–11282. https://doi.org/10.1523/JNEUROSCI.1416-16.2016

Li, W., Wang, Z., Syed, S., Lyu, C., Lincoln, S., O'Neil, J., Nguyen, A.D., Feng, I., Young, M.W., 2021. Chronic social isolation signals starvation and reduces sleep in Drosophila. Nature 597, 239–244. https://doi.org/10.1038/S41586-021-03837-0

Link, A.J., Mock, M.L., Tirrell, D.A., 2003. Non-canonical amino acids in protein engineering. Curr. Opin. Biotechnol. 14, 603–609. https://doi.org/10.1016/j.copbio.2003.10.011

Link, A.J., Vink, M.K.S., Agard, N.J., Prescher, J.A., Bertozzi, C.R., Tirrell, D.A., 2006. Discovery of aminoacyl-tRNA synthetase activity through cell-surface display of noncanonical amino acids. Proc. Natl. Acad. Sci. U. S. A. 103, 10180–10185. https://doi.org/10.1073/PNAS.0601167103

Liu, C., Plaşais, P.Y., Yamagata, N., Pfeiffer, B.D., Aso, Y., Friedrich, A.B., Siwanowicz, I., Rubin, G.M., Preat, T., Tanimoto, H., 2012. A subset of dopamine neurons signals reward for odour memory in Drosophila. Nat. 2012 4887412 488, 512–516. https://doi.org/10.1038/nature11304

Liu, W., Ganguly, A., Huang, J., Wang, Y., Ni, J.D., Gurav, A.S., Aguilar, M.A., Montell, C., 2019. Neuropeptide F regulates courtship in Drosophila through a male-specific

neuronal circuit. Elife 8, e49574. https://doi.org/10.7554/ELIFE.49574

Liu, X., Ramirez, S., Pang, P.T., Puryear, C.B., Govindarajan, A., Deisseroth, K., Tonegawa, S., 2012. Optogenetic stimulation of a hippocampal engram activates fear memory recall. Nature 484, 381–385. https://doi.org/10.1038/nature11028

Livingstone, M.S., Sziber, P.P., Quinn, W.G., 1984. Loss of calcium/calmodulin responsiveness in adenylate cyclase of rutabaga, a Drosophila learning mutant. Cell 37, 205–215. https://doi.org/10.1016/0092-8674(84)90316-7

Luan, H., Peabody, N.C., Vinson, C.R., White, B.H., 2006. Refined spatial manipulation of neuronal function by combinatorial restriction of transgene expression. Neuron 52, 425–36. https://doi.org/10.1016/j.neuron.2006.08.028

Macpherson, L.J., Zaharieva, E.E., Kearney, P.J., Alpert, M.H., Lin, T.-Y., Turan, Z., Lee, C.-H., Gallio, M., 2015. Dynamic labelling of neural connections in multiple colours by trans-synaptic fluorescence complementation. Nat. Commun. 6, 10024. https://doi.org/10.1038/ncomms10024

Maleszka, J., Barron, A.B., Helliwell, P.G., Maleszka, R., 2009. Effect of age, behaviour and social environment on honey bee brain plasticity. J. Comp. Physiol. A. Neuroethol. Sens. Neural. Behav. Physiol. 195, 733–740. https://doi.org/10.1007/S00359-009-0449-0

Mallory, H.S., Howard, A.F., Weiss, M.R., 2016. Timing of environmental enrichment affects memory in the house cricket, Acheta domesticus. PLoS One 11, 1–13. https://doi.org/10.1371/journal.pone.0152245

Mao, Z., Davis, R.L., 2009. Eight different types of dopaminergic neurons innervate the *Drosophila* mushroom body neuropil: anatomical and physiological heterogeneity. Front. Neural Circuits 3, 5. https://doi.org/10.3389/neuro.04.005.2009

Marella, S., Fischler, W., Kong, P., Asgarian, S., Rueckert, E., Scott, K., 2006. Imaging Taste Responses in the Fly Brain Reveals a Functional Map of Taste Category and Behavior. Neuron 49, 285–295. https://doi.org/10.1016/j.neuron.2005.11.037

Marter, K., Kobler, O., Erdmann, I., Soleimanpour, E., Landgraf, P., Müller, A., Abele, J., Thomas, U., Dieterich, D., 2019. Click Chemistry (CuAAC) and Detection of Tagged de novo Synthesized Proteins in Drosophila. BIO-PROTOCOL 9. https://doi.org/10.21769/bioprotoc.3142

McEwen, B.S., Sapolsky, R.M., 1995. Stress and cognitive function. Curr. Opin. Neurobiol. 5, 205–216. https://doi.org/10.1016/0959-4388(95)80028-X

McGuire, S.E., Le, P.T., Osborn, A.J., Matsumoto, K., Davis, R.L., 2003. Spatiotemporal rescue of memory dysfunction in Drosophila. Science 302, 1765–1768. https://doi.org/10.1126/SCIENCE.1089035

McGuire, S.E., Mao, Z., Davis, R.L., 2004. Spatiotemporal gene expression targeting with the TARGET and gene-switch systems in Drosophila. Sci. STKE 2004. https://doi.org/10.1126/stke.2202004pl6

Miyashita, T., Kikuchi, E., Horiuchi, J., Saitoe, M., 2018. Long-Term Memory Engram Cells Are Established by c-Fos/CREB Transcriptional Cycling. Cell Rep. 25, 2716-2728.e3. https://doi.org/10.1016/j.celrep.2018.11.022

Mockett, B.G., Guévremont, D., Elder, M.K., Parfitt, K.D., Peppercorn, K., Morrissey, J., Singh, A., Hintz, T.J., Kochen, L., Tom Dieck, S., Schuman, E., Tate, W.P., Williams, J.M., Abraham, W.C., 2019. Glutamate Receptor Trafficking and Protein Synthesis Mediate the Facilitation of LTP by Secreted Amyloid Precursor Protein-Alpha. J. Neurosci. 39, 3188–3203. https://doi.org/10.1523/JNEUROSCI.1826-18.2019

Modi, M.N., Shuai, Y., Turner, G.C., 2020. The Drosophila Mushroom Body: From Architecture to Algorithm in a Learning Circuit. Annu. Rev. Neurosci. 43, 465–484. https://doi.org/10.1146/ANNUREV-NEURO-080317-0621333

Mori, K., Sakano, H., 2021. Olfactory Circuitry and Behavioral Decisions. Annu. Rev. Physiol. 83, 231–256. https://doi.org/10.1146/ANNUREV-PHYSIOL-031820-092824

Neckameyer, W.S., Weinstein, J.S., 2005. Stress affects dopaminergic signaling pathways in Drosophila melanogaster. Stress 8, 117–131. https://doi.org/10.1080/10253890500147381

Ng, M., Roorda, R.D., Lima, S.Q., Zemelman, B. V., Morcillo, P., Miesenböck, G., 2002. Transmission of olfactory information between three populations of neurons in the antennal lobe of the fly. Neuron 36, 463–474. https://doi.org/10.1016/S0896-6273(02)00975-3

Ngo, J.T., Champion, J.A., Mahdavi, A., Tanrikulu, I.C., Beatty, K.E., Connor, R.E., Yoo, T.H., Dieterich, D.C., Schuman, E.M., Tirrell, D.A., 2009. Cell-selective metabolic labeling of proteins. Nat. Chem. Biol. 5, 715–717. https://doi.org/10.1038/NCHEMBIO.200

Niehues, S., Bussmann, J., Steffes, G., Erdmann, I., Köhrer, C., Sun, L., Wagner, M., Schäfer, K., Wang, G., Koerdt, S.N., Stum, M., RajBhandary, U.L., Thomas, U., Aberle, H., Burgess, R.W., Yang, X.L., Dieterich, D., Storkebaum, E., 2015. Impaired protein translation in Drosophila models for Charcot-Marie-Tooth neuropathy caused by mutant

tRNA synthetases. Nat. Commun. 6. https://doi.org/10.1038/ncomms8520

Ohkawa, N., Saitoh, Y., Suzuki, A., Tsujimura, S., Murayama, E., Kosugi, S., Nishizono, H., Matsuo, M., Takahashi, Y., Nagase, M., Sugimura, Y.K., Watabe, A.M., Kato, F., Inokuchi, K., 2015. Artificial association of pre-stored information to generate a qualitatively new memory. Cell Rep. 11, 261–269. https://doi.org/10.1016/j.celrep.2015.03.017

Okray, Z., Jacob, P.F., Stern, C., Desmond, K., Otto, N., Talbot, C.B., Vargas-Gutierrez, P., Waddell, S., 2023. Multisensory learning binds neurons into a cross-modal memory engram. Nature 617, 777–784. https://doi.org/10.1038/S41586-023-06013-8,

Owald, D., Felsenberg, J., Talbot, C.B., Das, G., Perisse, E., Huetteroth, W., Waddell, S., 2015a. Activity of defined mushroom body output neurons underlies learned olfactory behavior in Drosophila. Neuron 86, 417–427. https://doi.org/10.1016/j.neuron.2015.03.025

Owald, D., Lin, S., Waddell, S., 2015b. Light, heat, action: neural control of fruit fly behaviour. Philos. Trans. R. Soc. B Biol. Sci. 370, 20140211. https://doi.org/10.1098/rstb.2014.0211

Owald, D., Waddell, S., 2015. Olfactory learning skews mushroom body output pathways to steer behavioral choice in *Drosophila*. Curr. Opin. Neurobiol. 35, 178–184. https://doi.org/10.1016/j.conb.2015.10.002

Pavlov, I.P., 1927. Conditioned reflexes: An investigation of the physiological activity of the cerebral cortex. Ann. Neurosci. 17, 136. https://doi.org/10.5214/ANS.0972-7531.1017309

Pearce, E., Birken, M., Pais, S., Tamworth, M., Ng, Y., Wang, J., Chipp, B., Crane, E., Schlief, M., Yang, J., Stamos, A., Cheng, L.K., Condon, M., Lloyd-Evans, B., Kirkbride, J.B., Osborn, D., Pitman, A., Johnson, S., 2023. Associations between constructs related to social relationships and mental health conditions and symptoms: an umbrella review. BMC Psychiatry 23. https://doi.org/10.1186/S12888-023-05069-0

Perez-Orive, J., Mazor, O., Turner, G.C., Cassenaer, S., Wilson, R.I., Laurent, G., 2002. Oscillations and sparsening of odor representations in the mushroom body. Science 297, 359–365. https://doi.org/10.1126/SCIENCE.1070502

Pfeiffer, B.D., Ngo, T.-T.B., Hibbard, K.L., Murphy, C., Jenett, A., Truman, J.W., Rubin, G.M., 2010. Refinement of Tools for Targeted Gene Expression in *Drosophila*. Genetics 125, 21–27. https://doi.org/10.1534/genetics.166.4.1775

Potter, C.J., Tasic, B., Russler, E. V., Liang, L., Luo, L., 2010. The Q System: A Repressible

Binary System for Transgene Expression, Lineage Tracing, and Mosaic Analysis. Cell 141, 536–548. https://doi.org/10.1016/J.CELL.2010.02.025

Préat, T., 1998. Decreased Odor Avoidance after Electric Shock inDrosophila Mutants Biases Learning and Memory Tests. J. Neurosci. 18, 8534. https://doi.org/10.1523/JNEUROSCI.18-20-08534.1998

Qin, H., Cressy, M., Li, W., Coravos, J.S., Izzi, S.A., Dubnau, J., 2012. Gamma neurons mediate dopaminergic input during aversive olfactory memory formation in Drosophila. Curr. Biol. 22, 608–614. https://doi.org/10.1016/J.CUB.2012.02.014

Ramdya, P., Lichocki, P., Cruchet, S., Frisch, L., Tse, W., Floreano, D., Benton, R., 2014. Mechanosensory interactions drive collective behaviour in Drosophila. Nat. 2014 5197542 519, 233–236. https://doi.org/10.1038/nature14024

Ramos-Hryb, A.B., Ramirez, M.F., Lino-de-Oliveira, C., Pagani, M.R., 2021. Stress-mediated hyperactivity and anhedonia resistant to diazepam and fluoxetine in drosophila. Stress 24, 96–106. https://doi.org/10.1080/10253890.2020.1759547

Rampon, C., Jiang, C.H., Dong, H., Tang, Y.P., Lockhart, D.J., Schultz, P.G., Tsien, J.Z., Hu, Y., 2000. Effects of environmental enrichment on gene expression in the brain. Proc. Natl. Acad. Sci. U. S. A. 97, 12880–12884. https://doi.org/10.1073/PNAS.97.23.12880

Rattazzi, L., Piras, G., Brod, S., Smith, K., Ono, M., D'Acquisto, F., 2016. Impact of Enriched Environment on Murine T Cell Differentiation and Gene Expression Profile. Front. Immunol. 7. https://doi.org/10.3389/FIMMU.2016.00381

Razzoli, M., Andreoli, M., Maraia, G., Di Francesco, C., Arban, R., 2010. Functional role of Calcium-stimulated adenylyl cyclase 8 in adaptations to psychological stressors in the mouse: implications for mood disorders. Neuroscience 170, 429–440. https://doi.org/10.1016/J.NEUROSCIENCE.2010.07.022

Redondo, R.L., Kim, J., Arons, A.L., Ramirez, S., Liu, X., Tonegawa, S., 2014. Bidirectional switch of the valence associated with a hippocampal contextual memory engram. Nature 513, 426–430. https://doi.org/10.1038/nature13725

Riabowol, K.T., Fink, J.S., Gilman, M.Z., Walsh, D.A., Goodman, R.H., Feramisco, J.R., 1988. The catalytic subunit of cAMP-dependent protein kinase induces expression of genes containing cAMP-responsive enhancer elements. Nature 336, 83–86. https://doi.org/10.1038/336083A0

Ries, A.S., Hermanns, T., Poeck, B., Strauss, R., 2017. Serotonin modulates a depression-like state in Drosophila responsive to lithium treatment. Nat. Commun. 2017 81 8, 1–11. https://doi.org/10.1038/ncomms15738

Robertson, H.M., Warr, C.G., Carlson, J.R., 2003. Molecular evolution of the insect chemoreceptor gene superfamily in Drosophila melanogaster. Proc. Natl. Acad. Sci. U. S. A. 100, 14537–14542. https://doi.org/10.1073/PNAS.2335847100/SUPPL_FILE/5847CLUSTALX.TXT

Rosenberg, T., Gal-Ben-Ari, S., Dieterich, D.C., Kreutz, M.R., Ziv, N.E., Gundelfinger, E.D., Rosenblum, K., 2014. The roles of protein expression in synaptic plasticity and memory consolidation. Front. Mol. Neurosci. 7, 86. https://doi.org/10.3389/FNMOL.2014.00086/BIBTEX

Rosenzweig, M.R., Bennett, E.L., 1996. Psychobiology of plasticity: Effects of training and experience on brain and behavior. Behav. Brain Res. 78, 57–65. https://doi.org/10.1016/0166-4328(95)00216-2

Rosenzweig, M.R., Bennett, E.L., Krech, D., 1964. Cerebral effects of environmental complexity and training among adult rats. J. Comp. Physiol. Psychol. 57, 438–439. https://doi.org/10.1037/H0046387

Rosenzweig, M.R., Krech, D., Bennett, E.L., Diamond, M.C., 1962. Effects of environmental complexity and training on brain chemistry and anatomy: a replication and extension. J. Comp. Physiol. Psychol. 55, 429–437. https://doi.org/10.1037/H0041137

Sachdev, P.S., 2022. Social health, social reserve and dementia. Curr. Opin. Psychiatry 35, 111–117. https://doi.org/10.1097/YCO.0000000000000779

Saleh, A.M., Wilding, K.M., Calve, S., Bundy, B.C., Kinzer-Ursem, T.L., 2019. Non-canonical amino acid labeling in proteomics and biotechnology. J. Biol. Eng. 2019 131 13, 1–14. https://doi.org/10.1186/S13036-019-0166-3

Sano, Y., Shobe, J.L., Zhou, M., Huang, S., Shuman, T., Cai, D.J., Golshani, P., Kamata, M., Silva, A.J., 2016. CREB regulates memory allocation in the insular cortex. Curr Biol 176, 139–148. https://doi.org/10.1016/j.cub.2014.10.018.CREB

Savarit, F., Sureau, G., Cobb, M., Ferveur, J.F., 1999. Genetic elimination of known pheromones reveals the fundamental chemical bases of mating and isolation in Drosophila. Proc. Natl. Acad. Sci. U. S. A. 96, 9015–9020. https://doi.org/10.1073/PNAS.96.16.9015/ASSET/85A0F423-F99F-4814-9B03-2EFDB77C6613/ASSETS/GRAPHIC/PQ1592143003.JPEG

Schaefer, M.L., Wong, S.T., Wozniak, D.F., Muglia, L.M., Liauw, J.A., Zhuo, M., Nardi, A., Hartman, R.E., Vogt, S.K., Luedke, C.E., Storm, D.R., Muglia, L.J., 2000. Altered stress-induced anxiety in adenylyl cyclase type VIII-deficient mice. J. Neurosci. 20, 4809–4820. https://doi.org/10.1523/JNEUROSCI.20-13-04809.2000

Scheper, G.C., Van Der Knaap, M.S., Proud, C.G., 2007. Translation matters: protein synthesis defects in inherited disease. Nat. Rev. Genet. 2007 89 8, 711–723. https://doi.org/10.1038/nrg2142

Schloesser, R.J., Lehmann, M., Martinowich, K., Manji, H.K., Herkenham, M., 2010. Environmental enrichment requires adult neurogenesis to facilitate the recovery from psychosocial stress. Mol. Psychiatry 15, 1152–1163. https://doi.org/10.1038/MP.2010.34

Schwaerzel, M., Monastirioti, M., Scholz, H., Friggi-Grelin, F., Birman, S., Heisenberg, M., 2003. Dopamine and Octopamine Differentiate between Aversive and Appetitive Olfactory Memories in Drosophila. J. Neurosci. 23, 10495–10502. https://doi.org/10.1523/jneurosci.23-33-10495.2003

Scott, K., Brady, R., Cravchik, A., Morozov, P., Rzhetsky, A., Zuker, C., Axel, R., 2001. A chemosensory gene family encoding candidate gustatory and olfactory receptors in Drosophila. Cell 104, 661–73. https://doi.org/doi: 10.1016/s0092-8674(01)00263-x.

Sekeres, M.J., Mercaldo, V., Richards, B., Sargin, D., Mahadevan, V., Woodin, M.A., Frankland, P.W., Josselyn, S.A., 2012. Increasing CRTC1 function in the dentate gyrus during memory formation or reactivation increases memory strength without compromising memory quality. J. Neurosci. 32, 17857–17868. https://doi.org/10.1523/JNEUROSCI.1419-12.2012

Semon, R.W., 1921. The Mneme. Allen & Unwin, London.

Serra, M., Pisu, M.G., Floris, I., Cara, V., Purdy, R.H., Biggio, G., 2003. Social isolation-induced increase in the sensitivity of rats to the steroidogenic effect of ethanol. J. Neurochem. 85, 257–263. https://doi.org/10.1046/J.1471-4159.2003.01680.X

Shin, M., Copeland, J.M., Venton, B.J., 2018. Drosophila as a Model System for Neurotransmitter Measurements. ACS Chem Neurosci. 20, 1872–1883. https://doi.org/10.1021/acschemneuro.7b00456

Siegenthaler, D., 2019. Development and function of the Drosophila learning and memory center. Technische Universität Kaiserslautern, Germany.

Siegenthaler, D., Escribano, B., Bräuler, V., Pielage, J., 2019. Selective suppression and recall of long-term memories in Drosophila. PLoS Biol. 17, e3000400. https://doi.org/10.1371/journal.pbio.3000400

Siju, K.P., De Backer, J.-F., Grunwald Kadow, I.C., 2021. Dopamine modulation of sensory processing and adaptive behavior in flies. Cell Tissue Res. 2021 3831 383, 207–225. https://doi.org/10.1007/S00441-020-03371-X

Smith, T.D., Bhatnagar, K.P., 2019. Anatomy of the olfactory system. Handb. Clin. Neurol. 164, 17–28. https://doi.org/10.1016/B978-0-444-63855-7.00002-2

Sokolowski, M.B., 2010. Social interactions in “simple” model systems. Neuron 65, 780–794. https://doi.org/10.1016/J.NEURON.2010.03.007

Soto-Yéber, L., Soto-Ortiz, J., Godoy, P., Godoy-Herrera, R., 2018. The behavior of adult Drosophila in the wild. PLoS One 13. https://doi.org/10.1371/JOURNAL.PONE.0209917

Stensmyr, M.C., Dweck, H.K.M., Farhan, A., Ibba, I., Strutz, A., Mukunda, L., Linz, J., Grabe, V., Steck, K., Lavista-Llanos, S., Wicher, D., Sachse, S., Knaden, M., Becher, P.G., Seki, Y., Hansson, B.S., 2012. A conserved dedicated olfactory circuit for detecting harmful microbes in drosophila. Cell 151, 1345–1357. https://doi.org/10.1016/J.CELL.2012.09.046

Stewart, B.A., Atwood, H.L., Renger, J.J., Wang, J., Wu, C.F., 1994. Improved stability of Drosophila larval neuromuscular preparations in haemolymph-like physiological solutions. J. Comp. Physiol. A 175, 179–191. https://doi.org/10.1007/BF00215114

Suh, G.S.B., Wong, A.M., Hergarden, A.C., Wang, J.W., Simon, A.F., Benzer, S., Axel, R., Anderson, D.J., 2004. A single population of olfactory sensory neurons mediates an innate avoidance behaviour in Drosophila. Nat. 2004 4317010 431, 854–859. https://doi.org/10.1038/nature02980

Sun, H., Nishioka, T., Hiramatsu, S., Kondo, S., Amano, M., Kaibuchi, K., Ichinose, T., Tanimoto, H., 2020. Dopamine receptor DOP1R2 stabilizes appetitive olfactory memory through the Raf/MAPK pathway in Drosophila. J. Neurosci. 40, 2935–2942. https://doi.org/10.1523/JNEUROSCI.1572-19.2020

Takemura, Shin ya, Aso, Y., Hige, T., Wong, A., Lu, Z., Xu, C.S., Rivlin, P.K., Hess, H., Zhao, T., Parag, T., Berg, S., Huang, G., Katz, W., Olbris, D.J., Plaza, S., Umayam, L., Aniceto, R., Chang, L.A., Lauchie, S., Ogundeyi, O., Ordish, C., Shinomiya, A., Sigmund, C., Takemura, Satoko, Tran, J., Turner, G.C., Rubin, G.M., Scheffer, L.K., 2017. A connectome of a learning and memory center in the adult Drosophila brain. Elife 6. https://doi.org/10.7554/ELIFE.26975

Tanaka, N.K., Tanimoto, H., Ito, K., 2008. Neuronal assemblies of the *Drosophila* mushroom body. J. Comp. Neurol. 508, 711–755. https://doi.org/10.1002/cne.21692

Tavosanis, G., 2012. Dendritic structural plasticity. Dev. Neurobiol. 72, 73–86. https://doi.org/10.1002/DNEU.20951

Tayler, K.K., Tanaka, K.Z., Reijmers, L.G., Wiltgen, B.J., 2013. Reactivation of neural ensembles during the retrieval of recent and remote memory. Curr. Biol. 23, 99–106.

https://doi.org/10.1016/j.cub.2012.11.019

Tcherkezian, J., Brittis, P.A., Thomas, F., Roux, P.P., Flanagan, J.G., 2010. Transmembrane Receptor DCC Associates with Protein Synthesis Machinery and Regulates Translation. Cell 141, 632–644. https://doi.org/10.1016/J.CELL.2010.04.008

Technau, G.M., 2007. Fiber number in the mushroom bodies of adult Drosophila melanogaster depends on age, sex and experience. J. Neurogenet. 21, 183–196. https://doi.org/10.1080/01677060701695359

Technau, G.M., 1984. Fiber number in the mushroom bodies of adult drosophila melanogaster depends on age, sex and experience. J. Neurogenet. 1, 113–126. https://doi.org/10.3109/01677068409107077

Tempel, B.L., Bonini, N., Dawson, D.R., Quinn, W.G., 1983. Reward learning in normal and mutant Drosophila. Proc. Natl. Acad. Sci. U. S. A. 80, 1482–1486. https://doi.org/10.1073/PNAS.80.5.1482

Tonegawa, S., Liu, X., Ramirez, S., Redondo, R., 2015. Memory Engram Cells Have Come of Age. Neuron 87, 918–931. https://doi.org/10.1016/J.NEURON.2015.08.002

Trannoy, S., Redt-Clouet, C., Dura, J.M., Preat, T., 2011. Parallel processing of appetitive short- and long-term memories in *Drosophila*. Curr. Biol. 21, 1647–1653. https://doi.org/10.1016/j.cub.2011.08.032

Tully, T., Preat, T., Boynton, S.C., Del Vecchio, M., 1994. Genetic dissection of consolidated memory in Drosophila. Cell 79, 35–47. https://doi.org/10.1016/0092-8674(94)90398-0

Tully, T., Quinn, W.G., 1985. Classical conditioning and retention in normal and mutant Drosophila melanogaster. J. Comp. Physiol. A. 157, 263–77.

Turner, G.C., Bazhenov, M., Laurent, G., 2008. Olfactory representations by Drosophila mushroom body neurons. J. Neurophysiol. 99, 734–746. https://doi.org/10.1152/JN.01283.2007/ASSET/IMAGES/LARGE/Z9K0020887080005.JPEG

van Praag, H., Kempermann, G., Gage, F.H., 2000. Neural consequences of enviromental enrichment. Nat. Rev. Neurosci. 2000 13 1, 191–198. https://doi.org/10.1038/35044558

Vanderklish, P.W., Edelman, G.M., 2005. Differential translation and fragile X syndrome. Genes. Brain. Behav. 4, 360–384. https://doi.org/10.1111/J.1601-183X.2005.00134.X

Varela, N., Gaspar, M., Dias, S., Vasconcelos, M.L., 2019. Avoidance response to CO2 in the lateral horn. PLoS Biol. 17. https://doi.org/10.1371/JOURNAL.PBIO.2006749

Viktorinová, I., Wimmer, E.A., 2007. Comparative analysis of binary expression systems for directed gene expression in transgenic insects. Insect Biochem. Mol. Biol. 37, 246–254. https://doi.org/10.1016/J.IBMB.2006.11.010

Volgin, A.D., Yakovlev, O. V., Demin, K.A., De Abreu, M.S., Rosemberg, D.B., Meshalkina, D.A., Alekseeva, P.A., Friend, A.J., Amstislavskaya, T.G., Kalueff, A. V., 2018. Understanding the Role of Environmental Enrichment in Zebrafish Neurobehavioral Models. Zebrafish 15, 425–432. https://doi.org/10.1089/ZEB.2018.1592

Vosshall, L.B., Amrein, H., Morozov, P.S., Rzhetsky, A., Axel, R., 1999. A spatial map of olfactory receptor expression in the *Drosophila* antenna. Cell 96, 725–36.

Vosshall, L.B., Stocker, R.F., 2007. Molecular Architecture of Smell and Taste in Drosophila. Annu. Rev. Neurosci. 30, 505–533. https://doi.org/10.1146/ANNUREV.NEURO.30.051606.094306

Wachowiak, M., Shipley, M.T., 2006. Coding and synaptic processing of sensory information in the glomerular layer of the olfactory bulb. Semin. Cell Dev. Biol. 17, 411–423. https://doi.org/10.1016/J.SEMCDB.2006.04.007

Walter, T., Couzin, I.D., 2021. Trex, a fast multi-animal tracking system with markerless identi cation, and 2d estimation of posture and visual elds. Elife 10, 1–73. https://doi.org/10.7554/eLife.64000

Wang, D.O., Kim, S.M., Zhao, Y., Hwang, H., Miura, S.K., Sossin, W.S., Martin, K.C., 2009. Synapse- and stimulus-specific local translation during long-term neuronal plasticity. Science 324, 1536–1540. https://doi.org/10.1126/SCIENCE.1173205

Wang, X., Amei, A., De Belle, J.S., Roberts, S.P., 2018. Environmental effects on Drosophila brain development and learning. J. Exp. Biol. 221. https://doi.org/10.1242/jeb.169375

Wang, Z., Singhvi, A., Kong, P., Scott, K., 2004. Taste representations in the Drosophila brain. Cell 117, 981–991. https://doi.org/10.1016/j.cell.2004.06.011

Ward, A.J.W., Herbert-Read, J.E., Sumpter, D.J.T., Krause, J., 2011. Fast and accurate decisions through collective vigilance in fish shoals. Proc. Natl. Acad. Sci. U. S. A. 108, 2312–2315. https://doi.org/10.1073/PNAS.1007102108/SUPPL_FILE/PNAS.201007102SI.PDF

Waschke, L., Kamp, F., van den Elzen, E., Krishna, S., Lindenberger, U., Rutishauser, U., Garrett, D.D., 2025. Single-neuron spiking variability in hippocampus dynamically tracks sensory content during memory formation in humans. Nat. Commun. 2024 161 16, 1–9. https://doi.org/10.1038/s41467-024-55406-4

Webster, M.W., Weixlbaumer, A., 2021. The intricate relationship between transcription and translation. Proc. Natl. Acad. Sci. U. S. A. 118. https://doi.org/10.1073/PNAS.2106284118

Widmer, Y.F., Fritsch, C., Jungo, M.M., Almeida, S., Egger, B., Sprecher, S.G., 2018. Multiple neurons encode crebB dependent appetitive long-term memory in the mushroom body circuit. Elife 7. https://doi.org/10.7554/ELIFE.39196

Wilhelmy, N., 2020. Cellular analysis of long-term memory formation in Drosophila melanogaster. Technische Universität Kaiserslautern, Germany.

Wilhelmy, N.M., 2024. Formation and function of the Drosophila learning and memory centre. RPTU Kaiserslautern Landau, Germany.

Xie, H., Wu, Y., Jia, J., Liu, G., Zhang, Q., Yu, K., Guo, Z., Shen, L., Hu, R., 2013. Enrichment-induced exercise to quantify the effect of different housing conditions: A tool to standardize enriched environment protocols. Behav. Brain Res. 249, 81–89. https://doi.org/10.1016/J.BBR.2013.04.032

Xu, Y., Yan, Y., He, M., Liao, Z., Ran, D., Sun, X., Liu, Y., Wang, X., Huang, Y., Xu, H., Gu, H., 2015. A giant local interneuron modulates the rhythmic activities of the antennal lobe in Pupae Drosophila. Neurosci. Lett. 606, 82–87. https://doi.org/10.1016/J.NEULET.2015.07.014

Yamagata, N., Hiroi, M., Kondo, S., Abe, A., Tanimoto, H., 2016. Suppression of Dopamine Neurons Mediates Reward. PLOS Biol. 14, e1002586. https://doi.org/10.1371/JOURNAL.PBIO.1002586

Yamagata, N., Ichinose, T., Aso, Y., Plaçais, P.-Y., Friedrich, A.B., Sima, R.J., Preat, T., Rubin, G.M., Tanimoto, H., 2015. Distinct dopamine neurons mediate reward signals for short- and long-term memories. Proc. Natl. Acad. Sci. 112, 578–583. https://doi.org/10.1073/pnas.1421930112

Yamamoto, D., Koganezawa, M., 2013. Genes and circuits of courtship behaviour in drosophila males. Nat. Rev. Neurosci. 14, 681–692. https://doi.org/10.1038/NRN3567,

Yin, J.C., Wallach, J.S., Del Vecchio, M., Wilder, E.L., Zhou, H., Quinn, W.G., Tully, T., 1994. Induction of a dominant negative CREB transgene specifically blocks long-term memory in Drosophila. Cell 79, 49–58. https://doi.org/doi: 10.1016/0092-8674(94)90399-9.

Yiu, A.P., Mercaldo, V., Yan, C., Richards, B., Rashid, A.J., Hsiang, H.L.L., Pressey, J., Mahadevan, V., Tran, M.M., Kushner, S.A., Woodin, M.A., Frankland, P.W., Josselyn, S.A., 2014. Neurons Are Recruited to a Memory Trace Based on Relative Neuronal Excitability Immediately before Training. Neuron 83, 722–735.

https://doi.org/10.1016/J.NEURON.2014.07.017/ATTACHMENT/9DC12016-9323-406F-847B-8193623D3BE5/MMC2.PDF

Yoon, B.C., Jung, H., Dwivedy, A., O'Hare, C.M., Zivraj, K.H., Holt, C.E., 2012. Local Translation of Extranuclear Lamin B Promotes Axon Maintenance. Cell 148, 752–764. https://doi.org/10.1016/J.CELL.2011.11.064

Yu, D., Akalal, D.-B.G., Davis, R.L., 2006. *Drosophila* α/β Mushroom Body Neurons Form a Branch-Specific, Long-Term Cellular Memory Trace after Spaced Olfactory Conditioning. Neuron 52, 845–855. https://doi.org/10.1016/j.neuron.2006.10.030

Yu, D., Ponomarev, A., Davis, R.L., 2004. Altered Representation of the Spatial Code for Odors after Olfactory Classical Conditioning: Memory Trace Formation by Synaptic Recruitment. Neuron 42, 437–449. https://doi.org/10.1016/S0896-6273(04)00217-X

Zhang, T.Y., Keown, C.L., Wen, X., Li, J., Vousden, D.A., Anacker, C., Bhattacharyya, U., Ryan, R., Diorio, J., O'toole, N., Lerch, J.P., Mukamel, E.A., Meaney, M.J., 2018. Environmental enrichment increases transcriptional and epigenetic differentiation between mouse dorsal and ventral dentate gyrus. Nat. Commun. 2018 91 9, 1–11. https://doi.org/10.1038/s41467-017-02748-x

Zhang, X., Noyes, N.C., Zeng, J., Li, Y., Davis, R.L., 2019. Aversive Training Induces Both Presynaptic and Postsynaptic Suppression in Drosophila. J. Neurosci. 39, 9164–9172. https://doi.org/10.1523/JNEUROSCI.1420-19.2019

Zhou, C., Rao, Yong, Rao, Yi, 2008. A subset of octopaminergic neurons are important for Drosophila aggression. Nat. Neurosci. 2008 119 11, 1059–1067. https://doi.org/10.1038/nn.2164

Zhou, F., Tichy, A.M., Imambocus, B.N., Sakharwade, S., Rodriguez Jimenez, F.J., González Martínez, M., Jahan, I., Habib, M., Wilhelmy, N., Burre, V., Lömker, T., Sauter, K., Helfrich-Förster, C., Pielage, J., Grunwald Kadow, I.C., Janovjak, H., Soba, P., 2023. Optimized design and in vivo application of optogenetically functionalized Drosophila dopamine receptors. Nat. Commun. 2023 141 14, 1–18. https://doi.org/10.1038/s41467-023-43970-0

Zhou, Y., Won, J., Karlsson, M.G., Zhou, M., Rogerson, T., Balaji, J., Neve, R., Poirazi, P., Silva, A.J., 2009. CREB regulates excitability and the allocation of memory to subsets of neurons in the amygdala. Nat. Neurosci. 12, 1438–1443. https://doi.org/10.1038/nn.2405

1. Appendix

1.1 Results of statistical analysis

Table 4: List of detailed statistical results for boxplots and scatter plots.
Listed are the corresponding figures, the designation of the groups examined, the n-numbers, the mean values, the statistical analyses performed, and the p-values. If a post hoc test was performed, this is noted and the corrected p-values are given. Data were tested for normal distribution using the Shapiro-Wilk test. No statistical analysis was performed for Figures 10 and 20, which is indicated by the term not applicable (N/A).

figure	groups tested	n	mean	statistical test	p values
13C$_1$	control	44	10,61	two-tailed Mann-Whitney test	<0,0001
	pupae	58	0,78		
13C$_2$	control	55	10,55	two-tailed Mann-Whitney test	0,0986
	single male	75	9,75		
14D$_1$	control	56	10,5	two-tailed Mann-Whitney test	0,0762
	flipping	77	12		
14D$_2$	contorl	83	10,72	two-tailed Mann-Whitney test	<0,0001
	flipping + odor	78	14,06		
14D$_3$	control	60	10,83	unpaired, two-tailed t-test	<0,0001
	flipping + odor + virgins	77	14,6		
15	pupae	58	0,78	N/A	N/A
	single male	75	9,75		
	control	298	10,65		
	flipping	77	12		
	flipping + odor	78	14,06		
	flipping + odor + virgins	77	14,6		
16B	control	8	-0,88	unpaired, two-tailed t-test	0,2101
	odor	7	-8,65		
16C	control	8	-4,54	unpaired, two-tailed t-test	0,9309
	flipping	8	-4,21		
16D	control	8	-5,62	unpaired, two-tailed t-test	0,5573
	virgins	8	-9,76		
16E$_1$	control	20	-13,91	unpaired, two-tailed t-test	<0,0001
	odor + flipping	19	-39,91		
16E$_2$	control	33	7,61	two-tailed Mann-Whitney test	0,0004
	odor + flipping	30	10,97		
17C	Chrimson	13	5,15	two-tailed Mann-Whitney test	<0,0001
	EGFP	18	10,39		
20B	mock	8	-7,06	unpaired, two-tailed t-test	<0,0001
	paired	8	55,5		
20C	mock	9	3,34	unpaired, two-tailed t-test	<0,0001
	paired	8	36		
20E	mock	146	12,94	two-tailed Mann-Whitney test	0,0007
	paired	159	15,09		
23B	- retinal	9	-2,18	unpaired, two-tailed t-test	0,0278
	+ retinal	9	-11,5		
23C	- retinal	9	-5,47	unpaired, two-tailed t-test	0,5268
	+ retinal	9	-2,23		

24A	24h water	5	-53,84	unpaired, one-way ANOVA	Tukey's test: 0,9994; 0,9783; 0,5003; 0,3239
	48h water	5	-55,47		
	24h food	5	-65,68		
	48h food	5	-69,78		
24B	24h water	5	34,45	unpaired, one-way ANOVA	Tukey's test: 0,2093; 0,9758; 0,46; 0,7804
	48h water	5	19,99		
	24h food	5	23,58		
	48h food	5	27,3		
25C	Gr66a	8	-67,12	N/A	N/A
	MB077B	8	41,12		
$25D_1$	manual	8	-67,12	unpaired, two-tailed t-test	0,9568
	automated	8	-66,9		
$25D_2$	manual	8	41,12	unpaired, two-tailed t-test	0,1399
	automated	8	35,68		
$25E_1$	0,04	8	-72,92	N/A	N/A
	0,4	8	-69,96		
	1	8	67,93		
	2	8	67,9		
	3	8	-68,4		
	4	8	-67,85		
	5	8	-66,9		
	10	8	-62,11		
	15	8	-60,17		
$25E_2$	0,04	8	27,19	N/A	N/A
	0,4	8	29,99		
	1	8	32,57		
	2	8	34,63		
	3	8	35,28		
	4	8	35,75		
	5	8	35,68		
	10	8	31,97		
	15	8	29,62		
$25F_1$	0	8	4,72	N/A	N/A
	5	8	-36,63		
	10	8	-50,5		
	15	8	56,01		
$25F_2$	0	8	6,68	N/A	N/A
	5	8	21,63		
	10	8	29,53		
	15	8	24,91		
26A	control	5	-4,642	Kruskal-Wallis test	Dunn's test: 0,0012; 0,2313; 0,2313
	Gr66a	5	-74,12		
	conditioned	5	-17,16		
26B	control	5	-28,29	unpaired, one-way ANOVA	Tukey's test: 0,4105; <0,0001; <0,0001
	Gr66a	5	-39		
	conditioned	5	36,03		
27B	no retinal	28	-5,42	two-tailed Mann-Whitney test	0,001
	1st 48h retinal	27	-17,34		
27C	no retinal	16	2,4	unpaired, two-tailed t-test	<0,0001
	1st 48h retinal	16	-18,43		
27D	no retinal	17	4,06	unpaired, two-tailed t-test	0,001
	1st 48h retinal	17	-12,21		
27E	1st 48h retinal	19	-24,41	unpaired, one-way ANOVA	Tukey's test: 0,0012; 0,0098; 0,9800
	2nd 48h retinal	26	-9,03		
	96 retinal	12	-23,45		
27F	paired	20	-16,71	unpaired, two-tailed t-test	0,305
	unpaired	21	-11,83		

27G	paired	19	-13,64	unpaired, two-tailed t-test	0,3693
	unpaired	19	-9,329		
30B	2U x OK107-Gal80	8	-57,75	unpaired, one-way ANOVA	Tukey's test: 0,1699; 0,0186; 0,0002
	2U x D1R1-RNAi	8	-45,91		
	OK107-Gal80 x D1R1-RNAi	8	-27,08		
30C	2U x OK107-Gal80	9	-56,72	unpaired, one-way ANOVA	Tukey's test: 0,9685; 0,3788; 0,4902
	2U x UAS-D1R1-V2	8	-58,29		
	OK107-Gal80 x UAS-D1R1-V2	8	-49,16		
31B	- retinal + odor + shock + light	10	-37,59	unpaired, one-way ANOVA	Tukey's test: 0,6479; 0,2322; 0,7287
	+ retinal + odor + shock - light	11	-42,7		
	+ retinal + odor + shock + light	10	-33,14		
31C	- retinal + odor + shock + light	11	-42,52	unpaired, one-way ANOVA	Tukey's test: 0,9866; 0,3123; 0,3908
	+ retinal + odor + shock - light	11	-41,81		
	+ retinal + odor + shock + light	11	-48,56		
31D	- retinal + odor - shock + light	8	2,807	unpaired, one-way ANOVA	Tukey's test: 0,9560; 0,9882; 0,9900
	+ retinal + odor - shock - light	9	1,003		
	+ retinal + odor - shock + light	8	1,929		

1.2 Curriculum Vitae

Personal Data

Name:	Vanessa Burre
Nationality:	German

Education

2019 – now	**Ph.D. in Neuroscience** Thesis: “Analysis of associative olfactory learning and memory in Drosophila” Place: RPTU Kaiserslautern Supervisor: Prof. Dr. Jan Pielage
2016 – 2019	**Master of Science (M.Sc.)** in Molecular Cell Biology and Neurobiology Thesis: “Characterization of memory engram neurons in *Drosophila*” Place: Technical University of Kaiserslautern Supervisor: Prof. Dr. Jan Pielage
2012 – 2016	**Bachelor of Science (B.Sc.)** in Biosciences Thesis: “Tamoxifen induzierte tdTomato-Expression im auditorischen Hirnstamm bei Mäusen” Place: Technical University of Kaiserslautern Supervisor: Prof. Dr. Eckhard Friauf

1.3 Acknowledgements

First and foremost, I would like to thank Prof. Dr. Jan Pielage for the opportunity to pursue my PhD in his lab and for his continuous support throughout this project. I especially appreciate his encouragement during challenging phases of the behavioral experiments

I also thank Prof. Dr. Stefan Kins for kindly agreeing to serve as the second reviewer of this thesis.

I am grateful to all current and former lab members for the collaborative environment, helpful discussions, and the many shared moments beyond daily lab work. I would also like to thank everyone who took the time to proofread this thesis and contributed to improving it.

I would like to particularly acknowledge Hans-Peter, Patrick, and Simone for their support and reliability throughout my PhD. Their advice and willingness to help, even during stressful periods, made a real difference.

I am especially grateful to Nina Wilhelmy for her collaboration in the lab and, more importantly, for her friendship. Her support during my PhD meant a great deal to me, and I am deeply thankful to have her in my life. Even years later, despite the distance between us, our friendship remains, which I truly value.

Finally, I thank my family and friends for their encouragement. I am especially grateful to my husband Florian for his constant support, patience, and understanding throughout this journey. During the final phase of writing, he took on the full care of our daughter Paula so I could focus on finishing this thesis.